UNIVERSITAT ROVIRA I VIRGILI

GENERATION AND CONTROL OF LOCOMOTION FOR BIPED ROBOTS BASED ON BIOLOGICALLY INSPIRED APPROACHES.

Julián Efrén Cristiano Rodríguez

Dipòsit Legal: T 254-2016

Generation and control of locomotion for biped robots based on biologically inspired approaches

DOCTORAL THESIS

Author:

Julián Efrén Cristiano Rodríguez

Advisors:
Dr. Domènec Savi Puig Valls
Dr. Miguel Ángel García García

Departament d'Enginyeria Informàtica i Matemàtiques

UNIVERSITAT ROVIRA I VIRGILI

Tarragona

2015

UNIVERSITAT ROVIRA I VIRGILI
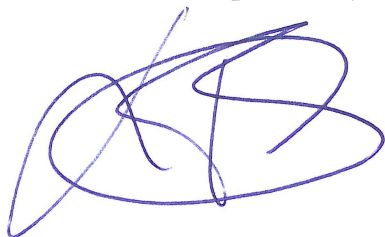
Departament d'Enginyeria Informàtica i Matemàtiques

Av. Paisos Catalans, 27

43007 Tarragona

Tel. +34 977 55 95 95

Fax. +34 977 55 95 97

We STATE that the present study, entitled "Generation and control of locomotion for biped robots based on biologically inspired approaches", presented by Julián Efrén Cristiano Rodríguez, for the award of the degree of Doctor, has been carried out under our supervision at the Departament d'Enginyeria Informàtica i Matemàtiques.

Tarragona, 16th November 2015.

Doctoral Thesis Supervisors,

Dr. Domènec Savi Puig Valls   Dr. Miguel Ángel García García

To God, thank you for walking by my side today and always.

To my parents Efrén and Blanca.

To my brother Juan and my sister Karen.

To my niece Silvia and my dear Lucía.

To the memory of my grandfather and my grandmother.

To my family and friends.

Abstract

This thesis proposes the use of biologically inspired control approaches to generate and control the omnidirectional gait of humanoid robots, adapting their movement to various types of flat terrain using multi-sensory feedback. The proposed locomotion control systems were implemented using Central Pattern Generator (CPG) networks based on Matsuoka's neuron model. CPGs are biological neural networks located in the central nervous system of vertebrates or in the main ganglia of invertebrates, which can control coordinated movements, such as those involved in locomotion, respiration, chewing or swallowing.

The fact that, in nature, human and animal locomotion is controlled by CPG networks has inspired the theory on which the present thesis is based. In particular, two closed-loop control architectures based on CPG-joint-space control methods have been proposed and tested by using both a simulated and a real NAO humanoid robot. The first control architecture identified some important features that a CPG-joint-space control scheme must have if a useful locomotion pattern is to be described. On the basis of this analysis, the second control architecture was proposed to describe well-characterized locomotion patterns. The new system, characterized by optimized parameters obtained with a genetic algorithm (GA), effectively generated and controlled locomotion patterns for biped robots on flat and sloped terrain.

To improve how the system behaves in closed loop, a phase resetting mechanism for CPG networks based on Matsuoka's neuron model has been proposed. It makes it possible to design and study feedback controllers that can quickly modify the locomotion pattern generated.

The results obtained show that the proposed control schemes can yield well-characterized locomotion patterns with a fast response suitable for humanoid robots with a reduced processing capability. These experiments also indicate that the proposed system enables the robot to respond quickly and robustly, and to cope with complex situations.

ii

Keywords: Biped locomotion, Robotics, Humanoid Robots, Adaptive control, Biologically inspired control, Central pattern generators, CPGs, Phase resetting, Matsuoka's oscillator.

Acknowledgements

I would like to express my gratitude to my advisors Dr. Domènec Savi Puig Valls and Dr. Miguel Ángel García García for giving me the opportunity to work under their academic supervision and for their dedication, guidance and support during these years.

I would like to thank my parents Efrén and Blanca, my brother Juan, my sister Karen, my niece Silvia and my dear Lucía for their love, encouragement and support. Likewise, the affection and support that I have received from all my family and friends in Colombia and Spain have been fundamental to me.

During the last years I have met many people from whom I have learnt a lot. To all of them, thank you very much for each of the great moments that we have shared and also for the great talks that I am completely sure we have had. I also would like to thank each of the former and current members of the Intelligent Robotics and Computer Vision Group for their companionship and friendship.

I would like to thank Fundación Carolina and Universitat Rovira i Virgili for the financial support given to me through a doctoral scholarship.

Last but not least, I want to express my gratitude to all those anonymous reviewers who have made useful revisions on my conference and journal publications.

Contents

Contents   vii

List of Figures

List of Figures xi

List of Tables

CHAPTER 1

Introduction

1.1 Motivation

Biped locomotion has long been of interest to researchers in neuroscience, robotics and other fields of research. However, the locomotion of legged robots involves complex dynamic systems from the mechanical, structural and control system points of view. Many control schemes have been proposed but despite the best efforts of the scientific community, the problem of biped locomotion has yet to be satisfactorily solved. At present, interest in humanoid robots is increasing because it is believed that they will be able to carry out a wide range of functions in the future: entertainment, dangerous tasks, rescue attempts, helping the disabled (Shukla et al., 2015), etc. Furthermore, the cost of producing these robots is being reduced, which is leading to their being used in a variety of scenarios. Many humanoid robots are now commercially available: for example, ASIMO (Sakagami et al., 2002), NAO

1

(Gouaillier et al., 2009, 2010), etc.

Humanoid robots are complex electromechanical systems that have been designed to have the appearance and the main features of human beings so that they can work and interact in the same environments as they do. The main features of these robots are the following: they have several degrees of freedom (DoF) so that they can control the whole body structure (arms, feet, head and trunk). Small humanoid robots normally use around 22 degrees of freedom to control the whole body and full-size biped robots use around 40 degrees of freedom. Most of their weight is located in their upper body and they have only two possible contact surfaces located on the soles of their feet.

Currently, the study of how legged living organisms move has led to biologically inspired approaches being applied to the problem of the locomotion of legged robots because these approaches take advantage of the real, efficient natural process observed in the locomotor system of living beings. In nature, biological systems do not perform complex computations and still efficiently solve a wide variety of complex control problems by using networks consisting of simple units.

Advances in neuroscience have shown clear evidence that rhythms in vertebrate and invertebrate animals are generated centrally and do not require sensory information. These rhythms are generated by Central Pattern Generators (CPGs). These are biological neural networks that can generate complex multi-dimensional rhythmical signals through the interconnection of mutually inhibiting and excitatory neurons. CPGs are located in the central nervous system of vertebrates (e.g., cat, lamprey and human) or in the main ganglia in invertebrates (e.g., leech, worm, and mollusc Tritonia diomedia) (Yu et al., 2014).

Human locomotion is based on the activity of networks of central pattern generators. These networks are located in the spinal cord. Afferent information from the periphery (i.e. the limbs) influences the central pattern and, conversely, the CPGs select afferent information according to the external requirement. Both the CPGs and the reflexes that mediate afferent input to the spinal cord are under the control of the brainstem (Dietz, 2003).

Several mathematical models have been proposed to mimic the behaviour observed in biological CPG networks. These models describe stable rhythmical output signals that can be easily controlled by using simple input signals which, in turn, can be used to modulate the CPGs output signals according to the current external sensory information. Nowadays, the big challenge is to design control systems inspired by how these networks function to control humanoid robots.

The fact that, in nature, human and animal locomotion is controlled by CPG networks has inspired the theory on which the present thesis is based. Controlling the locomotion of biped robots requires a robust control system that can deal with all the unexpected situations that can arise during motion. The system used by animals and human beings to control their legs is efficient and adaptive. They can cope with complex situations and adapt their behaviour to new challenging situations if required.

1.2 Objectives

1.2.1 General objective

This thesis proposes the use of biologically inspired control approaches to generate and control the omnidirectional gait of humanoid robots, adapting their movement on-line to various types of flat terrain using multi-sensory feedback. The main aim is to design a control strategy that generates and controls well-characterized locomotion patterns, for humanoid robots with reduced processing capability through simple but effective control strategies inspired biologically by minimizing the number of user-tuned, control parameters. The system must guarantee a fast response, describe well-characterized locomotion patterns comparable to previously proposed systems, and guarantee correct interaction between the soles of the robot's feet and the floor. It should enable the robot to deal with internal mismatches and external perturbations through feedback strategies that quickly modulate the well-characterized locomotion pattern. This thesis focuses on the research field of generation and control of biped locomotion based on Central Pattern Generator

networks implemented with non-linear oscillators that operate in the joint space.

1.2.2 Specific objectives

The specific objectives of this thesis are listed below:

1. To propose new control schemes based on new networks of non-linear oscillators and feedback strategies that generate well-characterized patterns to control the locomotion of biped robots, minimizing the number of control parameters and avoiding the computation of the inverse kinematics so that response is in real time even on hardware with low or moderate performance capabilities.

2. To develop an offline methodology that optimizes CPG parameters and generates omnidirectional gait modes for various types of flat terrain.

3. To propose an online methodology that automatically changes the CPG parameters and describes omnidirectional movements.

4. To propose an online feedback mechanism that controls the motion described for the humanoid robot using multi-sensory information that compensates for internal mismatches and external perturbations.

5. To implement the generation and control locomotion framework in C++ for the NAO humanoid Robot.

1.3 Overview

The rest of this dissertation is organized as follows:

Chapter 2 introduces some fundamental concepts of biped locomotion and reviews the relevant literature on control systems used for the locomotion control of humanoid robots. Finally, some fundamental concepts of CPG networks are presented and the CPG networks implemented with Matsuoka's neuron model are studied in detail.

Chapter 3 explains the design methodology used for the study of the two closed-loop control schemes proposed for the locomotion control of biped robots. These systems use CPG networks implemented by using Matsuoka's neuron model to generate and modulate the locomotion patterns. The experimental results validating

the proposed control schemes are also presented and discussed.

Chapter 4 presents a detailed description of the phase resetting mechanism designed for CPG networks based on Matsuoka's oscillator. Experiments in simulation and with a real application to closed-loop locomotion control of biped robots are presented to validate the mechanism. The proposed phase resetting mechanism is useful for robotics, biomedical and other control applications.

Chapter 5 summarizes the main contributions of this study and proposes some interesting future research. Finally, the list of publications is presented.

CHAPTER 2

State of the art

2.1 Biped locomotion

Biped locomotion is a form of terrestrial motion by which an organism changes its position through the coordinated movement of its rear limbs or legs. There are three possible types of bipedal locomotion: walking, running and hopping.

During bipedal walking the support leg changes frequently and the contact surfaces are the soles of the robot's feet and the floor. The periods of contact are called *single support mode* and *double support mode*. The former is the time during which the robot is supported on a single foot. The latter is the time during which both feet are in direct contact with the floor. In bipedal walking the sole of at least one foot must be in contact with the floor. If there are periods of time during which both feet leave the ground and there is no direct contact with the walking surface then the robot is considered to be running.

The walking motion of humanoid robots is commonly produced by the synchronized movement of its limbs and is usually calculated by solving the inverse kinematics problem. The motion can also be generated by using models in the Joint Space to determine the periodic movements that directly control the robot's joints. In both cases the motion must guarantee that the robot's body is stable. These joints are normally controlled using position, force or parallel force/position control schemes. To generate stable bipedal walking modes on natural terrain, the complex dynamic interaction between the robot and the unknown environment around it must be regulated through the information provided by its sensors. Therefore, this information needs to be analysed quickly so that loss of balance can be detected and the system can react as soon as possible.

On flat terrain, the most common concept used to guarantee the stable walking of a biped robot is the *Zero Moment Point* (ZMP) (Vukobratović and Borovac, 2004). This is defined as the point on the ground at which the sum of the moments of all active forces equals zero. It reduces the representation of the distribution of the ground reaction forces to a single point. If the ZMP is within the convex hull (*current support polygon*) of all the contact points between the feet and the ground, the gait is dynamically stable. This methodology, first proposed by Vucobratovik, makes it possible to control biped stability using either full (Park and Youm, 2007) or simplified dynamic models of the humanoid (Kajita et al., 2003).

The normal field of pressure forces for the robot's feet is equivalent to a single resultant force exerted at a single point where the resultant moment is zero. This is known as the *Centre of Pressure* (CoP). Figure 2.1 shows the graphical representation of the CoP location. In biped robots, the CoP is estimated by using the measures provided by the force sensors located in the soles of the robot's feet. The magnitude of the resultant force in the normal direction is expressed as:

$$F_{RN} = \sum_{i=1}^{n} F_{Ni},\tag{2.1}$$

where F_{Ni} is the magnitude of the force provided by the ith sensor in the z direction. Variable n is the number of force sensors located in the soles of the robot's feet
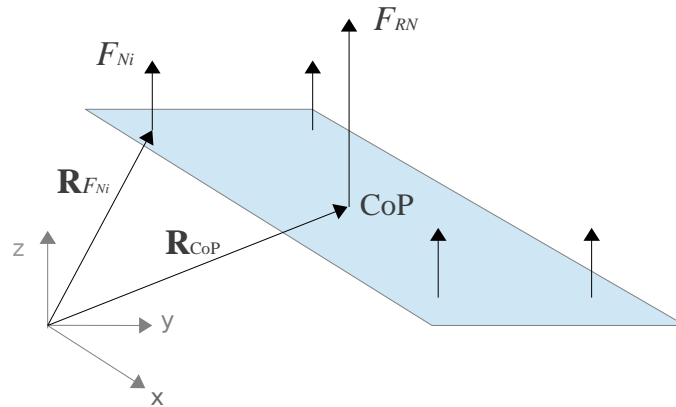
Figure 2.1: CoP location

(normally 8 for biped robots).

The location of the CoP with respect to the base-frame-origin, denoted as $\mathbf{R}_{\text{CoP}}$, can be calculated from:

$$\mathbf{R}_{\text{CoP}} = \frac{\sum_{i=1}^{n} \mathbf{R}_{F_{Ni}} F_{Ni}}{F_{RN}} \tag{2.2}$$

In humanoid robots with a balanced gait and on flat surfaces, the ZMP coincides with the CoP. Therefore, the ZMP is commonly calculated by estimating the CoP. During bipedal locomotion, the body's weight is continuously changing from one leg to the other, and the support polygon alternates from single to double support mode and vice versa. In order for walking to be stable on flat terrain, the ZMP must be within the polygon described by the current support polygon or the robot will fall.

The centre of masses (CoM) of a humanoid robot is mostly located near the robot's chest because it concentrates a large amount of mass. It is very important, then, to control the robot's chest position and orientation. Only by doing this can the location of the CoM also be controlled and balance be provided when unstable situations arise.

In bipedal locomotion some useful measures of the stability of the motion are: the *static stability margin* and the *dynamic stability margin*. The former is defined as the minimum distance between the vertical projection of the centre of mass in the current support polygon and the nearest support polygon's border to this projection. In order to guarantee static stability, the vertical projection of the centre of mass
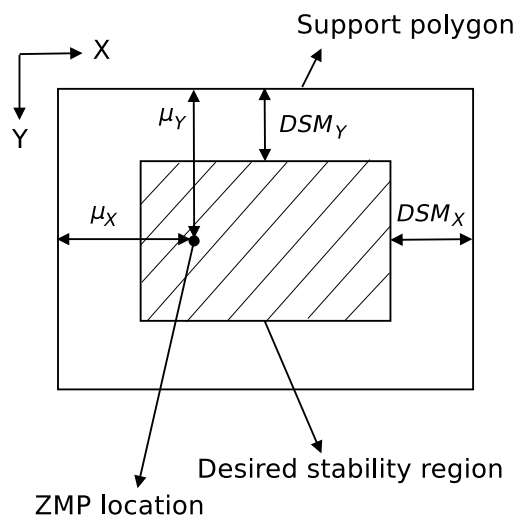
Figure 2.2: Desired dynamic stability margin

must remain inside the current support polygon.

The dynamic stability margin is defined as the minimum distance between the ZMP and the nearest border of the support polygon. The dynamic stability margin can be divided into the dynamic stability margin along the sagittal plane, μ_X, and the dynamic stability margin along the coronal plane, μ_Y (see fig. 2.2). In order to guarantee dynamic stability, the ZMP must remain inside the current support polygon.

The system of locomotion control for biped robots must maximize the stability margin at all times during motion in order to guarantee a stable walking pose. In order to guarantee more stable locomotion, a desired stability region is commonly defined by the values DSM_X and DSM_Y within the support polygon to prevent the ZMP from being too close to the support polygon's border. So, the support polygon is redefined as is shown in fig. 2.2.

In general, locomotion control systems for biped robots must ensure that the locomotion patterns generated guarantee the stability of the robot's body during walking by taking into account the robot's dynamics and the current interaction between the soles of the robot's feet and the terrain through the sensory information. Therefore, a system that properly and quickly integrates the information extracted from the current feedback signals is useful because it allows the robot to quickly react whenever there are disturbances.
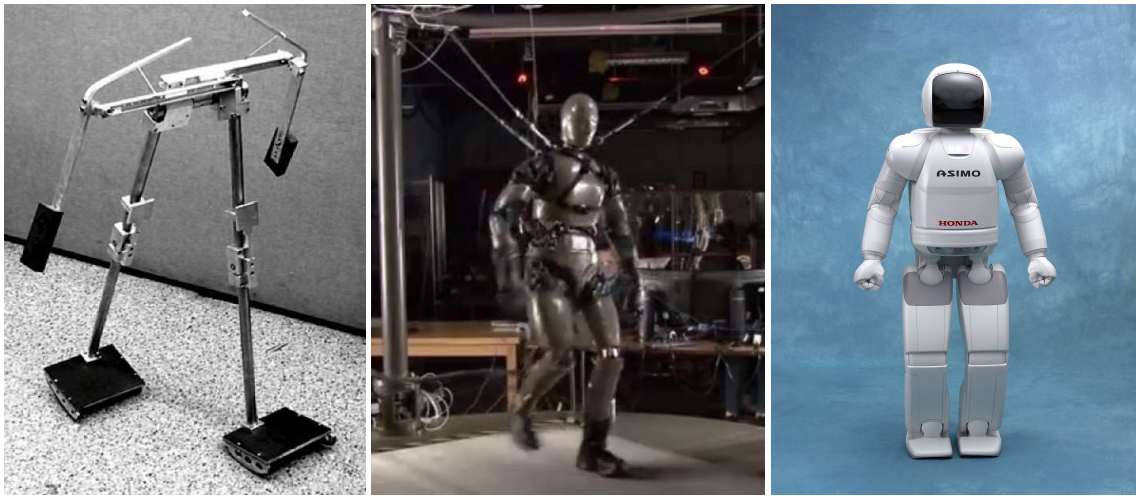
Figure 2.3: Three examples of biped robots. From left to right: Passive Dynamic Walker, Petman and Asimo.

2.2 Locomotion control systems for biped robots

Many control schemes have been proposed in recent years to generate and control the locomotion of biped robots on flat terrain. These control schemes are mainly designed to improve one or several of the most important aspects of walking. These aspects can be summarized as: *robustness*, *versatility* and *energy efficiency*. Robustness means that the system can cope with large unexpected disturbances that suddenly appear during motion. If the system is versatile then the control scheme can perform a wide range of different gaits in different directions, change speed, etc. Finally, an energy-efficient system attempts to guarantee that the power consumption of the system is as low as possible.

The specifications of the robot's hardware also need to be taken into account because the hardware determines the best control strategy to be implemented. For instance, if the robot does not have a powerful processor to perform extensive computations, then a control scheme that takes into account the whole robot's dynamics cannot be used. Hence, a control scheme must be implemented that requires fewer processing capabilities to be properly executed by the robot's hardware. Several approaches have been proposed for controlling the robot's joints motion depending on its structure and hardware. Some examples of biped robots are

shown in fig. 2.3. For instance, passive dynamic walkers are robots that are designed to be very energy efficient because the robot's mechanical structure is carefully built and naturally conducive to walking (McGeer, 1990). However, they are neither versatile nor robust and, therefore, it is difficult to use them in real environments.

A control system developed for the biped robot Petman,[1] designed by Boston Dynamics, has proved to be very robust and enables the robot to cope with considerable external disturbances. However, their results show that the control system is not very energy efficient or versatile when working in a real dynamic environment and the implementation seems to be very complex.

Another well-known robot called Asimo (Sakagami et al., 2002), manufactured by Honda, has been designed to be versatile. It can negotiate different walking surfaces, make turns, change its walking speed and also run (lift both feet off the ground). However, it cannot cope with external disturbances or unexpected situations because it is not very robust.

In general, a control strategy that takes into account the robot's hardware resources and the parameters to be improved (robustness, versatility and/or energy-efficiency) must be defined. The main objective for systems of locomotion control is to generate reference signals for the robot's joints, either as angular displacement or torque, so that motion is stable. These signals are mainly generated through pre-computed trajectories or trajectories computed in real-time by various control schemes.

The aim of this thesis is to design a control strategy for humanoid robots with reduced processing capability that can be versatile and robust. It will use simple but effective control strategies which take their inspiration from biology and will not solve the inverse kinematics problem.

Currently, several control strategies have been put forward for solving the biped locomotion problem. Despite the existence of several types of robots and control schemes, in this section, only the most common methods in the literature for generating and controlling the locomotion patterns for biped robots on flat terrain

---

[1]http://www.bostondynamics.com/robot%5Fpetman.html

are presented and classified in two categories.

The first category, the ZMP-based control methods, contains the approaches that use the ZMP location to generate locomotion patterns. To get a real-time response, these approaches often use a simplified representation of the robot that employs a simple and easily understandable formulation associated with the model used. The second category, the biologically inspired control methods, contains all those control schemes that have been proposed in the literature and which mimic the efficient functioning of the locomotion control performed by living beings. The most important feature of biological systems is their adaptability, which makes them ideal for coping with a variety of situations that can arise during biped locomotion.

2.2.1 ZMP-based control methods

ZMP-based control methods must guarantee that the ZMP remains inside the convex hull that encloses the support polygon described by the foot or feet that is/are in contact with the ground. The main inconvenience is that they require precise models of the robot and the environment, which leads to complex models that require good hardware specifications so that the calculations can be made for the system to work in real time. The most commonly used methodology for generating biped locomotion is a simplified dynamic model of the humanoid robot's body that describes the trajectories for the robot's arms and legs in the task space. These approaches mainly control the position of the Zero Moment Point (Vukobratović and Borovac, 2004), track the ZMP location and correct it through a feedback strategy so that the robot's balance can be recovered if necessary.

One of the most used models is the mass concentrated model. It simplifies the whole body dynamics to the centre of gravity motion by concentrating the whole-body mass at that point. It is the most suitable model for real-time applications, because it computes the walking motion faster. Two kinds of mass concentrated models have been used for attaining stable walking: the three dimensional linear inverted pendulum model (3D-LIPM) and the cart-table model (Kajita et al., 2003). A real-time pattern can be generated for biped walking by

analysing the dynamics of the motion of a three dimensional linear inverted pendulum model on an arbitrarily defined plane (Sugihara et al., 2002; Kajita et al., 2002). The 3D-LIPM models the humanoid robot motion by computing a smooth trajectory of a single mass (centre of mass), which follows the inverted pendulum laws under the gravity field; the constraint is to maintain the ZMP on the support polygon during walking in order to prevent the humanoid from falling down. Therefore, a stability controller for recovering balance is required to deal with internal mismatches and external perturbations.

In (Choi et al., 2007), a CoM/ZMP trajectory planning method with a humanoid simplified model was proposed to generate the stable movement for a humanoid robot. To guarantee the stability of the motion, a walking CoM/ZMP controller is used. Using the full dynamic model, an on-line pattern generator for bipedal walking control can be designed based on a ZMP preview control (Park and Youm, 2007). However, a humanoid robot with a good processing capability is required.

2.2.2   Biologically inspired control methods

Getting biped robots to walk requires a robust control system that can cope with a wide variety of unexpected events in real time. In recent years, biologically inspired control approaches have successfully been used to generate and control the motion of various types of robots (Bekey, 2005). These approaches have proven to be simple yet robust and reliable. This is due to the fact that animals and human beings do not solve complex formulations to generate movements and can react easily to changes in the environment.

Many of the behaviours currently studied by neuroscientists are rhythmic. If a behaviour is rhythmic, there will be many repetitions of very similar movements. Many rhythmic behaviours such as walking are generated by a specialized subset of neurons that control these behaviours. These neural networks can usually generate rhythmic patterns without outside stimuli; that is, the rhythm is intrinsic to the network and/or cells of the network. These networks are called Central Pattern Generators (CPG) and are commonly used to control the locomotion of biped

robots because they generate rhythmic signals easily by using simple input signals. Furthermore, the oscillations generated are stable and can be easily modulated to incorporate feedback.

The first studies about CPGs applied to biped locomotion were presented in (Taga et al., 1991; Taga, 1995), who investigated the use of CPGs for controlling the walking of a simulated humanoid robot on a 2D plane. The results showed that the CPG controller was robust to disturbances. In (Miyakoshi et al., 1998), the previous work was extended to 3D using a simplified model without arms or head. The results showed that it is possible to obtain a stable biped stepping motion and tolerance against external perturbations with a neural oscillator system. Unlike ZMP methodologies, bipedal locomotion based on CPGs does not require precise information about the environment. The CPG-based controllers interact with biomechanical and environmental constraints through sensory feedback to adapt to changes and learning. Endo et al. (2004) investigated the robustness of the CPG controllers for a walking robot. The robot does not have an upper body and it is supported by a boom, which helps with balancing. Subsequently, they applied a CPG controlled with biologically inspired feedback to control the humanoid robot QRIO. Experimental results show that this controller is robust to perturbations and environmental changes (Endo et al., 2005). CPGs with sensory feedback play an important role and provide a promising way to develop robust humanoid walking control, and efficient coupling between the robot and the environment.

Artificial CPGs can be used to control the robot's motion in either the task space (Liu et al., 2013b; Song and Hsieh, 2014) or the joint space (Nassour et al., 2013). The first approach aims at determining the Cartesian space trajectories of the robot's limbs. In this case, the individual signals for the robot's joints must be generated by solving the inverse kinematics, which is a time-consuming process. Alternatively, if motion is generated in the joint space, the CPG output signals are directly used to control the angular position of the robot's joints. Later, some of the main studies in the literature for CPG-based control systems are presented in order to summarize the current state-of-the-art in the field. These works indicate the growing interest in
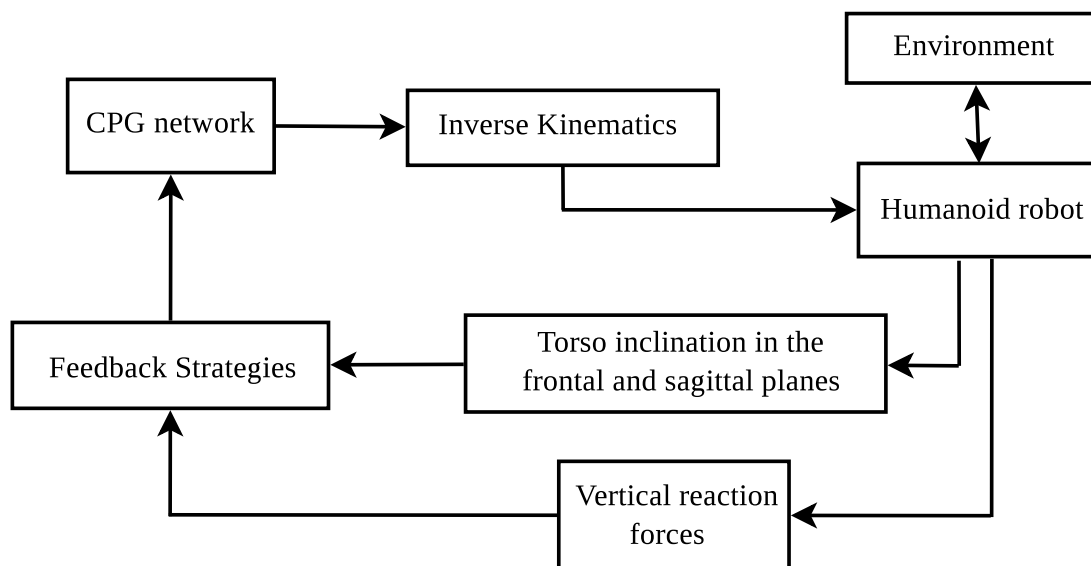
Figure 2.4: CPG-task-space control

the use of CPG-based control systems to generate closed-loop locomotion patterns for biped robots.

2.2.2.1   CPG-task-space control methods

Figure 2.4 presents the block diagram for a CPG-task-space control scheme. The signals generated by the CPG network are modulated through the feedback signals obtained by analysing the current sensory information provided by the robot's sensors. The aim is to control the limb trajectories in the Cartesian space. Therefore, the angular position of the robot's joints must be calculated by solving the inverse kinematics problem. Some of the studies in the literature on the locomotion control of biped robots in the CPG-task-space are presented below.

A CPG network that generates the stepping and propulsive motion for locomotion control of a biped robot was proposed in (Endo et al., 2008). The feedback pathways for propulsive motion were obtained through a gradient method, by using the pelvis angular velocity in the sagittal and coronal planes as inputs to generate a feedback signal that controls the trajectory of the legs in the direction of walking. Results on flat terrain were reported. Alternatively, a control system that generates the motion of a biped robot in the task-space by using nonlinear oscillators was presented in (Aoi and Tsuchiya, 2005). These movements are modulated by means of the signals
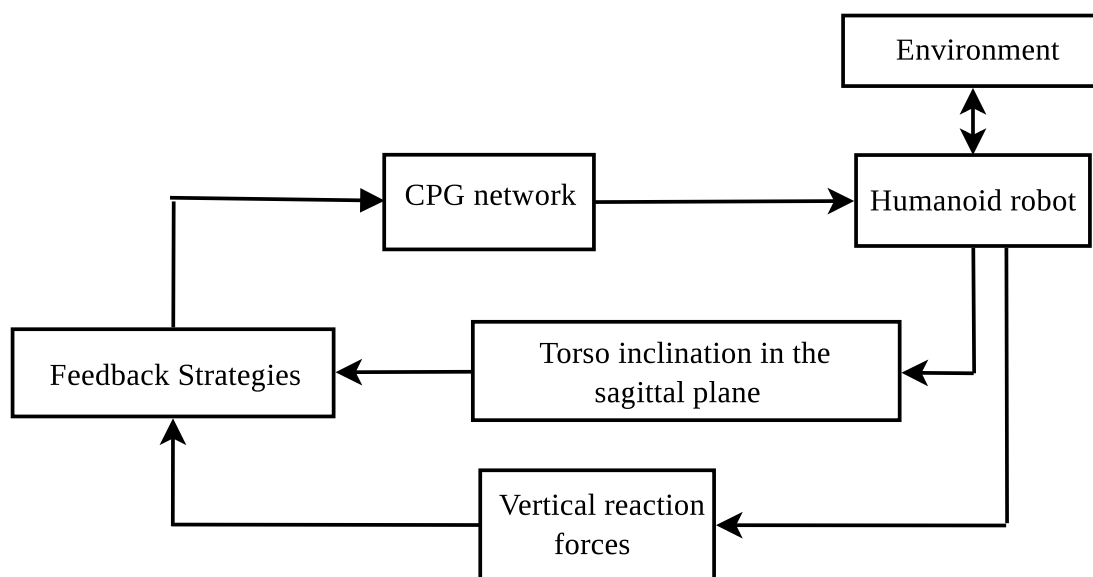
Figure 2.5: CPG-joint-space control

provided by touch sensors. Later, in (Aoi and Tsuchiya, 2007), the same authors extended their previous work to controlling the turning behaviour of the biped robot.

A pattern generator based on coupled oscillators is used in (Ha et al., 2011). The system is compensated directly with the data provided by the inertial sensors without real-time estimation of the current ZMP. In (Liu et al., 2013b), a CPG network is used to describe and modulate the trajectory of the robot's centre of gravity and, as a result, the trajectories of its limbs in the workspace. Experiments show that the robot can walk on both flat and inclined terrain with slopes of +/-10 degrees.

To generate stable static walking, Song and Hsieh (2014) proposed a pattern generator system for biped locomotion based on CPG networks. The system compensates for the slope of terrain with the pose of the upper-body's centre of gravity. The authors claim that the robot can walk on flat and inclined terrain with slopes of +/-7 degrees.

2.2.2.2 CPG-joint-space control methods

Figure 2.5 shows the block diagram of a CPG-joint-space control scheme. The signals generated by the CPG network are modulated through feedback signals obtained by analysing the current sensory information provided by the robot's sensors. The

system aims at controlling the angular position of the robot's joints directly with the output signals of the network. Some of the studies proposed in the literature for the locomotion control of biped robots in the CPG-joint-space are summarized below.

A CPG implemented with coupled nonlinear oscillators was proposed in (Righetti and Ijspeert, 2006) to control the biped locomotion of a humanoid robot. The system learns an arbitrary signal in a supervised framework. It modulates some parameters and introduces feedback signals provided by the robot's sensors. However, locomotion patterns must be defined in advance. In (Morimoto et al., 2008), the signals for the robot's joints are generated by using coupled oscillator models based on sensory information about the location of the centre of pressure and its velocity. Results on flat terrain were reported.

In turn, (Matos and Santos, 2012) proposed a feedback mechanism for phase regulation using load sensory information. The signals for the motors are specified in the joint-space through mathematical formulations that define the angular displacement, and the parameters that characterize the system's behaviour are hand-tuned. Subsequently, (Oliveira et al., 2013) proposed a multi-objective staged evolutionary algorithm to find the parameters that characterize the open-loop behaviour of the system. However, because the genetic algorithm used a reduced number of individuals and a hand-tuned gait was included as an individual in a random initial population, thus biasing the final convergence, there is no guarantee that the algorithm ends up exploring the whole search space or that it finds all the feasible solutions. The control system was tested on flat and sloped terrain with a maximum ascending slope of 4 degrees and a maximum descending slope of 2.5 degrees.

(Nassour et al., 2013) proposed a control scheme for qualitative adaptive reward learning with success failure maps applied to humanoid robot walking. However, their technique does not ensure stable interaction with the floor, since the robot tends to drag its feet when walking, which is likely to lead to falls on uneven terrain. The authors present results with the NAO walking on slopes of +/-10 degrees.

Table 2.1 summarizes the most representative closed-loop control schemes for

locomotion control of biped robots that have been successfully tested on small-size humanoid robots. All these approaches have been inspired by biological CPG networks.

2.2.2.3 Estimation of CPG network parameters through genetic algorithms

Genetic Algorithms have been used to determine the best combination of parameters that characterize the behaviour of CPG networks and to find the optimal set of parameters for the control system of various types of robots.

These algorithms are inspired by the mechanism of natural selection and natural genetics observed in nature. They use three basic operators to find the individuals with the highest fitness value according to the fitness function defined. These operators are: selection, crossover and mutation (Passino, 2004). In order to determine the best combination of parameters it is important that the fitness function used in the genetic algorithm assesses, sorts and classifies the individuals in each epoch in order to guarantee correct evolution over time.

In (Inada and Ishii, 2003), a five-step genetic algorithm is proposed for determining the optimal 271 parameters for a system for generating motion that uses a CPG network that describes an optimal locomotion pattern for a biped robot. (Kamimura et al., 2005) proposes a genetic algorithm to determine the optimal interconnection weights and the initial values for the variables of the CPG networks used to control the straight-line locomotion of a modular robotic system. In order to determine the system parameters for controlling the locomotion of a quadruped robot a genetic algorithm is used in (Liu et al., 2013a). The algorithm finds the weight of the interconnections between oscillators to generate appropriate phase relationships and realize the animal-like walking pattern. A bio-inspired system for controlling the locomotion of a biped robot based on Central Pattern Generators (CPGs) is proposed in (Oliveira et al., 2013). A multi-objective evolutionary algorithm is used to search for the best set of optimized CPG parameters through multiple objectives according to a staged evolution.

Table 2.1: CPG-based locomotion control systems tested on small size humanoid robots

Authors	Pattern generator	Feedback strategies	Tested terrain	Employed robot	Year
S. Aoi Aoi and Tsuchiya (2005)	Coupled oscillators (task space)	Phase resetting through the impact instant	Flat terrain	HOAP-1	2005
J. Morimoto Morimoto et al. (2008)	Coupled oscillators (joint space)	CoM used for modulation of phase resetting	Flat terrain Maximum obstacle height of 3.5mm	Qrio	2008
H. Inyong Ha et al. (2011)	Coupled oscillators (task space)	Balance controller through torque compensation	Flat terrain	Darwin	2011
V. Matos Matos and Santos (2012)	Coupled oscillators (joint space)	Phase regulation	Flat terrain Maximum ascending slope of 4 degrees Maximum descending slope of 2.5 degrees	Darwin	2012
C. Liu Liu et al. (2013b)	CPG-task space control (task space)	Modulation of the CoM trajectory	Flat terrain Maximum ascending slope of 10 degrees Maximum descending slope of 10 degrees	Nao	2013
J. Nassour Nassour et al. (2013)	Neurobiological-inspired learning algorithm (joint space)	Inertial sensor used to adjust the centre of oscillation of ankle joints	Flat terrain Maximum ascending slope of 10 degrees Maximum descending slope of 10 degrees	Nao	2013
K. Song Song and Hsieh (2014)	CPG-task space control (task space)	Posture controller	Flat terrain Maximum ascending slope of 7 degrees Maximum descending slope of 7 degrees	Nao	2014
Proposed approach Cristiano et al. (2015b)	CPG-joint space control (joint space)	Posture controller Stepping controller Stride length controller	Flat terrain Maximum ascending slope of 10 degrees Maximum descending slope of 10 degrees	Nao	2015

2.3 Central pattern generators

Central pattern generators are biological neural networks that can control coordinated movements, such as those involved in locomotion, respiration, chewing or swallowing. CPGs are able to generate rhythmical signals without any external sensory input, since they oscillate depending on the value of internal parameters and the interconnection weights between neurons. One of the most attractive features of CPGs is their ability to adapt the oscillations generated to external conditions by modulating the oscillatory parameters (i.e., frequency, amplitude, phase) from external feedback signals provided by a sensory subsystem. These features make the networks suitable for controlling the locomotion of humanoid robots.

2.3.1 Introduction

Advances in neuroscience have revealed the biological functioning of the locomotor system in humans and animals. This is an area in which neuroscience and robotics can complement each other. A wide variety of biologically-inspired control architectures have been studied in recent decades for closed-loop motion control of mobile robots, and most of them mimic the functionality of CPGs (Ijspeert, 2008; Yu et al., 2014). CPG-based models have interesting properties and may be an alternative to the classical methods proposed in the literature for controlling locomotion in robots (i.e., ZMP-based control, finite-state machines). CPG networks have been used to successfully control several types of robots (i.e., legged robots (Kimura et al., 2007), snake-like robots (Crespi and Ijspeert, 2008), salamander-like robots (Bicanski et al., 2013), reconfigurable robots (Kamimura et al., 2005), etc.). Some of the most important properties of CPGs are listed below:

- CPG models produce stable rhythmic patterns with stable limit cycles.
- The system based on CPG networks can be characterized by a reduced number of parameters which enable the system to generate multidimensional output signals with simple control signals.
- CPG models can be used to adapt the shape of the output signals generated by

modulating their parameters from feedback signals provided by the sensors so that the system's current state can be changed and synchronized in accordance with the real-time sensory information.

- Control systems based on CPG networks can use optimization (e.g., genetic algorithms) and learning algorithms (e.g., policy gradient method).

However, a global design methodology for developing CPG-based control systems has not been defined to get an optimal control system. The list below provides some important tips for designing a CPG-based control system:

- Determine the general architecture of the CPG-based control system by defining how the CPG network is going to be used inside the control loop.
- Design the CPG network topology and define the number of neurons. The topology depends on the number of outputs and the waveforms required by the system.
- Study how modulating the input signals and/or varying the CPG's internal parameters affects the CPG's output signals. The goal is to introduce feedback signals that can quickly adapt the activity of the CPG network to the real-time sensory information. It is very important to incorporate useful and well-characterized feedback controllers.

Many mathematical models have been proposed to model the neuron's dynamic response and build a CPG network of interconnected neurons. For instance, networks based on phase oscillators defined by systems of equations, which represent the phase behaviour, are used to directly control the phase of output signals by advancing or delaying their value (Aoi and Tsuchiya, 2007; Matos and Santos, 2012; Endo et al., 2004).

In this thesis a well-known neuron model proposed by Matsuoka (1985, 1987) is used to build the CPG networks. This model has been used in several studies because of its interesting properties (Taga et al., 1991; Park et al., 2010; Liu et al., 2011; Kimura et al., 2007; Huang et al., 2008; Kamimura et al., 2005; Endo et al., 2005, 2008; Zhang et al., 2011). Furthermore, Matsuoka's model makes the hardware implementation of these networks more straightforward (Nakada et al., 2005; Nakada

and Matsuoka, 2012). In CPG networks based on Matsuoka's model the oscillations are generated by the mutual inhibition of neurons which are represented by a continuous time variable model with a kind of fatigue or adaptation effect (see below).

2.3.2 Matsuoka's oscillator

The simplest CPG model proposed by Matsuoka (1985, 1987, 2011) is a non-linear oscillator that has widely been applied to robotic systems because it is at once simple and effective. It consists of two tonically excited neurons with a self-inhibitory effect, which are reciprocally linked via inhibitory connections. The block diagram of Matsuoka's oscillator can be seen in fig. 2.6 and its simplified representation in fig. 2.7. The system of equations that characterizes the behaviour of each neuron enables the amplitude, shape and frequency of the output signals generated to be controlled. Matsuoka's neuron model is used to build a neural network of N interconnected neurons, with the i-th neuron being defined by two differential equations with two state variables, u_i, v_i, and a single output, y_i:

$$\tau \dot{u}_i = -u_i - \sum_{j=1}^{N} w_{ij} y_j - \beta v_i + u_e + f_i \tag{2.3}$$
$$\tau' \dot{v}_i = -v_i + y_i$$
$$y_i = \max(0, u_i).$$

The amplitude of the neuron's output signal can be controlled through the external input u_e. The frequency of the output signals is determined by the values of τ, τ', w_{ij} and β. Term f_i is a feedback variable that can be used to control the output amplitude and synchronize the output signals with a periodic input signal by using the entrainment property of CPGs. In this way, this feedback variable adapts the behaviour of the neuron to external sensory stimuli. A detailed explanation of the entrainment property can be found in (Williamson, 1999). The weighting coefficients w_{ij} represent the bidirectional connection weights between the i-th and j-th neurons. These weights determine the phase difference between the output
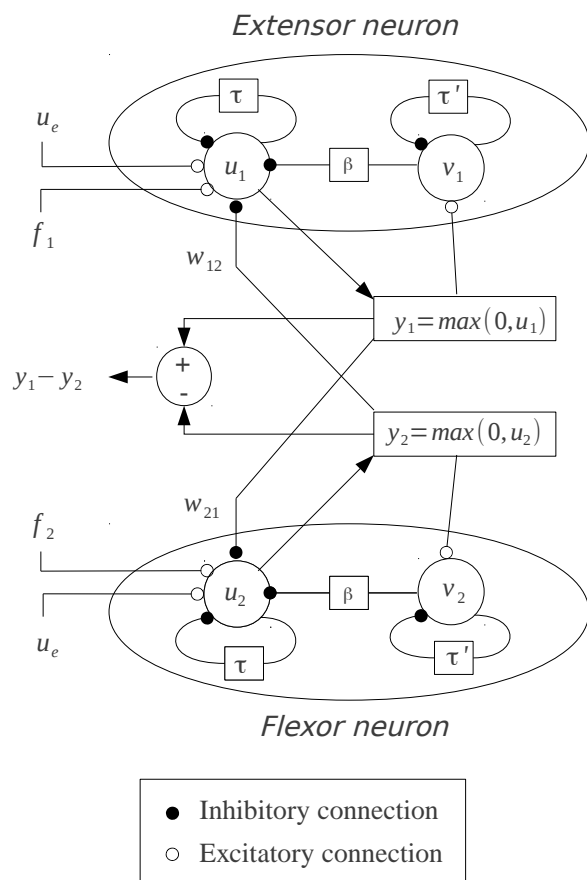
Figure 2.6: Schematic representation of Matsuoka's non-linear oscillator

signals of the interconnected neurons. All neurons within the network oscillate synchronously according to their internal parameters and network connections, converging to specific patterns and limit cycles. All constant parameters must satisfy certain constraints if oscillations are to be stable (Matsuoka, 1985, 2011).

In order to modulate the frequency of the output signal, Zhang et al. (2011) introduced an additional parameter, K_f, such that the time constants in (2.3) are reformulated as:

$$\tau = \tau_o K_f \qquad\qquad \tau' = \tau'_o K_f, \qquad\qquad (2.4)$$

where τ_o and τ'_o are the original time constants.

For Matsuoka's oscillator, after the mathematical expression of angular velocity presented in (Matsuoka, 2011) is reorganized and (2.4) included, the frequency of

Table 2.2: Internal parameters of Matsuoka's neurons

Parameter	Value	Parameter	Value
τ_o	0.2800	u_e	0.4111
τ_o'	0.4977	f_i	0
β	2.5000		

Table 2.3: Interconnection weights of Matsuoka's oscillator

$w_{1,2}$	2
$w_{2,1}$	2
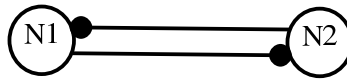
Figure 2.7: Simplified topology of 2-neuron Matsuoka's CPG (Matsuoka's oscillator)

the output signal can be expressed as:

$$\Gamma(K_f) \approx \frac{1}{2\pi K_f}\sqrt{\frac{1+\left(\frac{\beta}{w}-1\right)\left(\frac{\tau_o}{\tau_o'}+1\right)}{\tau_o\tau_o'}}. \qquad (2.5)$$

As is demonstrated in (Matsuoka, 2011), an oscillator generates a stable oscillation if the condition below is fulfilled:

$$1+\frac{\tau}{\tau'} \; < w \; < 1+\beta. \qquad (2.6)$$

The output signals generated by Matsuoka's oscillator with the parameters in tables 2.2 and 2.3 are shown in fig. 2.8. These parameters and weights were experimentally chosen in this thesis to yield output signals that resembled as closely as possible a sinusoidal wave. The value used for variable K_f was 0.7. In this case, there is no modulation of the oscillator's internal parameters. Figures 2.9 and 2.10 show examples of output signals obtained by varying the oscillator's internal parameters u_e and K_f, respectively. In fig. 2.9, the value used for variable K_f was 0.2. As can be seen, the modulation of these parameters affects the oscillator' output
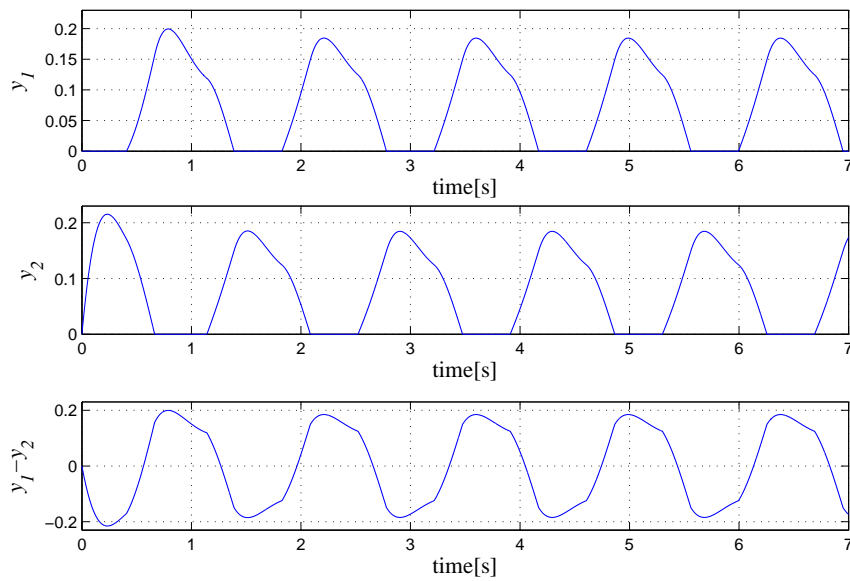
Figure 2.8: Output signals of Matsuoka's oscillator
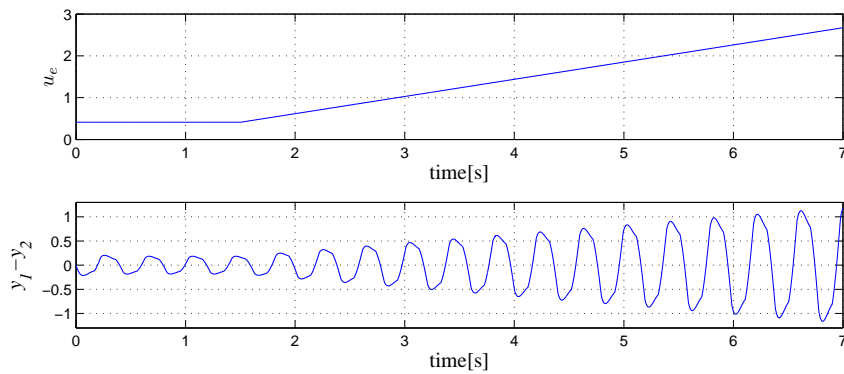
Figure 2.9: Example of amplitude modulation by varying parameter u_e

signals and gives a quick system response. As a result, the amplitude and frequency
of the output signals generated adapt quickly. There is no suitable control strategy
for specifying the phase of the output signals in real time. Therefore, in chapter 4 a
control mechanism is proposed and validated for modifying the phase of the output
signals generated by Matsuoka's oscillator or networks based on Matsuoka's neuron
model described with (2.3).
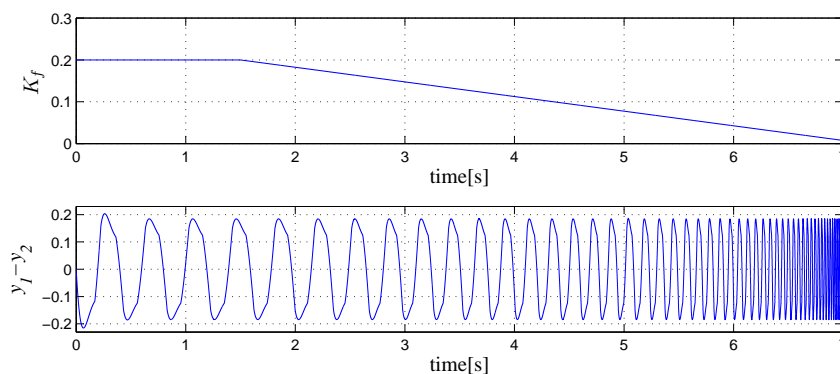
Figure 2.10: Example of frequency modulation by varying parameter K_f

2.3.3 CPG networks based on Matsuoka's neuron model

This section presents some examples of oscillations generated by CPG networks based on Matsuoka's neuron model. Figures 2.11, 2.13 and 2.15 show CPG network topologies proposed by Matsuoka and figs. 2.12, 2.14 and 2.16, respectively, show their corresponding output signals. The connection weights are shown in tables 2.4, 2.5 and 2.6. These weights were experimentally chosen in this thesis to yield output signals that resembled as closely as possible a sinusoidal wave. The output signals shown in these figures show the stable rhythmic patterns generated by each neuron. This feature makes these networks useful for control applications that require rhythmical signal within their control scheme.

Some of the CPG networks proposed by Matsuoka have been widely used in mobile robotics and other control applications because they are simple and effective (e.g., Endo et al., 2005, 2008; Zhang et al., 2011; Xu et al., 2009). Other topologies of CPG networks based on Matsuoka's neuron model have also been proposed for the locomotion control of mobile robots (e.g., Taga et al., 1991; Park et al., 2010; Liu et al., 2011; Kimura et al., 2007; Huang et al., 2008; Kamimura et al., 2005; Cristiano et al., 2013).

For instance, Kimura et al. (2007) proposed a system for the adaptive dynamic walking of a quadruped robot on natural ground by means of a control scheme based on a CPG network implemented with Matsuoka's neuron model. (Kamimura et al., 2005) report a unified framework for automatically designing an efficient locomotion
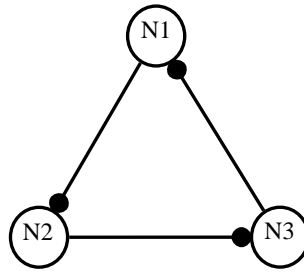
Figure 2.11: CPG network of 3 neurons as proposed in (Matsuoka, 1985)

controller that uses CPG networks based on Matsuoka's neuron model which is suitable for all modular robots.

Table 2.4: Interconnection weights of Matsuoka's 3-neuron CPG shown in fig. 2.11

$w_{1,1}$	0.0	$w_{1,2}$	0.0	$w_{1,3}$	2.5
$w_{2,1}$	2.5	$w_{2,2}$	0.0	$w_{2,3}$	0.0
$w_{3,1}$	0.0	$w_{3,2}$	2.5	$w_{3,3}$	0.0

Table 2.5: Interconnection weights of Matsuoka's 4-neuron CPG shown in fig. 2.13

$w_{1,1}$	0.0	$w_{1,2}$	0.0	$w_{1,3}$	0.0	$w_{1,4}$	2.5
$w_{2,1}$	2.5	$w_{2,2}$	0.0	$w_{2,3}$	0.0	$w_{2,4}$	0.0
$w_{3,1}$	0.0	$w_{3,2}$	2.5	$w_{3,3}$	0.0	$w_{3,4}$	0.0
$w_{4,1}$	0.0	$w_{4,2}$	0.0	$w_{4,3}$	2.5	$w_{4,4}$	0.0

Table 2.6: Interconnection weights of Matsuoka's 4-neuron CPG shown in fig. 2.15

$w_{1,1}$	0.0	$w_{1,2}$	0.0	$w_{1,3}$	2.0	$w_{1,4}$	0.5
$w_{2,1}$	0.5	$w_{2,2}$	0.0	$w_{2,3}$	0.0	$w_{2,4}$	2.0
$w_{3,1}$	2.0	$w_{3,2}$	0.5	$w_{3,3}$	0.0	$w_{3,4}$	0.0
$w_{4,1}$	0.0	$w_{4,2}$	2.0	$w_{4,3}$	0.5	$w_{4,4}$	0.0
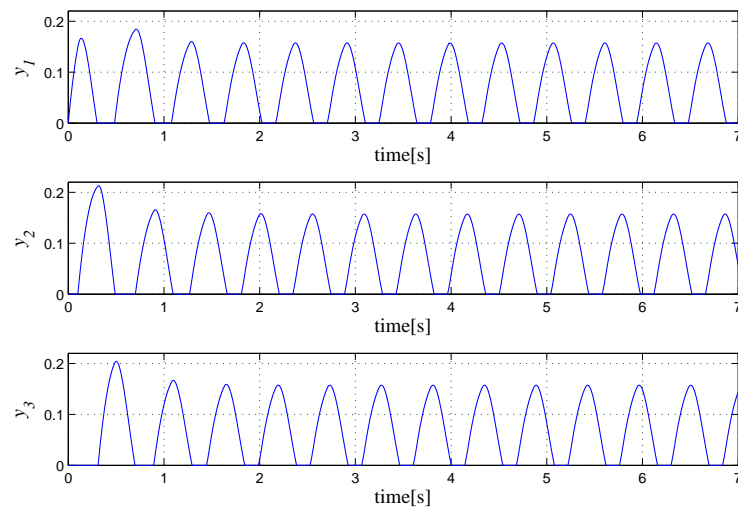
Figure 2.12: Output signals of the 3-neuron CPG shown in fig. 2.11
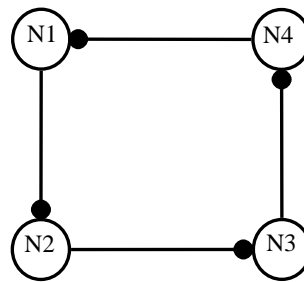
Figure 2.13: 4-neuron CPG network as proposed in (Matsuoka, 1985)
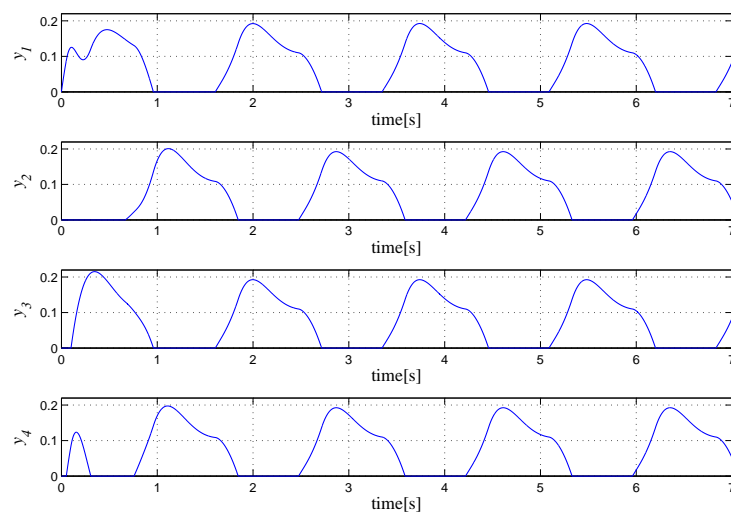
Figure 2.14: Output signals of 4-neuron CPG shown in fig. 2.13
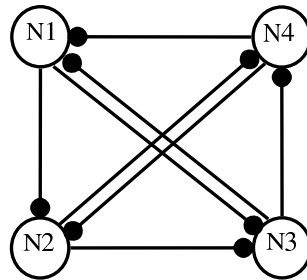
Figure 2.15: 4-neuron CPG network as proposed in (Matsuoka, 1985)
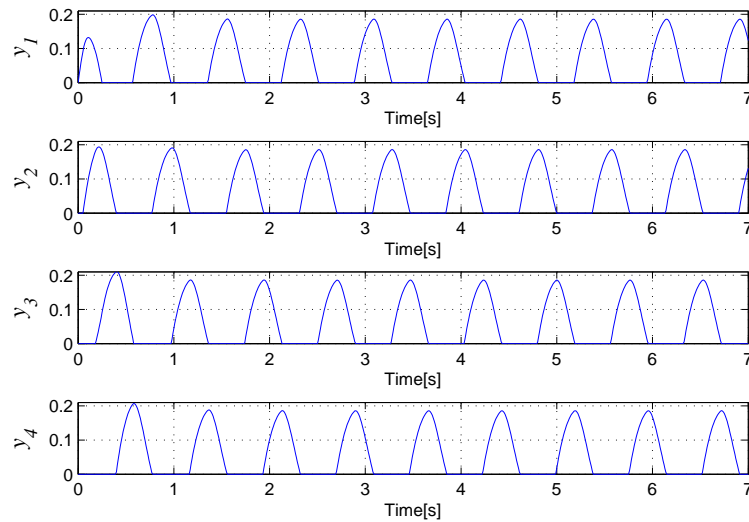
Figure 2.16: Output signals of the 4-neuron CPG shown in fig. 2.15

CHAPTER 3

Proposed systems for locomotion control of biped robots

In this chapter, two CPG-joint-space control schemes are proposed to control the locomotion of biped robots by using rhythmical signals generated by Central Pattern Generator (CPG) networks based on Matsuoka's neuron model. Previous approaches require a large number of parameters to characterize the generation and control of the locomotion pattern. Thus, the first control scheme proposed here was designed to have a reduced number of parameters and to be able to deal with obstacles on the walking surface.

The main features that a CPG-joint-space control system must have for the locomotion control of humanoid robots have also been identified. The system must generate a well-characterized locomotion pattern that can easily be modulated by the feedback signals provided by the robot's sensors and that guarantees a correct

interaction between the robot's feet soles and the floor. Genetic algorithms are used in this research to determine the combination of CPG network parameters that is best for generating optimal locomotion patterns for a defined fitness function. The systems proposed for the locomotion control of biped robots were tested by simulation and with a real humanoid robot.

The second control scheme proposed in this chapter was designed using the results obtained with the first control scheme. The aim was to define a system that generates well-characterized and optimal locomotion patterns that can be easily modulated and which guarantee correct interaction between the soles of the robot's feet and the floor. This has been identified as the main drawback of CPG-joint-space based control schemes because the signal generation process of the locomotion pattern is not easy to understand and the integration of new feedback signals to deal with complex situations is cumbersome. Also, the interaction between the soles of the robot's feet and the floor is not good enough, which limits the practical application of these approaches. Therefore, the locomotion pattern needs to interact properly with the floor, so that the system can control the real-time locomotion pattern described by the robot and cope with more complex situations.

Similar CPG-based systems for locomotion control of biped robots tested on sloped surfaces have previously been proposed in the literature. However, the most robust of those previous approaches need to solve the costly inverse kinematics (Liu et al., 2013b; Song and Hsieh, 2014), whereas the other approaches do not guarantee stable interaction with the floor, since the robot tends to drag its feet when walking, which is very likely to lead to falls on uneven terrain (Nassour et al., 2013). The results show that the proposed system, like the state-of-the-art for CPG-based control systems, can negotiate sloped surfaces (see table 2.1) and also generate well-characterized omnidirectional locomotion patterns that guarantee correct interaction with the floor.

Since the proposed control scheme is well-characterized, it can be incrementally improved by adding more controllers that allow the robot to deal with more complex situations. Also, the proposed approaches directly operate in the joint space, which

guarantees the system's quick response and also makes it especially suitable for direct hardware implementation with electronic circuits.

3.1 Introduction

The systems that control the locomotion of biped robots must naturally integrate three fundamental aspects: the robot's body, the environment and the control system. Such a control system basically consists of two main stages. The first stage generates the locomotion pattern, whereas the second introduces feedback into the system in order to modulate the current locomotion pattern so that stability can be recovered whenever unexpected situations appear as the robot is walking.

3.1.1 NAO humanoid robot

The proposed control schemes were validated in a NAO humanoid robot (Gouaillier et al., 2009, 2010). However, these can be easily adapted to other biped robots with a similar kinematic structure of joints after making the corresponding changes (robot model, limits for the genetic algorithm search space, etc.). NAO is a small-size humanoid 56 cm tall and weighing 4.8 kg. It has 21 degrees of freedom (1 for the pelvis, 5 for each leg, 2 for the head and 4 for each arm) (see fig. 3.1). It is also equipped with two cameras, an inertial measuring unit (2-axis gyrometer with 5% precision with an angular speed of 500°/s and 3-axis accelerometer with 1% precision with an acceleration of 2g), four sonars and four force sensors under each foot. The force sensors measure the change in resistance depending on the pressure applied and have a working range from 0 N to 25 N. These force sensors and their position are used to determine the CoP location (see section 2.1).

The motion of the robot's joints is performed through a joint position control-loop. Magnetic rotary encoders (MRE) are used to estimate the motors' angular position. The motors used in the NAO are Maxon coreless brush DC motors. There are two classes, with their respective reduction gears, which are driven by microcontrollers that use an algorithm similar to a PID controller to control the

joint position.

3.1.2 Robotics simulator

Nowadays, researchers can use powerful mobile robot simulators to test algorithms with a particular system before transferring them to real robots. The robot simulations in this study were performed with Webots (Michel, 2004), a commercial dynamic simulator that includes the physical models of various real robots, including the NAO humanoid robot and can simulate the dynamic interaction between robots and the simulated environment.

Several controllers were used in the simulation stage. One controller was implemented to generate and control the locomotion pattern of the simulated robot by using the proposed control schemes. This controller implemented the whole system for locomotion control: the CPG network, the motion controllers, the feedback controllers, etc. These systems will be described in detail in the sections below. A second controller was used to modify the simulated scenario by adding obstacles or by changing the friction coefficient, etc. A third controller was used to provide more detailed information about the physical variables and also to add external forces to particular locations within the robot's kinematic structure. Finally, a useful controller called the supervisor controlled the whole simulation environment by restarting the simulation or the diverse controllers separately when necessary and by controlling all the objects within the simulated scenario. The supervisor controller works as a master controller by executing the other controllers when necessary and therefore it was used to implement the GA. These controllers were implemented in C, C++ or Matlab.

The results obtained in the simulation stage were subsequently tested in the real robot. The control systems used for the real robot were implemented using the robot's SDK. The SDK is called NaoQi, which is also the name of the main software that runs on the robot and controls it. This framework was used to program NAO with the language C++. The algorithms implemented can also be tested in simulation by using Webots and with the real robot. The same code can be used if
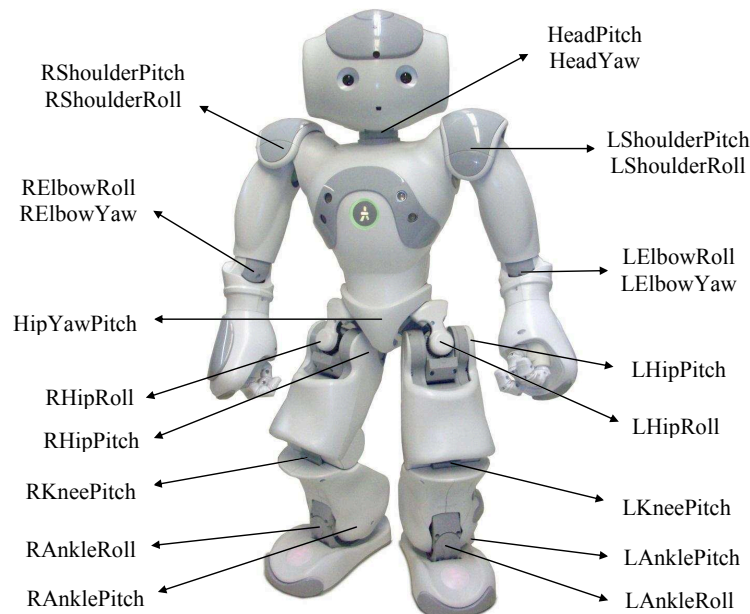
Figure 3.1: NAO humanoid robot
.

it is compiled for the corresponding platform.

3.2   First control scheme

This section presents a locomotion control system for biped robots that uses a network of Central Pattern Generators (CPGs) implemented with Matsuoka's oscillators. The behaviour of the system is controlled through a few parameters that are able to yield rhythmical signals. A network topology is proposed for controlling the generation of trajectories for a biped robot in the joint space in both the sagittal and coronal planes. The feedback signals are directly fed into the network to control the robot's pose and reset the phase of the locomotion pattern in order to prevent the robot from falling down whenever a risk situation arises. A Genetic Algorithm is used to find the optimal parameters for the system in open-loop. The system's behaviour in closed-loop was studied and analysed through extensive simulations. Finally, a real NAO humanoid robot was used to validate the control scheme proposed.
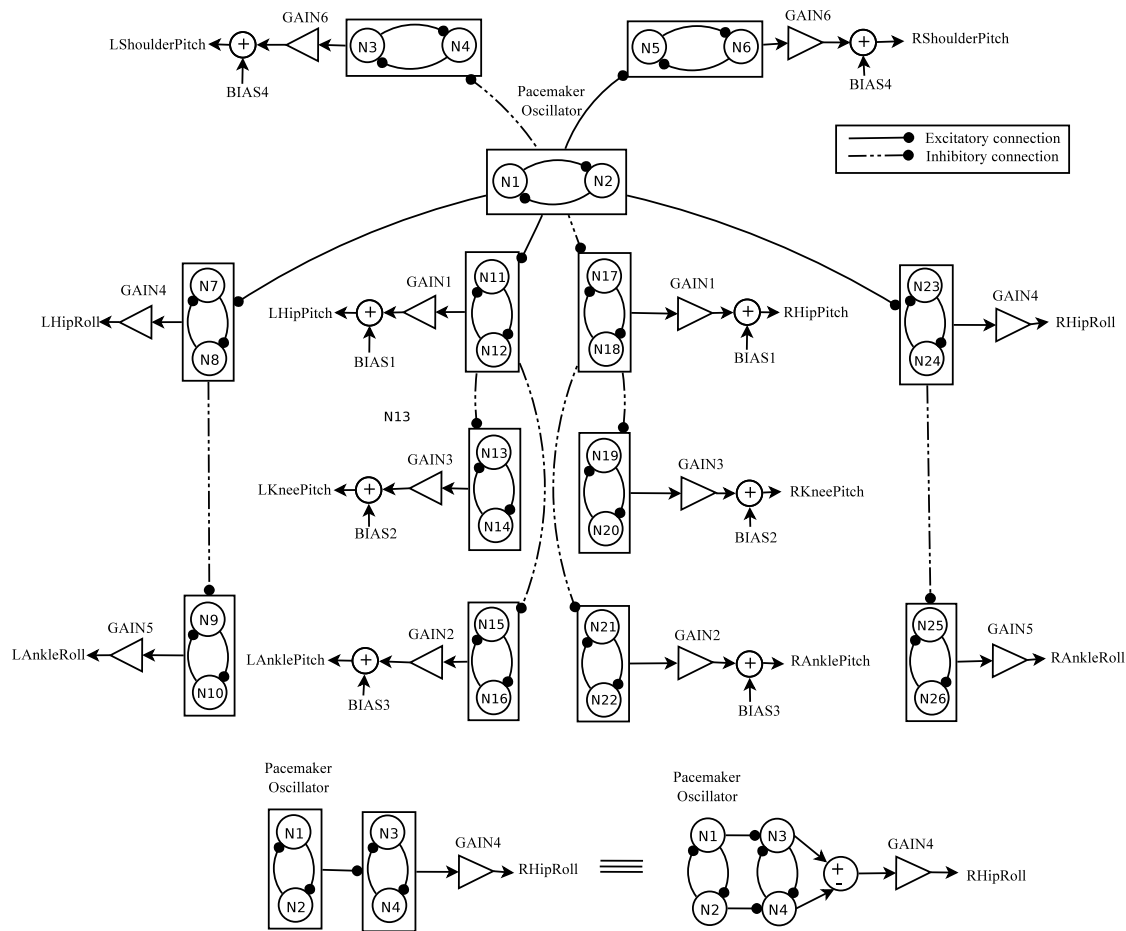
Figure 3.2: Proposed topology for the CPG network
.

3.2.1   CPG network topology

The proposed biped motion controller is based on a CPG network. Its goal is to generate the signals for the angular displacement of each of the robot's joints in order to describe a valid locomotion pattern. The combination of parameters of the proposed network was found by applying a genetic algorithm to evaluate the locomotion performance through dynamic simulations. The proposed CPG network was modelled by means of a set of interconnected non-linear oscillators previously proposed by Matsuoka. Table 2.2 shows the internal values used for each neuron and table 3.1 shows the corresponding connection weights used in the CPG network.

The main goal of the proposed CPG network is to generate stable locomotion patterns with stable limit cycles for controlling the motion of the humanoid robot.

Table 3.1: CPGs' interconnection weights

$w_{1,2}$	2.2829	$w_{2,1}$	2.2829	$w_{3,4}$	2.2829	$w_{4,3}$	2.2829	$w_{5,6}$	2.2829
$w_{6,5}$	2.2829	$w_{7,8}$	2.2829	$w_{8,7}$	2.2829	$w_{9,10}$	2.2829	$w_{10,9}$	2.2829
$w_{11,12}$	2.2829	$w_{12,11}$	2.2829	$w_{13,14}$	2.2829	$w_{14,13}$	2.2829	$w_{15,16}$	2.2829
$w_{16,15}$	2.2829	$w_{17,18}$	2.2829	$w_{18,17}$	2.2829	$w_{19,20}$	2.2829	$w_{20,19}$	2.2829
$w_{21,22}$	2.2829	$w_{22,21}$	2.2829	$w_{23,24}$	2.2829	$w_{24,23}$	2.2829	$w_{25,26}$	2.2829
$w_{26,25}$	2.2829	$w_{3,1}$	-1	$w_{4,2}$	-1	$w_{5,1}$	1	$w_{6,2}$	1
$w_{7,1}$	1	$w_{8,2}$	1	$w_{9,7}$	-1	$w_{10,8}$	-1	$w_{23,1}$	1
$w_{24,2}$	1	$w_{25,23}$	-1	$w_{26,24}$	-1	$w_{11,1}$	1	$w_{12,2}$	1
$w_{13,11}$	-1	$w_{14,12}$	-1	$w_{15,11}$	-1	$w_{16,12}$	-1	$w_{17,1}$	-1
$w_{18,2}$	-1	$w_{19,17}$	-1	$w_{20,18}$	-1	$w_{21,17}$	-1	$w_{22,18}$	-1

This network generates the motion of the robot's arms and synchronizes them with the motion of its legs in order to yield a more stable walking pattern. The proposed CPG network follows a master-slave topology, in which a central non-linear oscillator is used to drive the joints of the robot through slave oscillators associated with each of them.

The central oscillator is known as a pacemaker oscillator, since it generates the first electrical impulse or master signal that is propagated across the other oscillators in the various chains of the robot (left arm in the sagittal plane, right arm in the sagittal plane, left leg in the sagittal and coronal planes and right leg in the sagittal and coronal planes). The concept of pacemaker oscillator was introduced in (Aoi and Tsuchiya, 2005). However, they did not utilize it to directly control the angular displacement of joints with the CPG outputs. If the pacemaker oscillator does not have an input or feedback signal, its oscillations depend exclusively on its internal parameters.

The proposed CPG network has been designed to imitate the human gait, which has the following features:

1. The arms' motion in the sagittal plane is in anti-phase.
2. The legs' motion in the sagittal plane is in anti-phase.
3. The two motions mentioned above are in anti-phase: that is, the motion of the right arm is synchronized with the motion of the left leg, whereas the motion

of the left arm is synchronized with the motion of the right leg.

4. The coronal motion of legs is synchronized with the sagittal motion of legs in order to generate the periodic motion by changing the location of the centre of masses.

The large number of parameters is one of the main drawbacks when working with large CPG networks. In order to minimize this problem, all oscillators were configured with the same parameters presented in table 2.2. The parameters of the CPG network shown in fig. 3.2, which characterize the locomotion pattern of a biped robot are: seven gains (K_f, GAIN1 ,GAIN2, GAIN3, GAIN4, GAIN5, GAIN6) and four offsets (BIAS1, BIAS2, BIAS3, BIAS4). Parameter K_f can be used to change the walking speed, since it controls the frequency of the locomotion pattern, thus providing extra control on the robot's velocity (see section 2.3.2). This is an important feature, since the locomotion pattern's frequency can be modulated with a single parameter.

3.2.2 Automatic estimation of CPG network parameters

Evolutionary algorithms are typically used to solve high-dimensional optimization problems. These algorithms have proven to be a good way of finding the parameters associated with CPG networks. The genetic algorithm (GA) proposed in (Passino, 2004) was applied off-line to calculate the CPG network parameters with the objective of describing an optimal locomotion pattern in a straight line. Each individual of the genetic algorithm represents a different combination of parameters for the proposed CPG network. In particular, each individual is modeled by a chromosome with 11 traits that represent the combination of parameters of the CPG network (see fig. 3.3).

The genetic algorithm was initialized with a randomly selected initial population of 200 individuals. This number was heuristically set after a large number of simulations. The locomotion pattern associated with every individual was evaluated for 16 seconds using a dynamic simulator and a 3D synthetic model of the robot. The robot was allowed to walk a significant distance so that its fitness value could
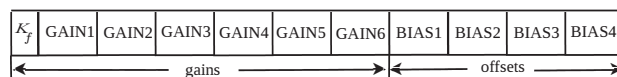
Figure 3.3: Chromosome structure

be calculated. If the robot fell down or oscillated considerably during the evaluation period, the fitness value was set to zero. Otherwise, its fitness value was calculated as follows. The individual with the best fitness score proceeded to the next generation. The other individuals were chosen by the roulette wheel selection rule. In particular, each individual was given a probability of being selected that was proportional to its fitness value. This rule made it possible to select individuals with a low score, thus preventing fast convergence of the genetic algorithm to a local maximum. The individual with the best fitness score and the individuals selected from the current generation constituted a mating pool. Crossover and mutation procedures were then applied in order to obtain the individuals of the next generation. The simulation stopped when a maximum number of generations was reached or the variation of the fitness function was lower than a given threshold ϵ ($\epsilon = 0.01$).

The fitness function used for sorting the individuals in each generation was formulated as (3.1), where vel represents the average straight line velocity, dev is the lateral deviation distance with respect to the straight line, α and γ are weighting coefficients.

$$f = \alpha(vel) - \gamma(dev) \tag{3.1}$$

3.2.3 Feedback strategies

This section presents some automatic feedback strategies implemented in the proposed CPG network to modulate the locomotion patterns obtained with the methodology explained above. This modulation was performed by analysing the feedback signals in order to compensate for internal mismatches or external perturbations. It exploits the ability of the CPGs to adapt their behaviour through external feedback variables introduced in the CPG model. The feedback strategies

are introduced into the system as explained below.

Phase resetting controller

Whenever a humanoid robot walks on flat terrain, it interacts with the floor through the soles of its feet. If the robot is walking at a constant speed on flat terrain, the elapsed times between the transition from the left to the right foot and from the right to the left foot should be approximately equal. This indicates that the walking pattern is symmetric and the robot is correctly interacting with the floor.

However, if the robot is walking on irregular terrain, the interaction times with the floor can be modified. For instance, if the robot steps on an obstacle or if it experiences an external perturbation, the interaction time could be longer or shorter for one or both interaction times. The information extracted from these time measures is used to synchronize the interaction between the feet and the floor by means of phase resetting. It aims to synchronize the pattern generation with the current interaction between the robot and the environment.

As explained above, the model proposed by Matsuoka for the non-linear oscillator was used in this thesis. To our knowledge, the phase resetting of the oscillator's output has not been implemented in Matsuoka's oscillator to control biped locomotion. In the study presented in (Nakada et al., 2011) by the same author, some initial studies about the phase resetting behaviour in the oscillator are presented. Two phase response curves of the oscillator for slow and fast dynamics are presented. These curves show that the phase shift introduced in the oscillator output depends on the oscillator's internal parameters and also on the current phase of the output signal. These phase response curves have a non-linear behaviour. In order to control the phase resetting through the current interaction times between the robot and the floor, the required phase difference needs to be accurately imposed. The phase resetting cannot be easily controlled with the phase response curves, since it may be required at any moment during the gait cycle due to irregularities in the walking terrain or perturbations that can be applied to the robot.

Therefore, an alternative strategy for controlling the phase resetting is proposed:

the feedback signals of the original Matsuoka's oscillator model can be used to control the phase of the oscillator's output signal. This is done by controlling the current state of the oscillator variables through the feedback signals in order to reset the phase of the output signal. How this feedback is introduced into the oscillator model is described below.

The mathematical model of each oscillator has two feedback variables, f_1 and f_2 (see fig. 2.6). If these variables have a positive value, they can be used to control the oscillator's output amplitude in real-time. Otherwise, if they are negative and have specific values, the time during which the output signal is disabled can be controlled and then turned on again in order to impose the required phase for the output signal. If these variables are set to zero, there is no effect on the oscillator output.

The phase resetting mechanism is implemented in the pacemaker oscillator. The output signal imposed by the central oscillator is propagated along the slave oscillators in order to synchronize the interaction between the robot and the floor in real-time, and prevent the robot from falling down due to instability.

The exact moment of impact between the sole of each robot's foot and the floor is detected by analysing the signals provided by the force sensors located in the soles of the feet. These force measures are used to calculate the time that elapses between the change in the robot's support leg. If this time is longer or shorter than some fixed limits determined by the current walking frequency, the phase resetting mechanism is activated to synchronize the interaction between the robot's feet and the floor. The phase resetting mechanism implemented for the pacemaker oscillator is defined by (3.2) and described in fig 3.4. The zero phase for the pacemaker oscillator signal is defined as the point of transition of the pacemaker oscillator amplitude from a negative value to a positive value.

$$
\xi_0(\phi) = \begin{cases} -\phi + \frac{13\pi}{15} & 0 < \phi \leq \pi \\ \\ -\phi + \frac{28\pi}{15} & \pi < \phi \leq 2\pi \end{cases}
\tag{3.2}
$$
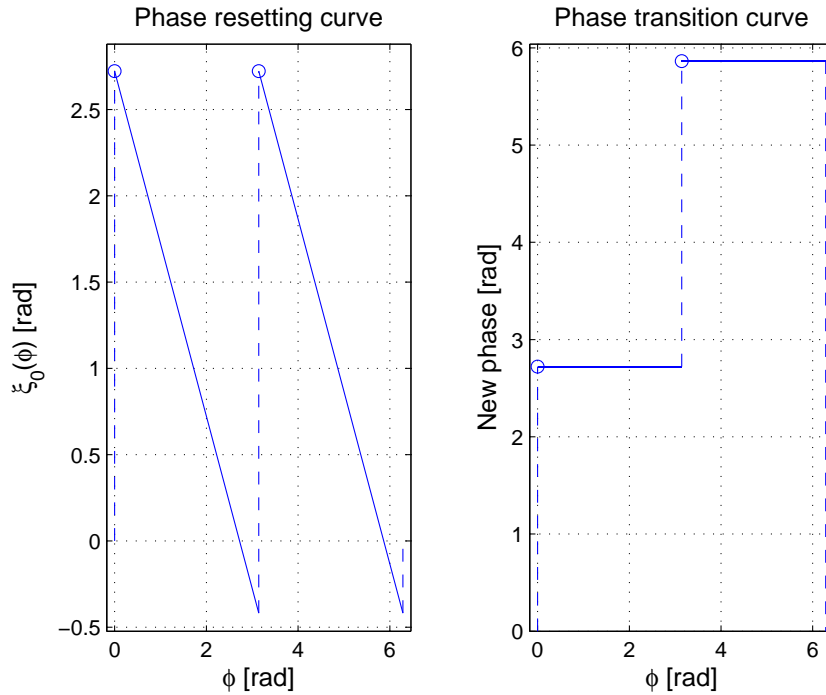
Figure 3.4: Phase resetting

Pose controller

In a bipedal gait, the robot's trunk pose during motion must be controlled since it has a higher concentration of mass and, therefore, plays an important role in the robot's stability. A feedback strategy is used to control the robot's pose by controlling the pose in the sagittal plane. In order to maintain the robot's trunk in a correct pose, parameter BIAS1 for controlling the pitch angle of the trunk is modified as follows:

$$BIAS1_{new} = BIAS1 + K_1(\theta_{trunk} - \hat{\theta}_{trunk}), \qquad (3.3)$$

where $BIAS1_{new}$ is the new value for the parameter BIAS1, θ_{trunk} is the reference value for the trunk inclination in the sagittal plane and $\hat{\theta}_{trunk}$ is the current inclination in the sagittal plane for the trunk provided by the robot's sensors.

Table 3.2: Fixed angles for other joints

Joint name	Angle [radians]	Joint name	Angle [radians]
HeadPitch	0	LShoulderRoll	0.23
HeadYaw	0	LElbowYaw	-1.51
RShoulderRoll	-0.23	LElbowRoll	-0.5
RElbowYaw	1.51	HipYawPitch	0
RElbowRoll	0.5		

3.2.4 Experimental results and discussion

A NAO humanoid robot was used to validate the proposed controller. The proposed CPG network, shown in fig. 3.2, aims to imitate the main features of the human gait and describe a biped motion by specifying the phase differences for 12 joints of the sagittal and coronal planes. The network can generate a 3D motion in both simulated and real environments. The motion of the arms is controlled by defining the position of the shoulders in the sagittal plane. The other joints in the arms, hip and head have constant angles that aim to mimic an upright walking pose. These angles are shown in table 3.2.

The genetic algorithm works in coordination with the control system based on a CPG network and the robot simulator to estimate the best combination of CPG parameters within the predefined search space. The aim is to control the signals of the robot's joints through the CPG network and generate an optimal locomotion pattern. The crossover probability was set to 80 percent and the probability of mutation to 10 percent. These values were heuristically set after a large number of simulations.

When the frequency of the locomotion pattern is higher than 2.28 Hz, the simulator cannot reproduce the real interaction between the soles of the feet and the floor, which leads to a noticeable deviation between the simulated motion pattern and the real one. Therefore, the maximum frequency allowed for the simulated locomotion pattern was set to 2.28 Hz, which is reached with $K_f = 0.2$.

Table 3.3 shows the different limits that have been heuristically defined for the gains and offsets. These limits define the search space of the genetic algorithm. Figure 3.5 shows the simulation results for optimal straight line locomotion. The

Table 3.3: Genetic algorithm search space

CPG network parameters	Parameter range	CPG network parameters	Parameter range
GAIN1	0.01 - 1.00	BIAS1	-0.90 - 0.00
GAIN2	0.01 - 1.00	BIAS2	0.5 - 1.2
GAIN3	0.01 - 0.50	BIAS3	-0.70 - 0.00
GAIN4	0.01 - 0.50	BIAS4	1 - 2
GAIN5	0.01 - 0.50	K_f	0.2 - 0.5
GAIN6	0.01 - 1.00		
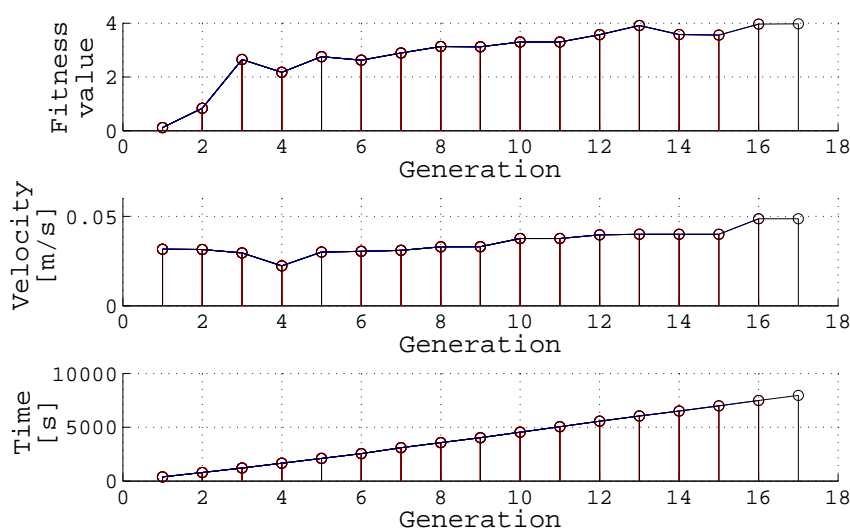
Figure 3.5: Simulation results obtained with the genetic algorithm

weighting coefficients α and γ have heuristically been set to 80 and 100, respectively. The CPG parameters shown in table 3.4 were finally obtained by means of the proposed methodology. The genetic algorithm was initialized with an initial population of 200 chromosomes. The total simulation time was 132 minutes on an Intel Core 2 Quad Q9400 processor at 2.66 GHz with 8GB of RAM.

In order to feedback the system, the phase resetting mechanism described above was implemented in the pacemaker oscillator. One example of the phase resetting mechanism is shown in fig. 3.6. The value of parameter K_1 in (3.3) was experimentally set to 10 to control the robot's vertical pose.

To test the robustness of the proposed closed-loop system, an environment with various classes of obstacles on the walking terrain was designed. These obstacles

Table 3.4: CPG network parameters found by the GA

CPG network parameters	Value	CPG network parameters	Value
GAIN1	0.24555	BIAS1	-0.60598
GAIN2	0.18665	BIAS2	0.70700
GAIN3	0.11685	BIAS3	-0.30590
GAIN4	0.40850	BIAS4	1.4797
GAIN5	0.43000	K_f	0.462
GAIN6	1.00000		
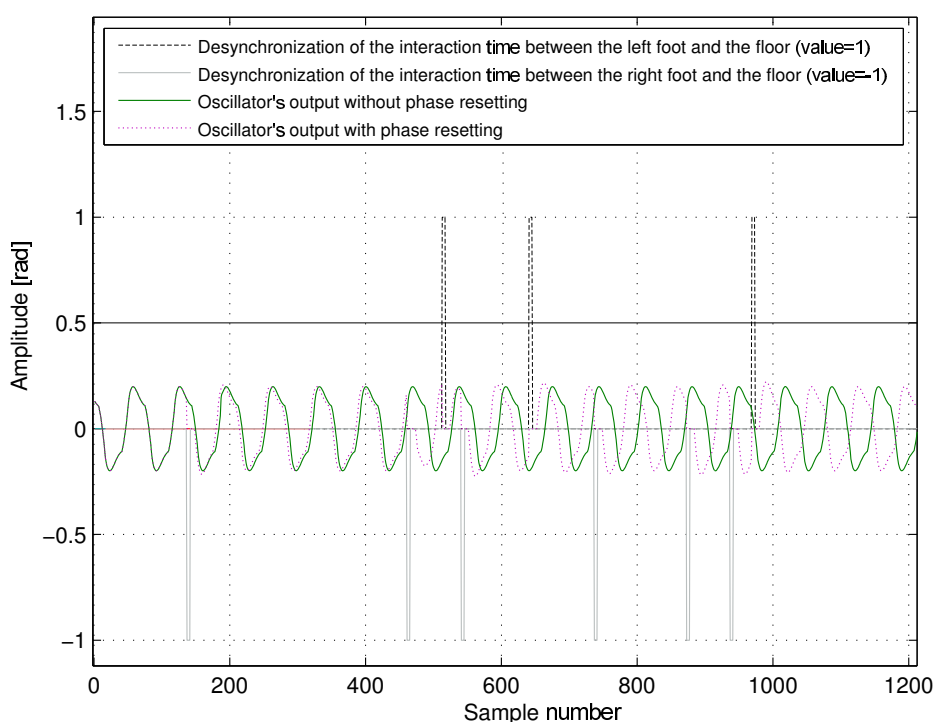
Figure 3.6: Phase resetting example for the pacemaker oscillator

are round, triangular and rectangular as can be seen in the simulation experiments. The shape of these obstacles implies that the soles of the robot's feet are subject to forces from different directions while it is walking and, therefore, there are different types of perturbation. These perturbations are used to test the robustness of the feedback system and to prevent the robot from falling down while it is exposed to unexpected situations. The system provides feedback to the locomotion pattern that is generated on-line so that the joint signals that prevent the robot from falling down can be modified. The proposed methodology was validated on a real NAO humanoid robot. Videos comparing the results obtained in simulation and the real environments
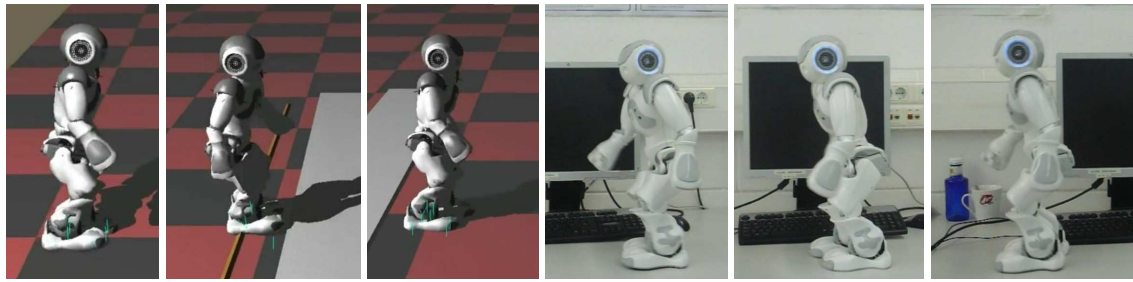
Figure 3.7: Snapshots of the simulation and real experiments

can be seen on the companion website.[1] Some snapshots with simulated and real experiments are shown in fig. 3.7.

3.2.5   Conclusion

A control architecture has been proposed to control the locomotion of a biped robot by using a CPG network based on Matsuoka's oscillators. A new CPG network has been proposed whose parameters are determined by evolutionary computation so that optimal biped locomotion patterns can be generated. These patterns are generated in the joint-space by controlling the angular displacement of the robot's joints in both the sagittal and coronal planes. A feedback mechanism is introduced into the network to modulate the locomotion patterns in accordance with the current sensory feedback and compensate for internal mismatches and external perturbations. The feedback is performed by controlling the robot's pose and the interaction between the robot and the floor through phase resetting of the pacemaker oscillator. Other approaches require a large number of parameters to characterize the locomotion pattern generated by the CPG network. However, our control scheme has been designed to characterize the system's behaviour with as few parameters as possible. Also, the signals are generated with CPG networks implemented with Matsuoka's oscillator which make it easy to incorporate feedback signals and modulate the output signals in real-time so that obstacles on the walking surface can be dealt with.

Experimental results have validated the proposed methodology in a NAO humanoid robot. It can be easily adapted to other biped robots with a similar

---

[1]Companion website: http://deim.urv.cat/%7Erivi/NAO%5FROBOT2013.html

joint structure after the corresponding changes have been made (robot model, limits for the genetic algorithm search space, etc.).

3.3   Second proposed control scheme

This section proposes another closed-loop system for CPG-based locomotion control of biped robots that operates in the joint space. The control scheme studied above identified some ways in which the system can be improved so that it can deal with more complex situations. Velocity was not defined as an input parameter. Thus, in the new control scheme proposed in this section, the required velocity is incorporated into the fitness function.

For the soles of the robot's feet to interact better with the floor for different velocities, a restriction that guarantees the ground clearance along the motion is incorporated, which has been identified as one of the drawbacks of the CPG-joint space control schemes. The first scheme discussed above did not measure stability. Therefore, an indicator of the accumulated stability has been added to the new fitness function to guarantee a large stability margin throughout the motion for the required velocity. This maximizes stability and allows the robot to deal with more complex situations. Furthermore, the locomotion pattern is generated by a new control scheme with another CPG network and controllers that easily determine and characterize the effect of each parameter in the locomotion pattern generated.

The new system has been designed to allow biped robots to perform omnidirectional walking on flat terrain and to walk on unknown sloped surfaces. Feedback signals generated by the robot's inertial and force sensors are directly fed into the CPG to automatically adjust the locomotion pattern over flat and sloped terrain in real time.

The proposed system belongs to the joint-space category, as the CPG output signals directly drive the angular position of the robot's joints. In terms of walking speeds and types of terrain, the results are comparable to those reported in (Liu et al., 2013b), even though it is a task-space approach and must continuously solve the

Table 3.5: CPGs' interconnection weights

$w_{1,1}$	0.0	$w_{1,2}$	0.0	$w_{1,3}$	2	$w_{1,4}$	0.5
$w_{2,1}$	0.5	$w_{2,2}$	0.0	$w_{2,3}$	0.0	$w_{2,4}$	2
$w_{3,1}$	2	$w_{3,2}$	0.5	$w_{3,3}$	0.0	$w_{3,4}$	0.0
$w_{4,1}$	0.0	$w_{4,2}$	2	$w_{4,3}$	0.5	$w_{4,4}$	0.0

computationally intensive inverse kinematics of the robot. Our approach, however, directly operates in the joint space, which guarantees a quick response and makes it especially suitable for direct hardware implementation with electronic circuits. The performance of the proposed control system has been assessed through both simulation and real experiments on an NAO humanoid robot.

3.3.1   CPG network topology

The proposed control system consists of a CPG network based on Matsuoka's neuron model (Matsuoka, 1985). The CPG used is based on a network of four interconnected neurons with mutual inhibition previously proposed by Matsuoka. The topology of the CPG is shown in fig. 2.15. The network was chosen because it generates oscillatory output signals in phase and anti-phase and with phase differences of $\frac{\pi}{2}$ and $\frac{3\pi}{2}$ radians. These phase differences are sufficient to control the robot's movement directly in the joint space, as shown in (Morimoto et al., 2008). In the present study, however, the CPG network directly drives the robot's joints instead of the phase oscillators used in (Morimoto et al., 2008). The interconnection weights between the neurons of the CPG, which were set according to (Endo et al., 2008), are shown in table 3.5. The system proposed here is advantageous since it facilitates the hardware implementation of the proposed control system as in (Nakada et al., 2005) and (Lewis et al., 2005).

The CPG's neurons are defined according to Matsuoka's neuron model (see (2.3)). The internal parameters that determine the behaviour of each neuron are summarized in table 2.2. In this study, the proposed control system was tested on the NAO platform. Notwithstanding, the same control system can easily be adapted to other

humanoid robots with a similar kinematic structure. Here, the controllers proposed in (Morimoto et al., 2008) were used to determine the angle in radians of the following joints of the NAO robot:

$$
\begin{aligned}
RHipPitch &= bias1 + a(-\xi(y_1 - y_3) + (y_2 - y_4)) \qquad (3.4)\\
LHipPitch &= bias1 + a(\xi(y_1 - y_3) - (y_2 - y_4))\\
LKneePitch &= bias2 + b(y_2 - y_4)\\
RKneePitch &= bias2 + b(y_4 - y_2)\\
RAnklePitch &= bias3 + c(\xi(y_1 - y_3) + (y_2 - y_4))\\
LAnklePitch &= bias3 + c(-\xi(y_1 - y_3) - (y_2 - y_4))\\
RHipRoll = LHipRoll &= d(y_2 - y_4)\\
LAnkleRoll = RAnkleRoll &= e(y_4 - y_2)\\
RShouldPitch &= bias4 + f(y_1 - y_3)\\
LShouldPitch &= bias4 - f(y_1 - y_3)
\end{aligned}
$$

These controllers not only generate the locomotion patterns directly with the output signals generated by the 4-neuron CPG network shown in fig. 2.15, but together with the CPG outputs they make it possible to implement the stepping controller by using the entrainment property of CPG networks. The information provided by the robot's force sensors is used directly and a quick response in real-time is guaranteed (see below).

The controllers depend on 10 internal parameters: 4 biases ($bias1, ..., bias4$ and 6 gains (a, b, c, d, e, f). The parameter ξ controls the stride length. This and the locomotion frequency, which is controlled through the value of K_f, determine the robot's walking velocity. By taking into account the relationship between locomotion frequency and stride length observed in the human gait (Danion et al., 2003), table 3.6 shows the pairs (K_f, ξ) that were experimentally chosen in this study for five reference velocities of the NAO robot, which span the same speed range as tested

in (Matos and Santos, 2012). The remaining joints were experimentally set to the constant values shown in table 3.7 to yield a stable upright position.

Table 3.6: Parameters related to locomotion frequency and stride length for some velocities in accordance with human gait

Velocity [cm/s]	1	3	5	7	9
K_f	1.0010	0.8546	0.7410	0.6583	0.6046
ξ	1.1318	1.3445	1.5760	1.8262	2.0950

3.3.2   Automatic estimation of CPG network parameters

The genetic algorithm (GA) proposed in (Passino, 2004) was applied in simulation to estimate the best combination of all internal parameters of the locomotion controllers specified above. The individuals of each generation were sorted and classified through a fitness function that assesses various constraints.

The GA's fitness function evaluates each individual of the current population at the end of a constant simulation period (t_{sim}) of 30 seconds in which the robot is allowed to walk using Webots real-time simulator. In particular, the fitness function that is maximized to sort out the individuals evaluated by the GA in each generation is the sum of four terms.

The first term applies a Gaussian function to the difference between the required straight line velocity and the velocity reached at the end of the simulation period for the individual evaluated. To obtain a Gaussian function with a small width, ρ is defined as 0.0018.

$$Fitness_1 = \exp\left(-\frac{(vel_{required} - vel_{end})^2}{\rho} \right) \qquad (3.5)$$

The second term applies a Gaussian function to the difference between the distance that the robot should travel in a straight line at the required velocity by the end of the simulation period and the final distance travelled by the individual evaluated. The term is maximized if the robot follows a straight path throughout the simulation period.

Table 3.7: NAO's joints with constant angles

Joint name	Angle (rad)	Joint name	Angle (rad)
$HeadPitch$	0	$LShouldRoll$	0.23
$HeadYaw$	0	$LElbowYaw$	-1.61
$RShouldRoll$	-0.23	$LElbowRoll$	-0.5
$RElbowYaw$	1.61	$HipYawPitch$	0
$RElbowRoll$	0.5		

$$Fitness_2 = \exp\left(-\frac{(dist_{required} - dist_{end})^2}{\rho}\right) \tag{3.6}$$

The distance required is calculated according to:

$$dist_{required} = vel_{required} * t_{sim} \tag{3.7}$$

The third term corresponds to the deviation distance with respect to the straight-line path at the end of a simulation period t_{sim}. To maximise it, the deviation is negated. The term is maximized when the robot reaches the desired destination along the straight path at the end of the simulation period.

$$Fitness_3 = -|\lambda_{end}| \tag{3.8}$$

The fourth term is the percentage of time within the simulation period that the robot's ZMP stability margin is above a given threshold. The term is maximized when the robot's stability is optimal during the various motion stages (both single-support and double-support modes). Each individual of the GA is evaluated for 30 seconds. Each 40 ms the dynamic stability margin is computed and if the value is above a given threshold, a variable called *counter* is increased. The maximum value for this counter is given by:

$$counter_{max} = \frac{30000}{40} = 750 \tag{3.9}$$

Then, the fitness value is calculated according to the following expression:

$$Fitness_4 = \frac{counter}{counter_{max}} \tag{3.10}$$

The total fitness value is defined as:

$$Fitness = \sum_{i=1}^{4} Fitness_i \tag{3.11}$$

The parameter required as input for the genetic algorithm is the required straight line velocity ($vel_{required}$). The total fitness is calculated according to (3.11). The maximum value of the fitness function is 3. According to the experimental results, the solutions found by the GA with a fitness values above a predefined threshold equal to 2.4 are considered to be valid locomotion patterns.

In order to obtain acceptable locomotion patterns, two restrictions were imposed on the solutions yielded by the GA. The first restriction prevents solutions with large torso inclinations. In particular, solutions with a torso inclination of above 16 degrees were rejected. At lower thresholds, the GA found hardly any valid solutions, whereas higher thresholds led to unnatural bent postures while walking. The second restriction has to do with ground clearance. The foot swing must be parallel to the floor and with the sole's height higher than 1.0 cm for the swing leg most of the time. This guarantees that the robot can interact correctly with the floor and avoid small obstacles.

The chromosome structure consists of 10 traits associated with the respective gains and biases that constitute the internal parameters of the locomotion controllers: (a, b, c, d, e, f) and ($bias1$, $bias2$, $bias3$, $bias4$). Table 3.8 shows the intervals allowed for those parameters, which constitute the GA's search space. The limits were experimentally delimited by taking into account the range of variation of the optimum solutions found by the GA after an extensive set of executions.

3.3.3 Feedback strategies

To adjust the locomotion pattern over flat, ascending and descending terrain in real time, some feedback pathways have been proposed for the control system described

Table 3.8: Genetic algorithm search space

CPG parameters	Parameter range	CPG parameters	Parameter range
a	0.1 to 0.5	f	0 to 2
b	0.4 to 0.9	$bias1$	-1.7 to 0.5
c	0.1 to 0.5	$bias2$	0.5 to 2
d	0.95 to 2.15	$bias3$	-1 to -0.2
e	0.95 to 2.15	$bias4$	1.35 to 1.43

above. The controllers described below have been implemented and tested in a NAO humanoid robot.

Posture controller

The posture controller keeps the robot's trunk in an upright position by using information provided by the robot's gyrometer and accelerometer. The trunk inclination in the sagittal plane can be controlled by changing the value of parameter $bias1$. This parameter is set proportionally to the difference between the reference inclination θ and the current trunk inclination estimated by the sensors, $\hat{\theta}$, as well as to the derivative of that difference.

$$bias1 = bias1_0 + k_1(\theta - \hat{\theta}) + k_2 \frac{d(\theta - \hat{\theta})}{dt}, \tag{3.12}$$

where $bias1_0$ is the original $bias1$ parameter.

Stepping controller

The stepping controller regulates the interaction between the robot's feet and the ground by synchronizing the output signals generated by the CPG with the real-time interaction between the robot and the floor by using the measures provided by the force sensors located in the soles of the robot's feet. This synchronization is performed by using the entrainment property of neural oscillators. Thus, the frequency of the locomotion pattern generated is adjusted according to the current interaction between the soles of the feet and the floor. This allows the control

system to compensate for both external perturbations and mismatches related to the robot's mechanical parts. Furthermore, if the stride length is set to zero, this controller guarantees correct stepping.

Let L_f, L_b, L_l and L_r be the force measures corresponding to the four force sensors located at the front, back, left and right positions of the left foot, respectively. Likewise, let R_f, R_b, R_l and R_r be the corresponding force measures for the right foot. The stepping controller is defined as:

$$F_L = L_f + L_b + L_l + L_r \tag{3.13}$$
$$F_R = R_f + R_b + R_l + R_r$$
$$f_1 = f_2 = k_3(-F_L + F_R)$$
$$f_3 = f_4 = -f_1,$$

where f_1, f_2, f_3 and f_4 are the feedback inputs described in (2.3) and corresponding to the four neurons of the CPG (see fig. 2.15).

Basically, the feedback signals f_1, f_2, f_3 and f_4 synchronize the frequency of the CPG's output signals in order to generate the locomotion pattern according to the real-time frequency of interaction between the robot and the floor. A simulation experiment showing the behaviour of this controller is shown in fig. 3.8.

Stride length controller

The stride length controller modulates the stride length ξ by taking into account the stability margin along the sagittal plane, μ_X, which is measured in centimetres (see fig. 2.2). The goal is to decrease the stride length whenever the stability margin is reduced in order to recover stability. The stride length is redefined as:

$$\xi = \begin{cases} k_4\mu_X, & \mu_X <= \kappa \\ \xi_0, & \mu_X > \kappa \end{cases} \tag{3.14}$$
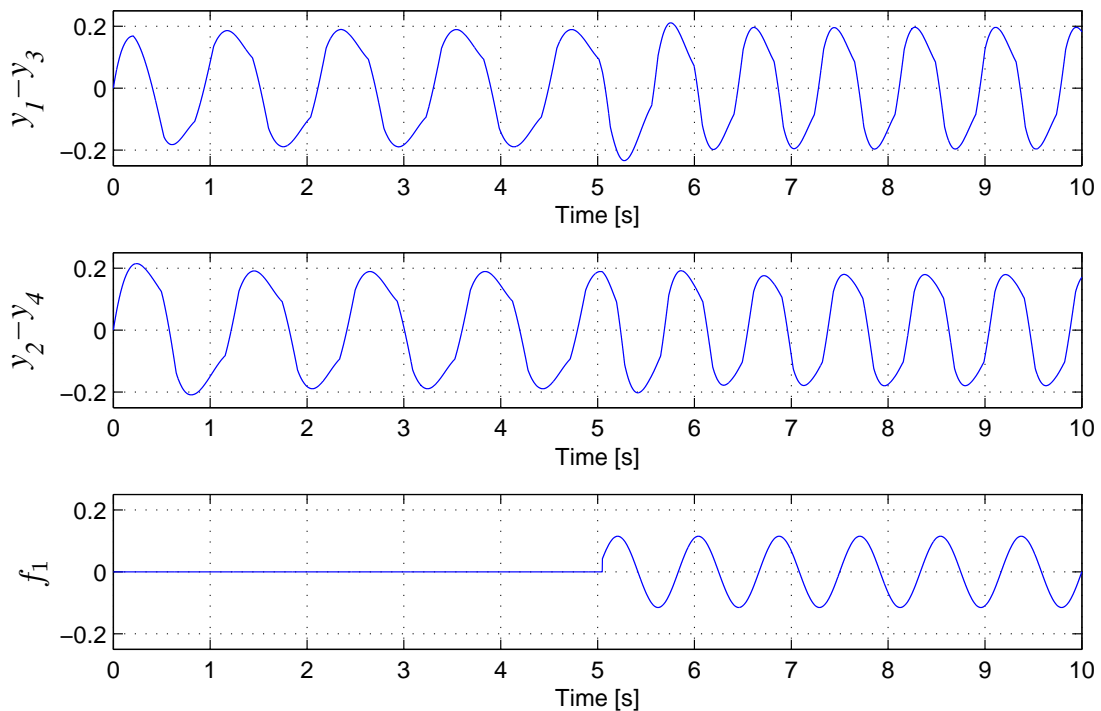
Figure 3.8: Simulation experiment with the stepping controller behaviour

where κ is a threshold and ξ_0 is the original stride length.

3.3.4   Omnidirectional controller

A joint located in the robot's pelvis is used to control the walking direction and describe a circular motion in either the clockwise or counterclockwise directions. This joint in the NAO is referred to as $HipYawPitch$ (see fig. 3.1). The following controller is used to determine its angle in radians:

$$HipYawPitch = k_5(y_1 - y_3), \tag{3.15}$$

where y_1 and y_3 are the corresponding CPG output signals and k_5 is a variable whose magnitude is inversely proportional to the curvature radius and whose sign determines whether the direction of circular motion is clockwise (negative sign) or

counterclockwise (positive sign).

3.3.5 Experimental results and discussion

Genetic algorithm results

The locomotion control system proposed was tested on a Webots simulator and a real NAO biped robot. To determine the gains and biases of the locomotion controllers for any given velocity, the GA interacts with the Webots simulator through a supervisor controller and evaluates the individuals from every generation. A total of 12000 individuals were evaluated, so a wide range of possible solutions within the search space were covered. Each individual requires the simulation of the robot while walking in straight line during the evaluation period, which was set to 30 seconds.

The proposed system was evaluated at five reference velocities: 1, 3, 5, 7 and 9 cm/s, which span the same speed range tested in (Matos and Santos, 2012). For each reference velocity, the GA was executed 50 times in order to find how best to combine the internal parameters of the locomotion controllers. The GA stops whenever the fitness function does not significantly vary for a predefined number of generations (3 generations with a fitness variation below 0.001) or the maximum number of generations is reached (8). Only the solutions whose fitness values were above a predefined threshold (2.4) were selected and the median of their corresponding parameters computed.

Table 3.9 shows the median values of the parameters for the five velocities tested. A total of seven solutions had a fitness value above the predefined threshold for 1, 3 and 7 cm/s, whereas four solutions passed that threshold for 5 and 9 cm/s. These solutions represent optimal locomotion patterns for the given reference velocities. Intermediate velocities can be obtained without changing the selected pattern by slightly modifying the values of the stride length, ξ, and/or the frequency gain, K_f. The results of one execution of the genetic algorithm to obtain the parameters that describe a locomotion pattern for a straight line velocity of 5 cm/s are shown in fig 3.9.

Figures 3.10, 3.11, 3.12, 3.13 and 3.14 show the ZMP location and the footsteps
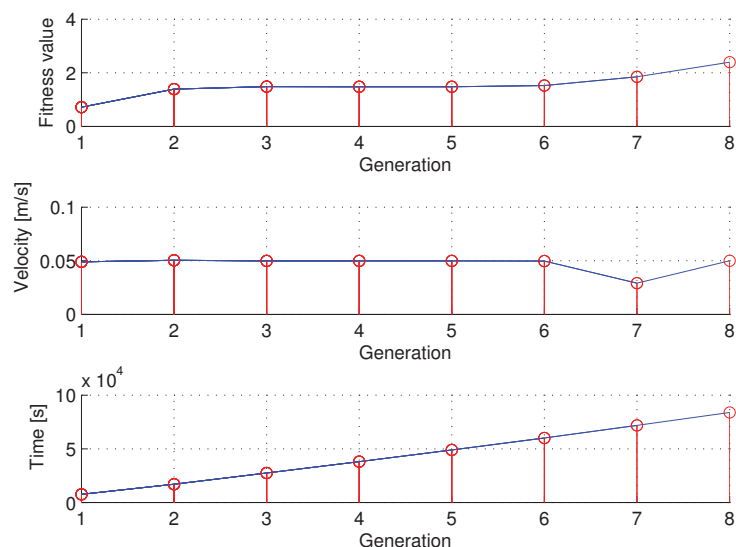
Figure 3.9: Simulation results obtained for one execution of the genetic algorithm

Table 3.9: Optimal parameters of locomotion controllers found by the GA for several velocities

Velocity [cm/s]	1	3	5	7	9
a	0.19016	0.28748	0.33363	0.36681	0.40146
b	0.40524	0.58164	0.67348	0.72823	0.90000
c	0.20877	0.20030	0.22286	0.28086	0.35967
d	1.68173	1.84968	1.93682	1.94680	2.01228
e	2.14299	2.07704	1.93374	1.83895	1.67558
f	0.73806	0.85100	0.93300	1.21052	1.28011
bias1	-0.99668	-0.88754	-1.02878	-1.08941	-1.09422
bias2	1.68364	1.47947	1.47344	1.41980	1.50161
bias3	-0.74073	-0.68465	-0.62478	-0.54938	-0.54021
bias4	1.37688	1.37644	1.36787	1.35089	1.42999

described for each of the five locomotion patterns obtained through the median values calculated from several executions of the GA for each of the reference velocities: 1, 3, 5, 7 and 9 cm/s, respectively. The ZMP location was calculated by estimating the CoP location using the measures of force provided by the sensors in the sole of each robot's foot and its location. The spatial reference system is located at the point at which the robot starts to walk. In the plots, the positive x-axis represents the direction that the robot walks in a straight line. The positive y-axis points the robot's right leg and the positive z-axis points the robot's head. In all the plots, the
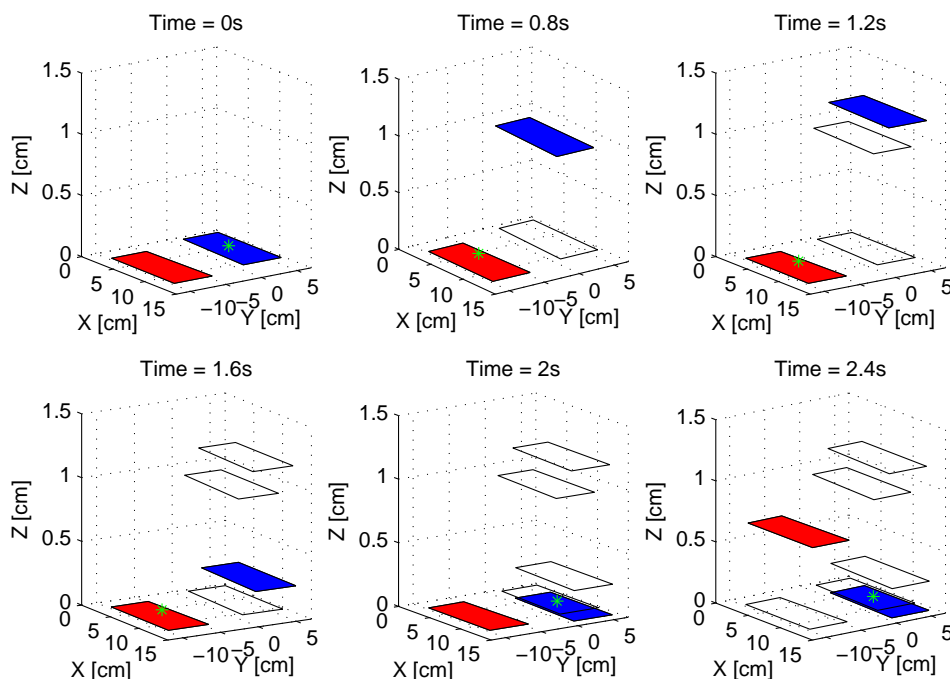
Figure 3.10: Locomotion pattern obtained for 1 cm/s
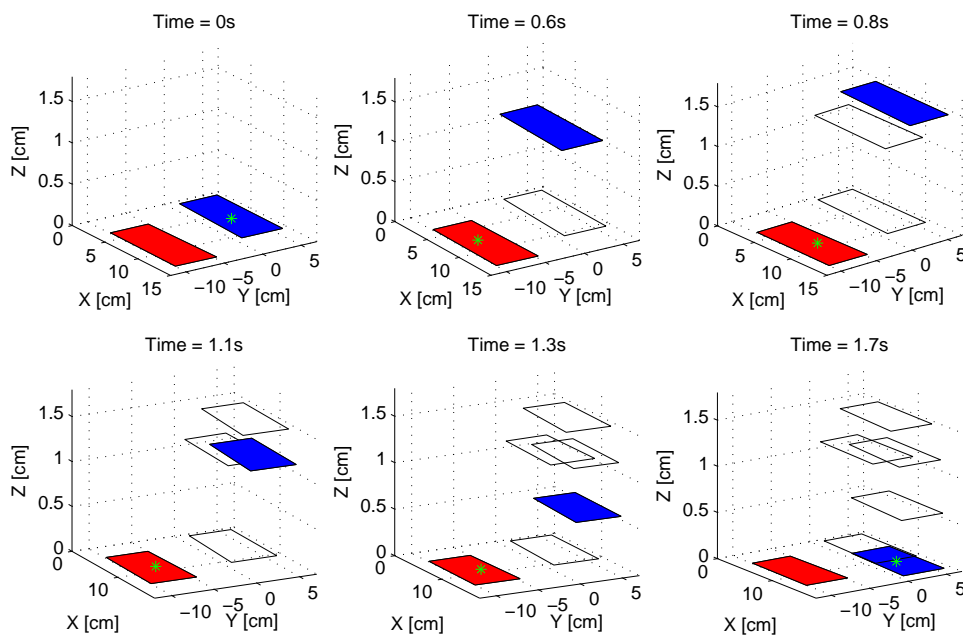
Figure 3.11: Locomotion pattern obtained for 3 cm/s

footsteps are colored blue and red for the robot's left and right soles, respectively.
The location of the ZMP is shown in green. As can be seen, for each figure and
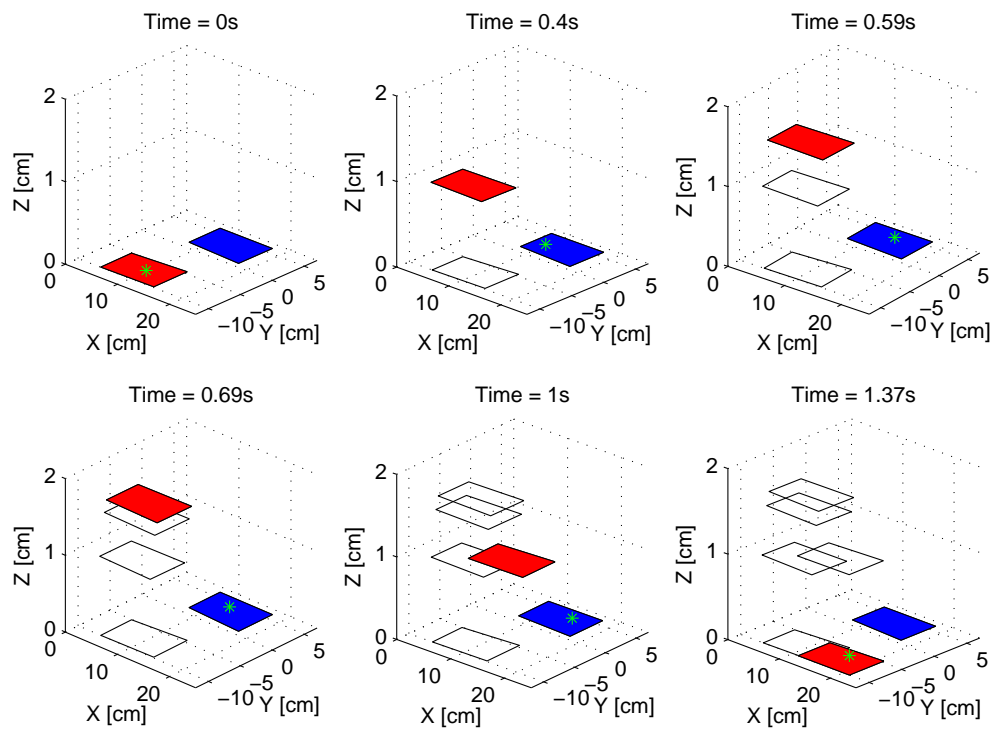
Figure 3.12: Locomotion pattern obtained for 5 cm/s
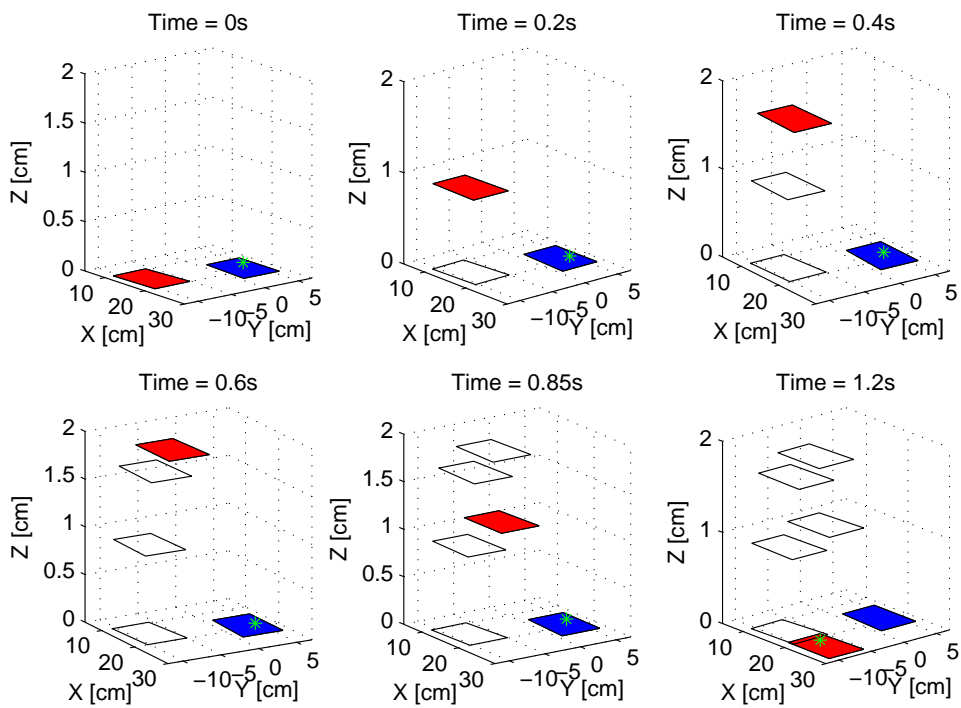
Figure 3.13: Locomotion pattern obtained for 7 cm/s
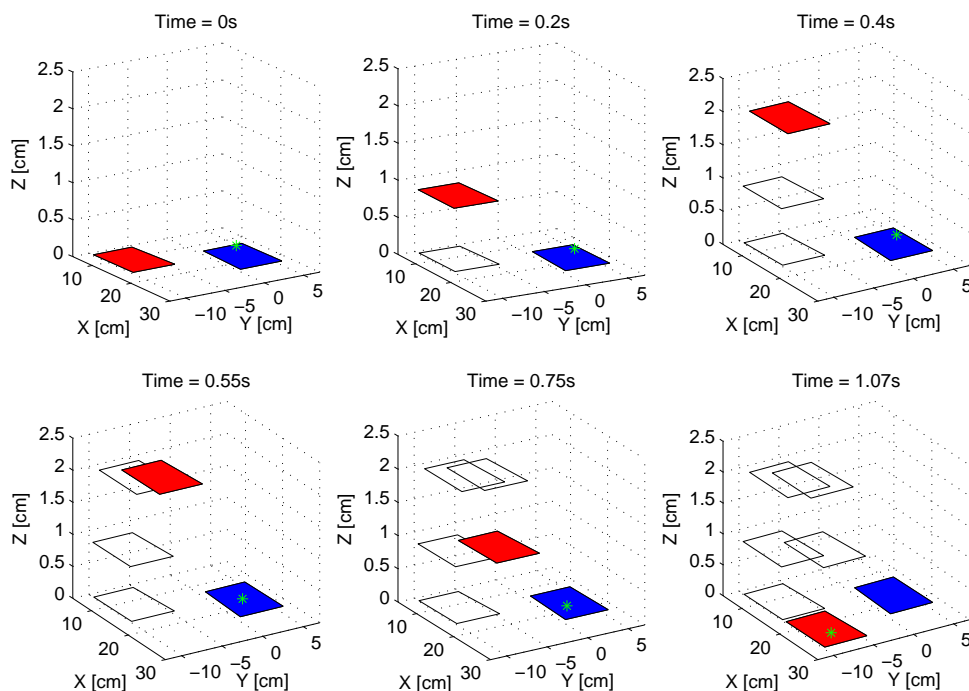
Figure 3.14: Locomotion pattern obtained for 9 cm/s

for all the velocities tested, the dynamic stability margin of each locomotion pattern is large for most of the time, which guarantees stable walking. This is consistent with the term introduced in the GA's fitness function to find the combination of parameters that best describe a stable locomotion pattern. It can also be seen that the maximum height of the sole is higher than 1 cm in each locomotion pattern, which is consistent with the restriction imposed in the GA.

Experiments on flat and inclined surfaces

The control scheme proposed was evaluated in simulation studies and in the real world using a workspace that consisted of an ascending 10-degree slope, followed by a flat surface and a final descending 10-degree slope. The robot started and stopped walking on the flat surface on both sides of the slope. Experimental results showing the behaviour of the overall system in both the simulated and real versions of the workspace can be found on the companion website.[2] Figure 3.15 shows a sequence

---

[2]Companion website: http://deim.urv.cat/%7Erivi/NAO%5F2014.html

3.3. Second proposed control scheme 61

of snapshots showing the performance of the system while the robot successfully traverses the workspace. Similar studies have been made with the same humanoid robot and CPG-based locomotion control on sloped surfaces. However, the most robust of those previous approaches needed to solve the costly inverse kinematics problem (Liu et al., 2013b; Song and Hsieh, 2014), whereas the other approaches did not ensure stable interaction with the floor, since the robot tended to drag its feet when walking, which is very likely to lead to falls on uneven terrain (Nassour et al., 2013).
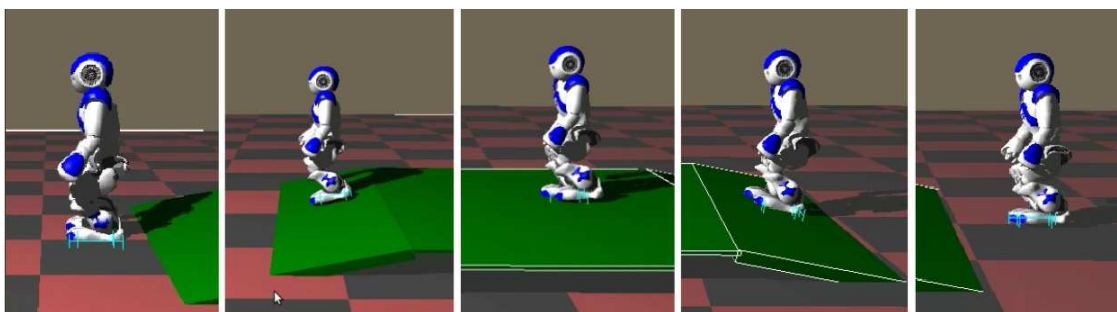
Figure 3.15: System behaviour in closed-loop

Step length modulation

Using the parameters found by the GA for the velocity of 5 cm/s, variable ξ was modulated to change the straight-line velocity on-line. Figure 3.16 shows the relation between the robot's measured straight-line velocity while variable ξ is modulated. This is another option for controlling the velocity of the locomotion pattern in real-time with the proposed control scheme. Figure 3.17 presents the footsteps generated by the robot when variable ξ is used to modify the walking velocity on-line.

Frequency modulation

Variable K_f can be modulated to change the frequency of the locomotion pattern and, therefore, its velocity. Figure 3.18 shows the relation between the robot's measured straight-line velocity while variable K_f is modulated. The set of parameters used were those obtained for the locomotion pattern at 5 cm/s.
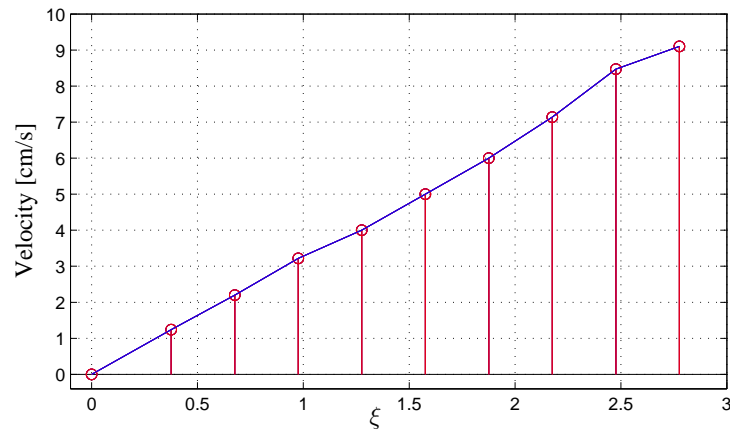
Figure 3.16: Straight-line velocity Vs. ξ for the locomotion pattern found for 5 cm/s
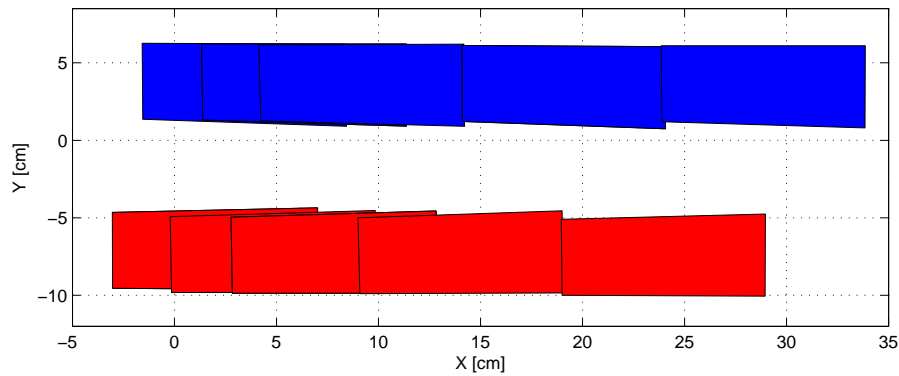
Figure 3.17: Footsteps obtained by varying parameter ξ from 0.676 to 2.176. The set of parameters used were those found for the locomotion pattern at 5 cm/s
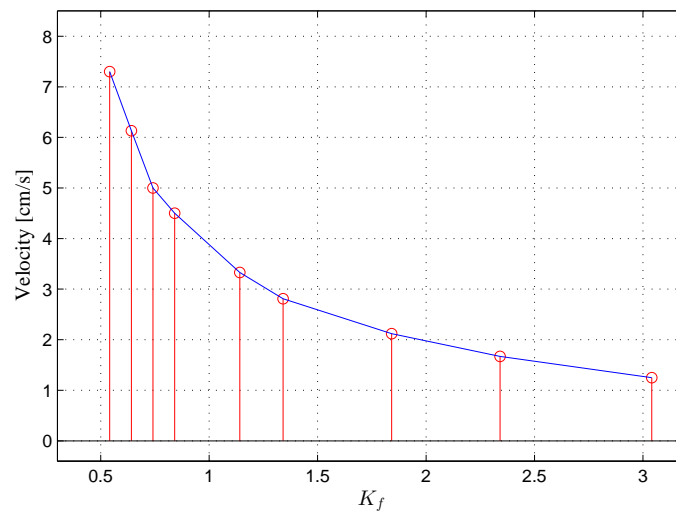
Figure 3.18: Velocity modulation by varying parameter K_f

Omnidirectional locomotion experiments

By using (3.15), which describes the omnidirectional controller, in combination with the parameters shown in tables 3.6, 3.7 and 3.9, we executed a genetic algorithm. The aim was to find the best value for the variable k_5 and to describe the desired omnidirectional locomotion pattern described by a circumference of radius r. The reference trajectory to be tracked is described in fig. 3.19.

A procedure similar to the one used to find the locomotion parameters that describe straight-line walking was used. In this case, the fitness function was minimized and described by a single term associated with the sum of the accumulated error between the desired trajectory and the trajectory described with the current combination of parameters and the value k_5 to be assessed. The input of the genetic algorithm was the desired curvature radius. The locomotion patterns previously found by the GA for 5 cm/s and the omnidirectional controller were used by the new GA to find the required omnidirectional trajectory. Figure 3.20 depicts the curvature radius described by the robot using the omnidirectional controller for different values of the omnidirectional gain k_5. The vertical asymptote for $k_5 = 0$ corresponds to straight-line motion. These gains were found by the GA.
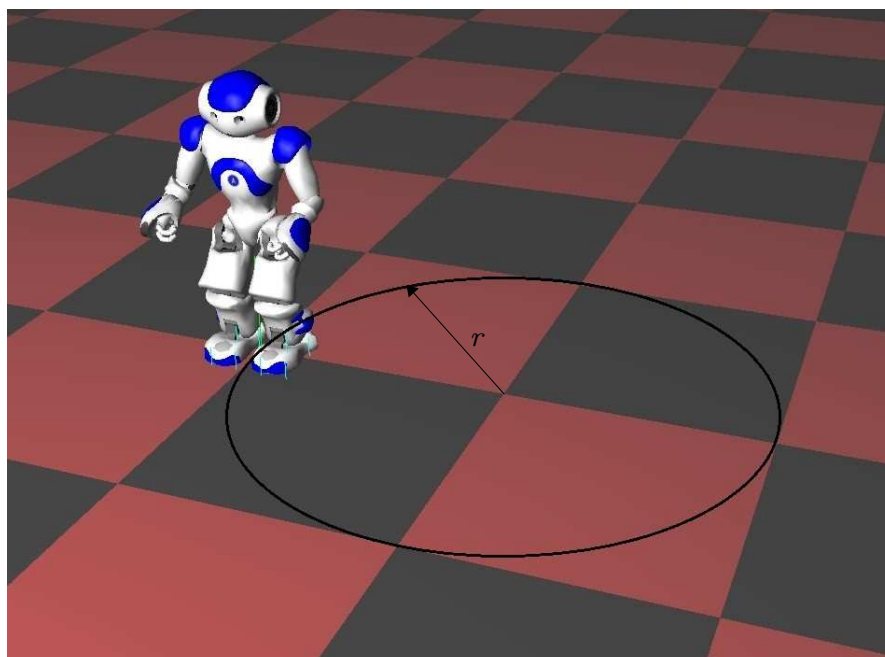
Figure 3.19: Desired trajectory

Figures 3.21 and 3.22 show the footsteps obtained from some of the experiments. The results indicate that the proposed control scheme enables the robot to describe omnidirectional locomotion patterns and circles of various radii and to freely navigate in real dynamic changing scenarios.
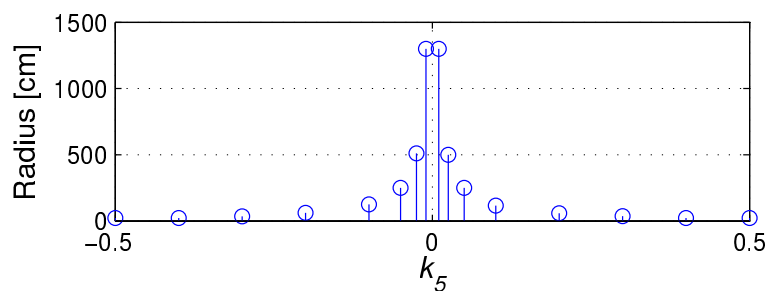
Figure 3.20: Curvature radius for several values of k_5
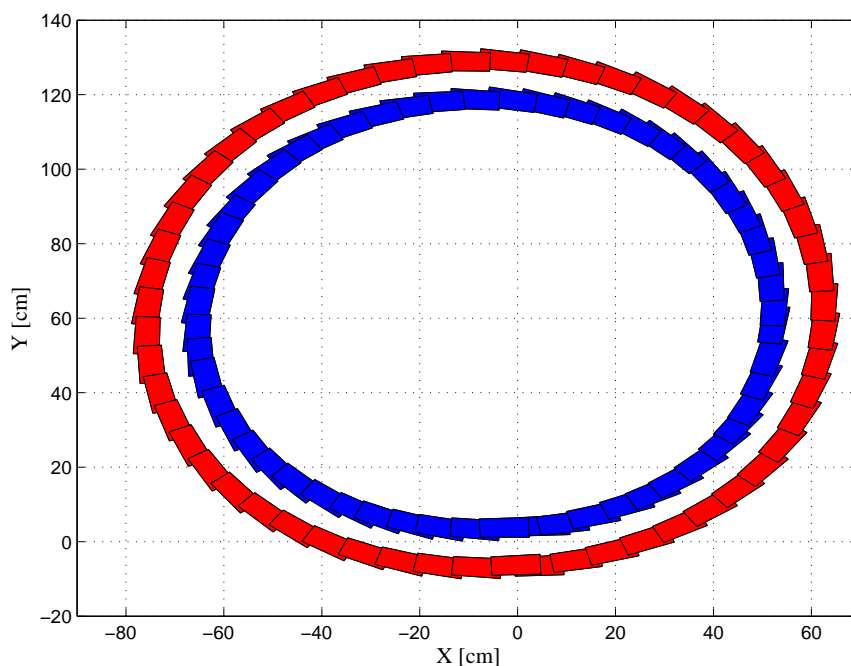
Figure 3.21: Omnidirectional locomotion example in the counter-clockwise direction. In this experiment the value for variable k_5 was 0.4

Figure 3.23 shows an example of a circular motion described by the robot using the omnidirectional controller and the optimal parameters found for the walking velocity of 5 cm/s. The stride length ξ in this case was set to zero so that the robot could turn round. The value of k_5 was set to 0.3, thus yielding a turning
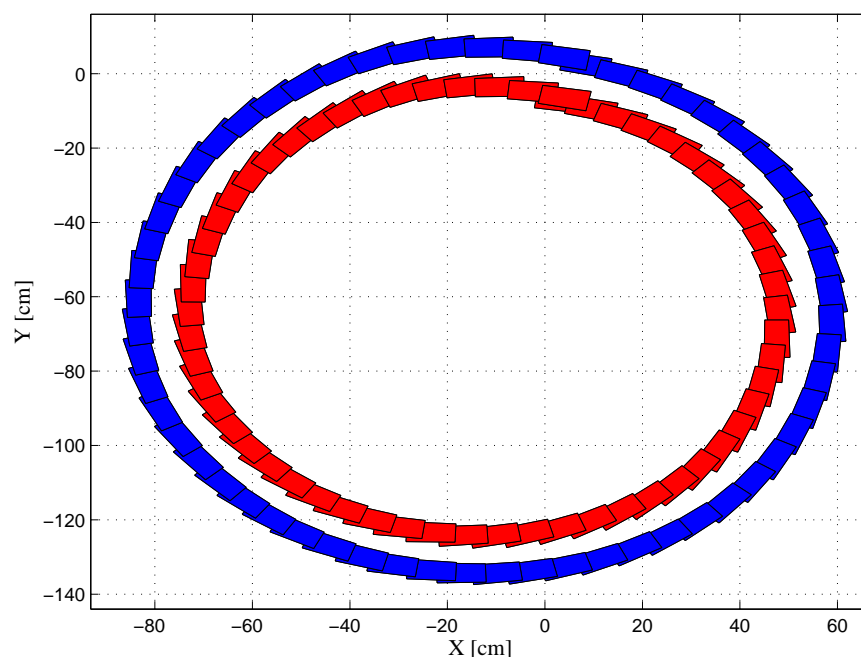
Figure 3.22: Omnidirectional locomotion example in the clockwise direction. In this experiment the value for variable k_5 was -0.4

velocity of 7.2°/s in the counterclockwise direction. Figure 3.24 presents the footstep trajectories obtained when the robot changes from a circular locomotion pattern in the clockwise direction to a straight-line locomotion pattern and finally to a circular locomotion pattern in the counter-clockwise direction. The proposed control system can be used to change the locomotion pattern on-line and describe the required omnidirectional walking trajectory according to the real-time interaction between the robot and the environment. At the moment of transition between locomotion patterns it is important to guarantee stability. Therefore a good strategy is to change the locomotion pattern at the moment at which the stability margin is large.
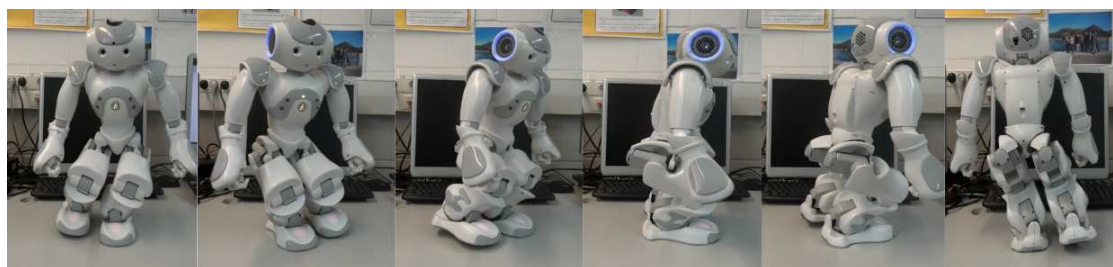
Figure 3.23: Turning behaviour with the omnidirectional controller
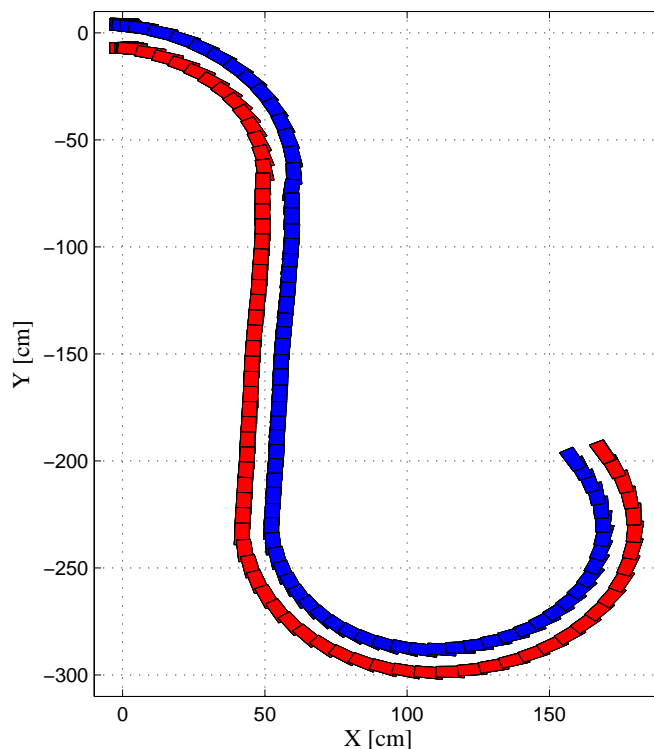
Figure 3.24: Online change in the direction of the locomotion pattern obtained for 5 cm/s. In this experiment the value of parameter k_5 is modified from -0.4 to 0 and finally to 0.4

The values of parameter ξ used to vary the step length and parameter K_f used to modify the locomotion pattern's frequency can be modulated to achieve a desired velocity in rad/s that describes a circular motion with radius r. Thus, the genetic algorithm could also be applied in order to estimate the best combination of values k_5, K_f and ξ to describe the desired circular motion with a required speed in rad/s. Future work will include a detailed study of the parameters, k_5, K_f and ξ so that the optimal locomotion pattern for a desired velocity can be described.

3.3.6 Conclusion

This section presents a closed-loop system for the omnidirectional locomotion control of biped robots on flat surfaces and for locomotion control on sloped surfaces that operates in the joint space, thus avoiding the high computational cost of continuously evaluating the inverse kinematics, which is mandatory for control systems that

operate in the task space. The output signals generated by a robust CPG network based on Matsuoka's neuron model directly control the angular position of the robot's joints through a set of controllers whose optimal configuration of internal parameters was computed using an evolutionary Genetic Algorithm given a desired walking speed in a straight line. The relationship between locomotion frequency and stride length for each reference velocity was obtained in agreement with the patterns established for the human gait.

Feedback signals generated by the robot's inertial and force sensors are directly fed into the CPG so that the locomotion pattern over flat and sloped terrain can be automatically adjusted in real time. In addition, omnidirectional motion is achieved by controlling the pelvis motion. The performance of the proposed control system was assessed by both simulation and real experiments on a NAO humanoid robot, and the approach was shown to be effective. The same control system can be applied to other families of humanoid robots with a similar kinematic structure.

The proposed system belongs to the joint-space category, as the CPG output signals directly drive the angular position of the robot's joints, and yields results comparable to those reported in (Liu et al., 2013b) in terms of walking speeds and types of terrain, although the latter is a task-space approach that requires solving the inverse kinematics problem, which limits the response time to unexpected events and may end up compromising the robot's safety. The proposed CPG guarantees that the open-loop control system generates a locomotion pattern that correctly interacts with the floor. It also straightforwardly modulates the locomotion patterns through sensory feedback so that the robot can cope with uneven terrain and transitions between different types of ground, and facilitates additional feedback controllers. This is a very important feature because it enables the system to be improved incrementally by adding controllers so that more complicated situations can be coped with.

Several recent studies have proposed CPG-based control approaches to solve the biped locomotion problem. However, the main problem of these approaches is that the signal generation process is not very clear. Thus, most of them cannot

be incrementally improved. As has been shown in this section the proposed control system incrementally improves the well-characterized motion described by the system, because each of the variables has a clear effect on the final locomotion pattern. The system can be continually improved by adding new controllers so that more complex situations can be dealt with during biped locomotion. The proposed control scheme has proved to be versatile enough to describe several types of locomotion patterns and is robust enough to deal with disturbances that appear on the walking surface and various slopes on the walking terrain.

3.4   Summary

In this chapter, two control schemes based on CPG-joint-space control methods have been proposed. Two CPG networks based on Matsuoka's neuron model have been proposed and integrated into the control system. The systems were designed by minimizing the number of parameters that characterize their behaviour, which were found by genetic algorithms with a fitness function. This function plays a fundamental role in the results obtained because it determines the shape and main features of the locomotion pattern. Therefore, it is very important to define a fitness function that properly assesses the current described locomotion pattern. The process is performed by assessing the main indicators of the locomotion pattern described by the current combination of parameters that need to be evaluated if the walking pattern is to be optimal.

The location of the centre of masses plays an important role in the robot's stability, as can be seen from the results obtained by using the GA. When the stability criteria are taken into account in the fitness function, as is the case of the second control scheme, the solutions found by the GA describe a locomotion pattern with a lower location of the centre of masses. In this study the most important criterion was the versatility and the robustness of the system. Future work will calculate the robot's power consumption so that it can be reduced without affecting the robot's stability when needed.

Some feedback strategies have been studied so that systems could be provided with feedback pathways able to deal with obstacles and inclined terrain. As was shown, several controllers can be introduced into the control scheme to cover different types of perturbation. The control system implemented enables learning to be incorporated into the feedback strategies through on-line modification of the feedback controllers' parameters.

The results indicate that CPG-joint-space control methods are a promising way of solving the biped locomotion problem by using simple but effective adaptive systems. This chapter has presented a detailed methodology for developing a system for the locomotion control of biped robots using biologically inspired models. A design strategy has been defined for a control system that uses CPG networks and genetic algorithms to characterize and model the generation and control of locomotion patterns for biped robots.

CHAPTER 4

Phase resetting mechanism

In this chapter, a new control strategy is proposed for resetting the phase of the rhythmical signals generated by Central Pattern Generator (CPG) networks based on Matsuoka's oscillator. The main contribution of the proposed phase resetting scheme is its predefined constant response time given a single-pulse perturbation and an arbitrary phase resetting curve (PRC) that can be modified at any time. Phase resetting is a feature of physiological oscillating systems, which can be utilized in robotics and other control applications as a feedback strategy to provide robust adaptation to unexpected external stimuli. The technique can be applied to CPG networks based on Matsuoka's neuron model. This phase resetting strategy is assessed through simulation and a real application of locomotion control of a biped robot.

4.1   Introduction

Experiments performed by physiologists on real neurons have driven the definition of mathematical models of artificial neurons and neural networks that try to mimic the behaviour of their biological counterparts. The CPGs in this thesis are based on the mathematical model proposed by Matsuoka (1985, 1987). By adjusting some internal parameters, this model straightforwardly modulates the amplitude and frequency of the oscillations generated (see section 2.3.2). However, there was no suitable control strategy for specifying the phase of the output signals in real-time. Therefore, in this chapter a control mechanism is proposed and validated in order to modify the phase of output signals generated by Matsuoka's oscillator or networks based on Matsuoka's neuron model described using (2.3).

Biological neurons and CPGs exhibit a behaviour known as *phase resetting* (Tass, 1999; Ding and Glanzman, 2011), in which the phase of the output signals generated by the CPG changes whenever a single-pulse perturbation is applied. The main effect of biological phase resetting is to synchronize the various internal processes, such as locomotion, with external stimuli based on information provided by the sensory subsystem. The phase resetting behaviour is commonly represented by a phase response (resetting) curve (PRC) (Granada et al., 2009; Galán et al., 2005), which indicates the phase shifts applied to the current oscillatory output signal according to the phase in which the external pulse perturbation occurs. An alternative representation is the phase transition curve (PTC), which defines the new phase of the output signal as a function of the phase in which the external perturbation is applied.

A theoretical analysis of phase resetting on Matsuoka's oscillators presented in (Nakada et al., 2011, 2013) describes the phase response properties of the oscillators after their internal parameters have been properly selected and derives their intrinsic PRCs. Using this approach, Nakada and Matsuoka (2012) proposed implementing Matsuoka's oscillator in an integrated circuit and applying it to phase resetting. However, real control applications require tailor-made PRCs, such as those proposed

in (Nakanishi et al., 2006; Nomura et al., 2009) to be implemented for closed-loop locomotion control of legged robots. To our knowledge, no phase resetting mechanism with a predefined constant response time given a single-pulse perturbation and allowing the definition of arbitrary PRCs has previously been proposed for CPG networks based on Matsuoka's oscillator.

In this chapter, a new feedback signal is introduced into the neuron's mathematical model proposed by Matsuoka to control the phase of the oscillator's output signals and determine its phase resetting response. The scheme can be applied to adaptive control systems using any topology of CPG network based on Matsuoka's neuron model. The proposed phase resetting mechanism can implement predefined arbitrary PRCs and modify the PRC specification at any time. So the feedback controllers can learn online by straightforwardly modifying the input PRC. An important feature of the proposed phase resetting mechanism is its fast response time, which makes it particularly suitable for real-time applications.

4.2   Phase resetting in robotics

The PRCs observed in spontaneously oscillating physiological systems have fixed shapes determined by the physical properties of biological neurons. In robotics control, however, PRCs can be of any shape and can be modified on-line so that learning capabilities can be incorporated in the implementation of adaptive feedback controllers. In particular, several works have studied and discussed the phase resetting mechanism for the locomotion control of legged robots (e.g. Nakanishi et al., 2006; Nomura et al., 2009; Aoi et al., 2010, 2012b,a; Aoi and Tsuchiya, 2006). They have shown that this mechanism contributes to the design of more robust controllers.

For locomotion controllers based on CPG networks, it is therefore necessary to define phase resetting mechanisms compatible with the mathematical models upon which those networks are based. In particular, for CPG networks based on phase oscillators defined by systems of equations that directly represent the phase dynamics of the output signals, the phase resetting mechanism is well defined since the phase

value is a variable of the system that can be controlled directly (Aoi and Tsuchiya, 2007; Matos and Santos, 2012; Endo et al., 2004).

However, for CPG networks with oscillators based on mutual inhibiting neurons, such as those based on Matsuoka's oscillator, there is no methodology for implementing a required PRC in an arbitrary network topology. A recent study by Matsuoka shows a phase resetting implementation for Matsuoka's oscillator (Nakada et al., 2013). However, the PRC in that approach has a fixed shape determined by the selection of the oscillator's internal parameters. So it is not possible to implement arbitrary PRCs, which, as mentioned in the section above, are necessary if the phase resetting mechanism is to be used in robotics, biomedical and other control applications.

4.3   Proposed phase resetting

The phase resetting scheme proposed here has been tested on two basic CPG models proposed by Matsuoka (1985), which are based on the neuron model defined in (2.3). They have been widely used in mobile robotics (e.g. Endo et al., 2008) and other control applications (e.g. Zhang et al., 2011). Figure 2.6 shows Matsuoka's simplest 2-neuron CPG-model, widely known as Matsuoka's oscillator, which generates periodic output signals in both phase and contra-phase. In turn, fig. 2.15 shows a 4-neuron CPG model that generates oscillatory output signals in phase, contra-phase and with phase differences of $\frac{\pi}{2}$ and $\frac{3\pi}{2}$ radians, respectively. Figure 2.8 and fig. 2.16 show the output signals for those CPG models. The phase difference between output signals is determined by the internal parameters of the neurons, the network topology and the interconnection weights. These parameters and weights have been experimentally chosen in this thesis to yield output signals with a shape resembling as much as possible a sinusoidal wave provided the weights and internal parameters do not change. In particular, table 2.2 shows the values of the neuron's internal parameters, whereas the network interconnection weights are given in table 4.1 and table 4.2, respectively. These CPGs generate periodic output signals with stable

Table 4.1: Interconnection weights of Matsuoka's oscillator

$w_{1,2}$	2
$w_{2,1}$	2

limit cycles.

Table 4.2: Interconnection weights of Matsuoka's 4-neuron CPG

$w_{1,1}$	0.0	$w_{1,2}$	0.0	$w_{1,3}$	2.2	$w_{1,4}$	2.2
$w_{2,1}$	2.2	$w_{2,2}$	0.0	$w_{2,3}$	0.0	$w_{2,4}$	2.2
$w_{3,1}$	2.2	$w_{3,2}$	2.2	$w_{3,3}$	0.0	$w_{3,4}$	0.0
$w_{4,1}$	0.0	$w_{4,2}$	2.2	$w_{4,3}$	2.2	$w_{4,4}$	0.0

The proposed phase resetting scheme is based on shifting the phase of every output signal of the CPG at a specific time instant t from its current phase ϕ_t to a desired phase at time $t + \triangle t$, $\phi_{t+\triangle t}$, as specified in the PRC, where $\triangle t$ is a predefined constant time interval. This is done by temporarily boosting the frequency of the CPG's signal in such a way that the new phase is reached by $\triangle t$. In order to do this, the relationship between parameter K_f and the CPG's oscillation frequency needs to be established, and the phase of the CPG's output signals online needs to be estimated. This process is applied to all output signals of the CPG simultaneously. These stages are fully described below.

4.3.1 Frequency characterization

As discussed in section 2.3.2, the frequency of the CPG's output signals is determined by the time constants τ and τ' if parameters β and w_{ij} are kept constant. Parameter K_f was introduced in (2.4) to modulate the oscillation period.

The closed-form relationship between K_f and the oscillation frequency Γ was identified from (2.5) and obtained for each network by fitting the following hyperbolic function using least-squares:

Table 4.3: Proportionality constants for the analysed CPG networks and corresponding coefficients of determination

	a_μ	R^2
2-neuron CPG	1.9869	0.99
4-neuron CPG	1.1022	0.99
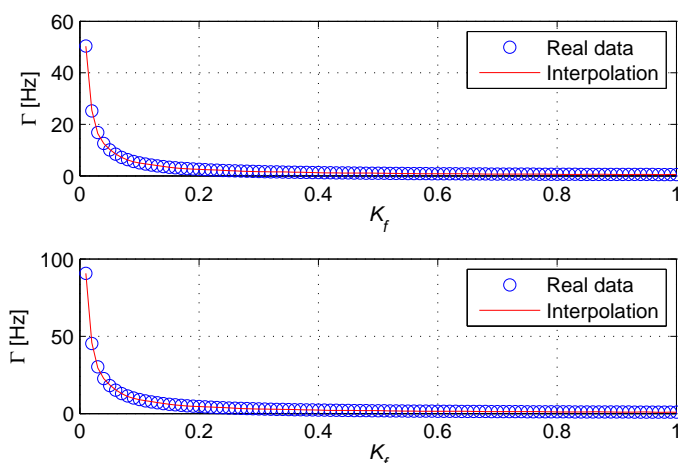
Figure 4.1: Frequency vs. K_f for the 2-neuron CPG (top) and 4-neuron CPG (bottom)

$$\Gamma(K_f) = \frac{1}{a_\mu K_f}, \quad K_f > 0 \tag{4.1}$$

The data pairs required for the least-squares procedure for each network were obtained by simulating the corresponding network with different values of K_f. Then, the fundamental frequency of the output signal for the corresponding K_f value was calculated from its Fourier transform. The data pairs and the corresponding fitted hyperbolic functions for both the 2-neuron and 4-neuron CPGs are shown in fig. 4.1. Table 4.3 shows the values of the proportionality constant a_μ in (4.1) experimentally obtained for the two CPG networks described in this section, as well as the coefficients of determination of the fitting process. For Matsuoka's oscillator (2-neuron CPG), the theoretical value of constant a_μ derived by equating (2.5) and (4.1) is 1.9890, which shows that the value obtained experimentally is similar to the theoretical one. For Matsuoka's oscillator, the mathematical expression for the

Table 4.4: Parameters of the piecewise phase function for the 2-neuron CPG and corresponding coefficients of determination

a_0	121434.5398	a_1	1992007.9194	a_2	10892461.4031	a_3	19853936.8566	R^2	0.99
b_0	19.5414	b_1	332.2828	b_2	2059.5606	b_3	4496.4205	R^2	0.99
c_0	2.0498	c_1	4.03396	c_2	-5.7558	c_3	23.4629	R^2	0.99
d_0	6.2818	d_1	-54.4002	d_2	199.2711			R^2	0.99
e_0	-16827.9477	e_1	278539.5229	e_2	-1536655.8403	e_3	2826034.4273	R^2	0.99
y_{min}	-0.1845	l_1	-0.1820	l_2	-0.1248	l_3	0.1494		
l_4	0.1798	y_{max}	0.1845						

Table 4.5: Parameters of the piecewise phase function for the 4-neuron CPG and corresponding coefficients of determination

a_0	3959.7697	a_1	65829.0423	a_2	364872.5258	a_3	674249.9305	R^2	0.99
b_0	1.5567	b_1	8.6703	b_2	34.6959	b_3	157.3163	R^2	0.99
c_0	1.5021	c_1	2.9551					R^2	0.99
d_0	1.4519	d_1	6.9924	d_2	-34.5365	d_3	227.5252	R^2	0.99
e_0	-1918.2598	e_1	32108.0716	e_2	-178969.1693	e_3	332706.7092	R^2	0.99
y_{min}	-0.1860	l_1	-0.1775	l_2	-0.0100	l_3	0.0141		
l_4	0.1760	y_{max}	0.1860						

frequency of the output signals is defined theoretically as (2.5). However, determining the mathematical expression of the frequency of the output signals for other networks is not straightforward. Therefore, the approximate value of frequency estimated by using the aforementioned procedure is generally valid.

4.3.2 Online phase estimation

Once the CPG network reaches a stable oscillation state, it generates periodic signals whose shapes depend on the internal parameters of its neurons, the network topology and interconnection weights, as shown in fig. 2.8 and fig. 2.16 for the 2-neuron and 4-neuron CPG, respectively. Both the phase and contra-phase signals generated by the CPG are combined to generate a *reference signal y*. In particular, for the 2-neuron CPG shown in fig. 2.7, $y = y_1 - y_2$, whereas for the 4-neuron CPG shown in fig. 2.15, $y = y_1 - y_3$. The reference signal is considered to be at phase 0 at its minimum amplitude (lowest peak) and at phase π at its maximum amplitude

(largest peak). Therefore, the signal is between phases 0 and π radians whenever its first derivative is positive (ascending slope).

The aim of this stage is to estimate the phase of the aforementioned reference signal based on its amplitude at any time instant, since the shape of that reference signal as a function of its phase is the same independently of the CPG's oscillating frequency defined by parameter K_f. In particular, for each CPG, a phase function $\phi(y)$ that relates the amplitude of the reference signal to its associated phase is defined as:

$$\phi(y) = \begin{cases} \phi^+(y) & dy/dt \geq 0 \\ \pi + \phi^+(-y) & dy/dt < 0, \end{cases} \tag{4.2}$$

where $\phi^+(y)$ is the phase function corresponding to the ascending slope of the reference signal. Due to the complexity of the waveforms generated by CPGs, function $\phi^+(y)$ was defined through polynomial fitting using the least-squares of a set of data pairs (amplitude, phase) obtained by simulating the CPGs and sampling the ascending slope of their corresponding reference signals. This sampling process is performed for a fixed value of $K_f = 0.7$, since the amplitude of the reference signal in steady state and its corresponding phase are the same for any frequency. In order to yield a fitting error lower than one degree, a polynomial of degree 20 would be necessary. However, since that phase function must be evaluated at every control cycle, computing such a high-order polynomial would be very inefficient. Therefore, function $\phi^+(y)$ was defined as a piecewise function of five low-order polynomials (see (4.3)). These polynomials were fitted through least-squares given the sampled data pairs (amplitude vs. phase). The coefficients and limits of each polynomial were found experimentally to yield a good fitting with polynomials of low order.

Figures 4.2 and 4.3 show the definition of $\phi^+(y)$ for the 2-neuron and 4-neuron CPG, respectively. The coefficients of the five low-order polynomials and the corresponding coefficients of determination are given in table 4.4 and table 4.5, respectively. The plots shown in the third row of fig. 4.4 were calculated using the polynomials found previously. These plots confirm that the same shape is obtained
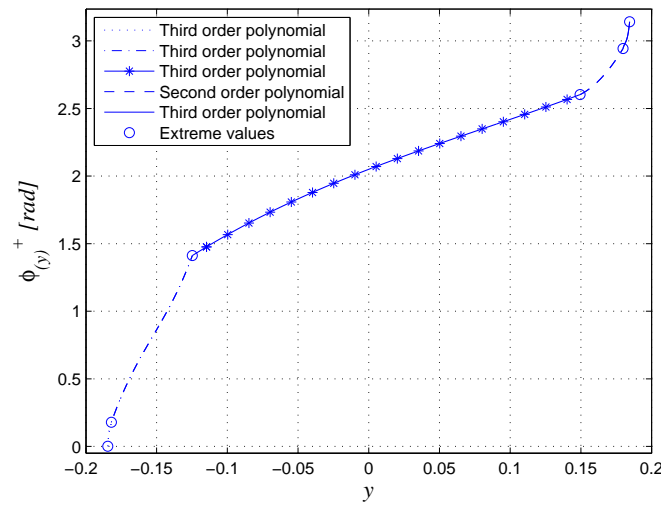
Figure 4.2: Piecewise phase function for the 2-neuron CPG

for different frequencies of the corresponding signal in steady state (after 1.8 seconds
of elapsed time).

$$\phi^+(y) = \begin{cases} \sum_{i=0}^{n_1} a_i y^i & y_{min} \leq y < l_1 \\[2em] \sum_{i=0}^{n_2} b_i y^i & l_1 \leq y < l_2 \\[2em] \sum_{i=0}^{n_3} c_i y^i & l_2 \leq y < l_3 \\[2em] \sum_{i=0}^{n_4} d_i y^i & l_3 \leq y < l_4 \\[2em] \sum_{i=0}^{n_5} e_i y^i & l_4 \leq y \leq y_{max} \end{cases} \tag{4.3}$$

4.3.3 Phase resetting strategy

Let $\xi(\phi)$ be a given phase resetting curve (PRC), which indicates the phase shifts
that must be applied to the CPG's reference signal according to its current phase,
which is estimated from its amplitude by $\phi(y)$, as defined in (4.2). The goal of phase
resetting is to apply the required phase shift at a given time instant t_0 in such a way
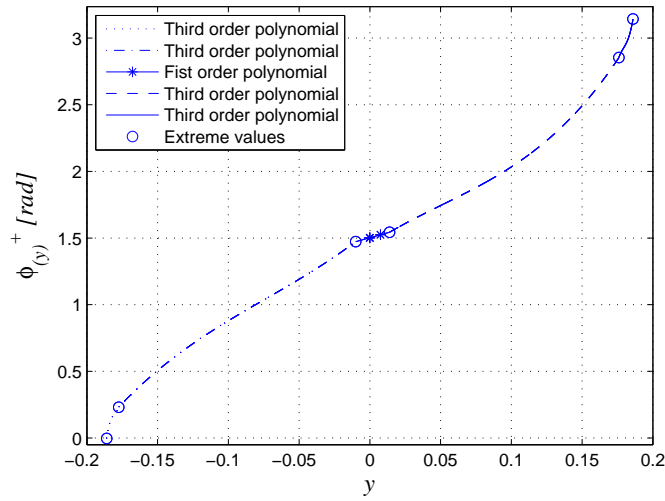
Figure 4.3: Piecewise phase function for the 4-neuron CPG

that the phase shift is effective by a predefined time interval Δt for all the CPG's outputs y_i. Let y_{t_0} be the amplitude of the CPG's reference signal at t_0. Since the PRC defines phase shifts between -2π and 2π, an equivalent positive phase shift $\Delta\phi_{t_0}$ is defined as:

$$\Delta\phi_{t_0} = \begin{cases} \xi(\phi(y_{t_0})) & \xi(\phi(y_{t_0})) \geq 0 \\ 2\pi + \xi(\phi(y_{t_0})) & \xi(\phi(y_{t_0})) < 0 \end{cases} \tag{4.4}$$

The angular velocity corresponding to a variation of $\Delta\phi_{t_0}$ radians over Δt seconds is:

$$\omega_{t_0} = \frac{\Delta\phi_{t_0}}{\Delta t} \tag{4.5}$$

In turn, the angular velocity of the CPG's reference signal is obtained from its frequency (4.1):

$$\omega = 2\pi\Gamma(K_f) = \frac{2\pi}{a_\mu K_f} \tag{4.6}$$

Therefore, from time t_0 to $t_0 + \Delta t$ the original angular velocity ω of the reference signal needs to be changed to ω_{t_0} to ensure that the desired phase is achieved at the end of that interval. This is done by introducing a pulse function, $\delta_f(t - t_0)$, which
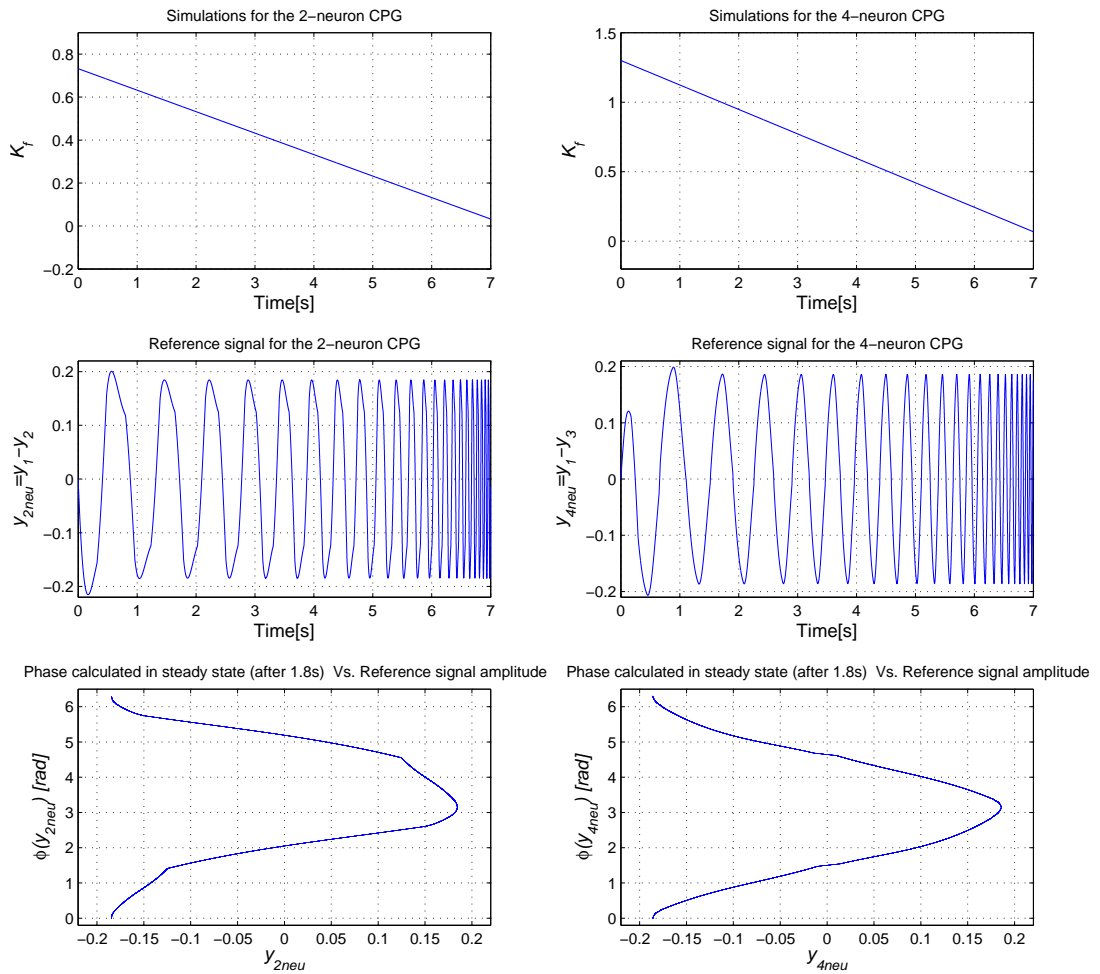
Figure 4.4: Simulation results for the 2-neuron and 4-neuron CPG

modulates the value of K_f only during that interval and which constitutes a new control input of the CPG:

$$\omega = \frac{2\pi}{a_\mu K_f \delta_f(t - t_0)} \tag{4.7}$$

This pulse function is defined as follows:

$$\delta_f(t - t_0) = \begin{cases} A_\delta & t_0 \leq t \leq t_0 + \Delta t \\ 1 & \text{otherwise,} \end{cases} \tag{4.8}$$
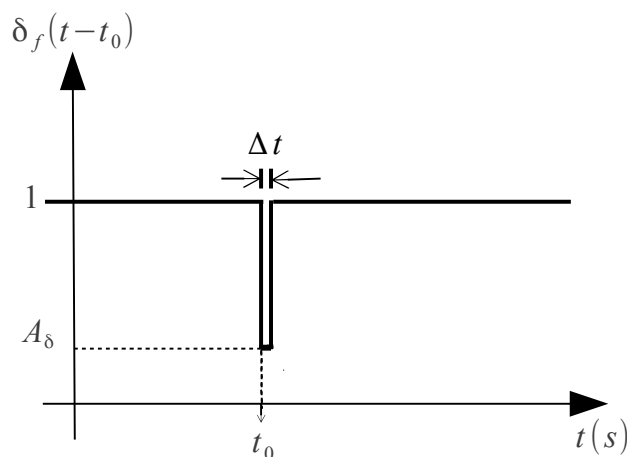
Figure 4.5: Pulse function

where:

$$A_\delta = \frac{2\pi}{a_\mu K_f \omega_{t_0}} \tag{4.9}$$

Figure 4.5 shows the graphical representation of the pulse function. The pulse width, Δt, is defined to obtain a phase resetting control with a bounded response time. That time can be increased or decreased depending on the problem to be solved and the hardware resources available. The pulse width is set to 10 ms.

4.4 Experimental results and discussion

4.4.1 Simulation results

Figures 4.7, 4.9, 4.11, and 4.13 show some simulation results of the proposed phase resetting scheme for the 2- and 4-neuron CPGs shown in figs. 2.7 and 2.15. As an example, the PRCs respectively defined by (4.10), (4.11), (4.12) and (4.13) for the 2- and 4-neuron CPGs have been used. These functions are shown in fig. 4.6, fig. 4.8, fig. 4.10 and fig. 4.12, respectively, along with the corresponding phase transition curves in order to highlight the new phase after the phase resetting scheme has been applied. Those PRCs can be conveniently tailored to the problem to be solved.

$$\xi_1(\phi) = \left\{ \begin{array}{ll} -\phi + \frac{\pi}{2} & 0 \leq \phi < 2\pi \end{array} \right. \tag{4.10}$$

Figure 4.6: Example of phase resetting curve and corresponding phase transition curve for the 2-neuron CPG
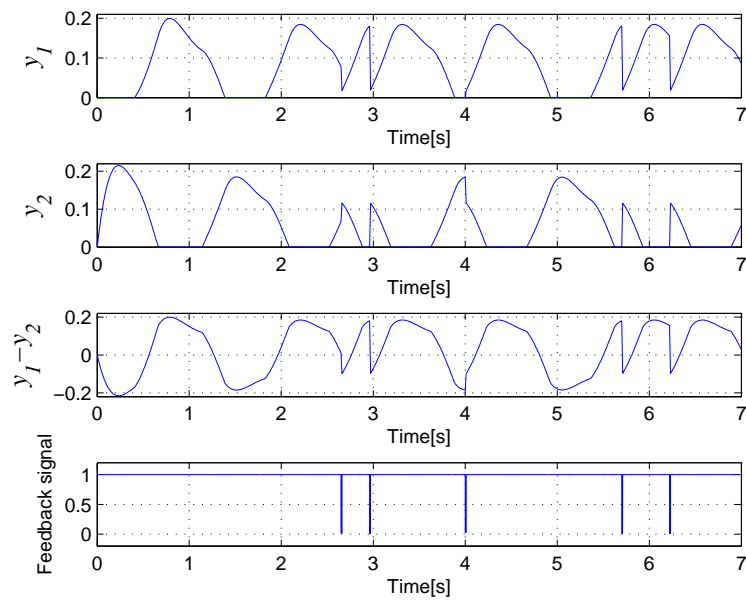
Figure 4.7: Example of phase resetting for the 2-neuron CPG by using the PRC shown in fig. 4.6

$$\xi_2(\phi) = \left\{ \begin{array}{ll} \pi \sin \phi & 0 \leq \phi < 2\pi \end{array} \right. \tag{4.11}$$

$$\xi_3(\phi) = \left\{ \begin{array}{ll} -\phi + \frac{\pi}{2} & 0 \leq \phi < \pi \\ \\ -\phi + \frac{3\pi}{2} & \pi \leq \phi < 2\pi \end{array} \right. \tag{4.12}$$

Figure 4.8: Example of phase resetting curve and corresponding phase transition curve for the 2-neuron CPG
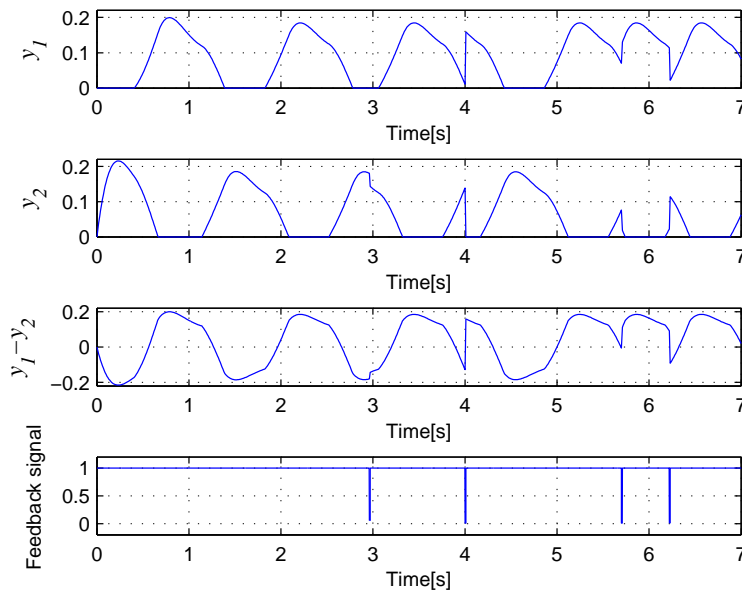
Figure 4.9: Example of phase resetting for the 2-neuron CPG by using the PRC shown in fig. 4.8

$$\xi_4(\phi) = \left\{ \begin{array}{ll} \frac{\pi}{2}\sin(2\phi) & 0 \leq \phi < 2\pi \end{array} \right. \tag{4.13}$$

The proposed phase resetting scheme can support on-line learning by redefining the PRC function $\xi(\phi)$ at run time. Therefore, it enables the system to modify the behaviour of the closed-loop controller in accordance with, for example, previous observations made by the system. This is advantageous for adaptive robot control.

Figure 4.10: Example of phase resetting curve and corresponding phase transition curve for the 4-neuron CPG
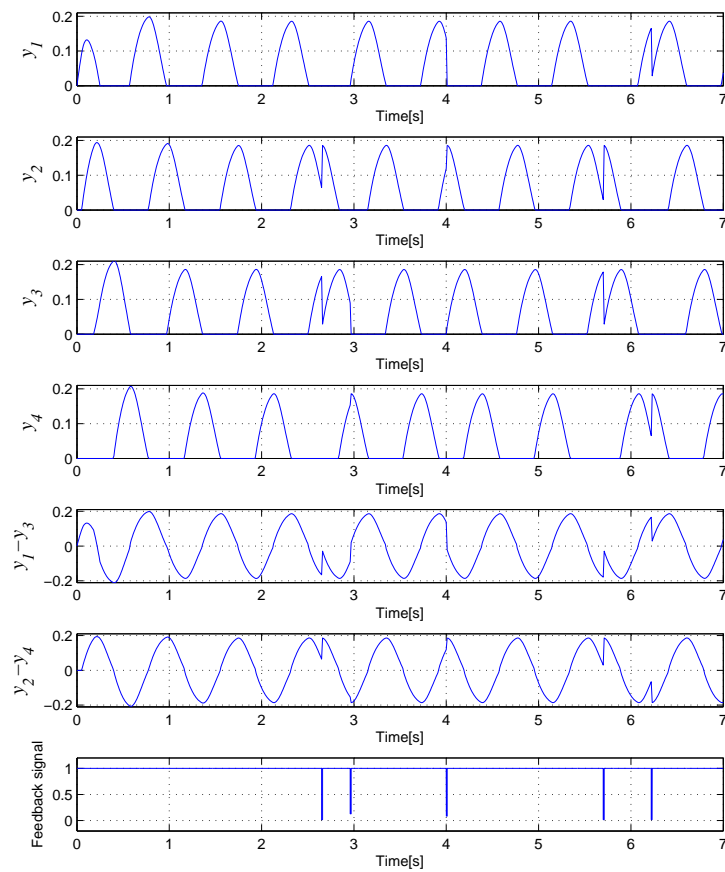
Figure 4.11: Example of phase resetting for the 4-neuron CPG by using the PRC shown in fig. 4.10
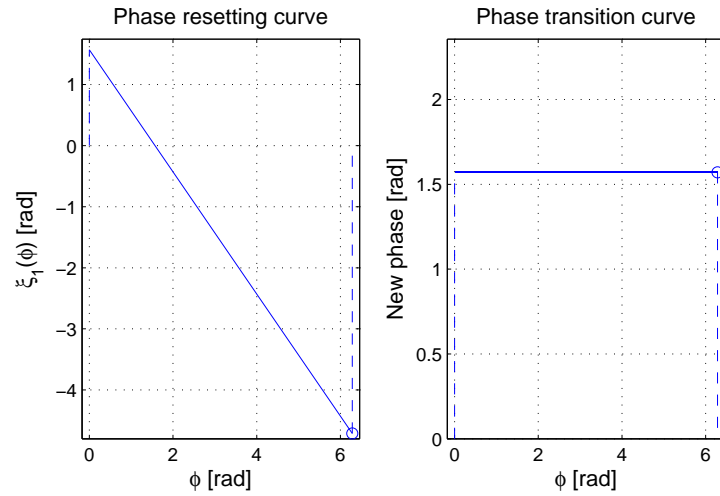
Figure 4.12: Example of phase resetting curve and corresponding phase transition curve for the 4-neuron CPG
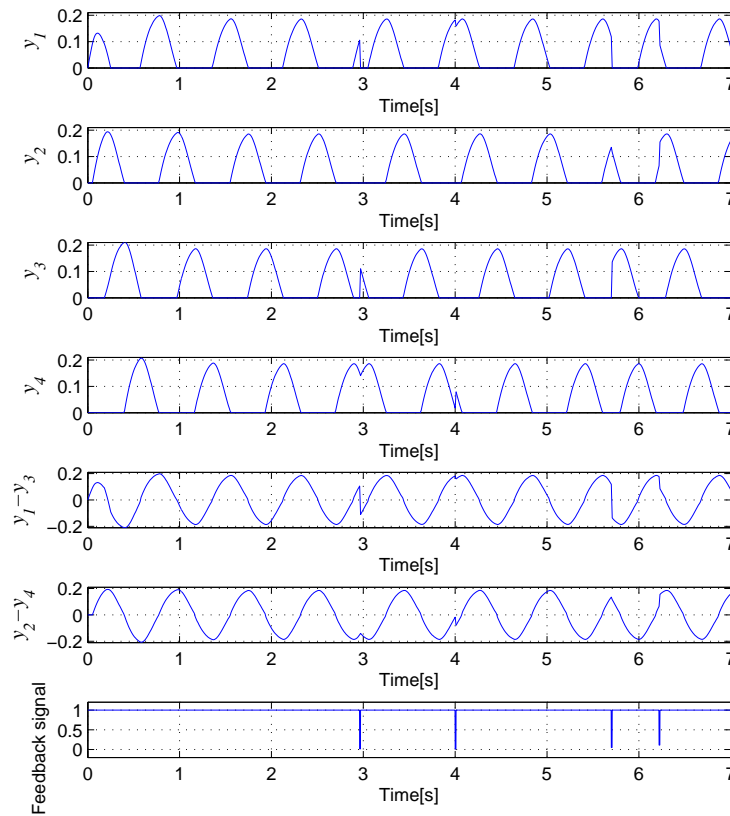
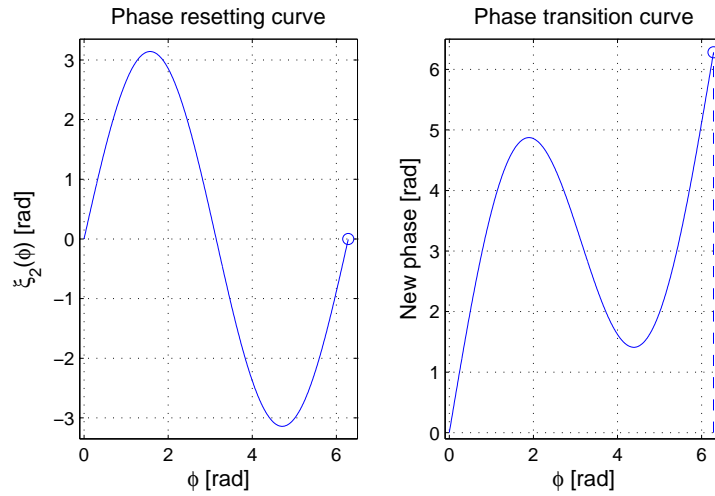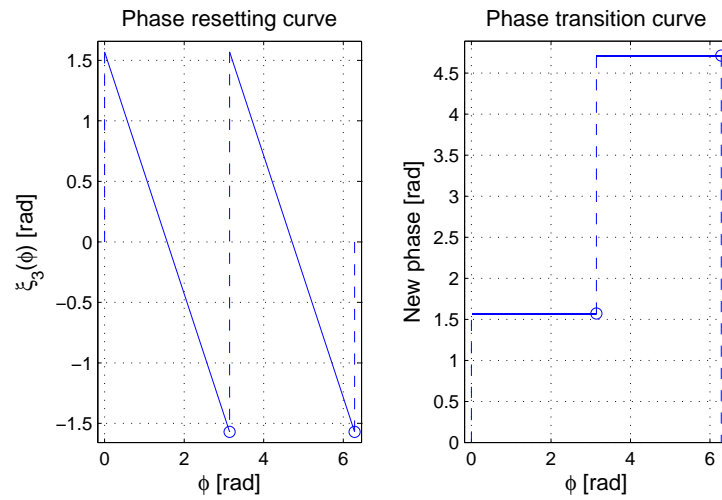**Figure 4.13:** Example of phase resetting for the 4-neuron CPG by using the PRC shown in fig. 4.12
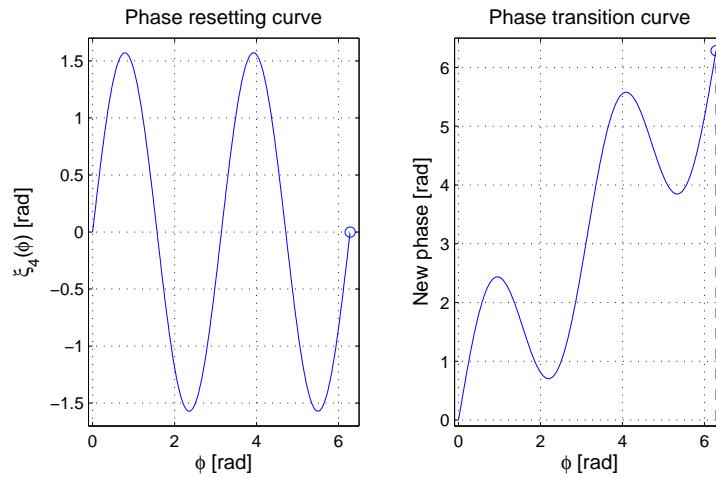
In addition, the system can use a variety of PRCs to robustly cope with various external stimuli gathered by its sensors.

4.4.2 Application to bipedal locomotion: Fast synchronization of the interaction between the robot's feet and the terrain

This section discusses a practical application of the proposed phase resetting scheme to closed-loop locomotion control of biped robots for synchronizing the interaction between the robot's feet and the walking surface. In particular, the proposed control scheme was implemented in the CPG network previously proposed in section 3.2.1 for controlling the locomotion of a NAO humanoid robot. Figure 3.2 shows the schematic representation of that CPG network, whose parameters are described in section 3.2. This CPG network consists of a Matsuoka master oscillator that drives a subset of slave Matsuoka oscillators whose outputs control the angular displacement of the robot's joints. The topology of these oscillators is shown in fig. 2.6.

In humanoid robots, phase resetting has been proposed for synchronizing the interaction between the robot's feet and the walking surface (Aoi and Tsuchiya, 2007; Nakanishi et al., 2004). Namely, every time a robot's foot comes into contact with the floor, the phase of the locomotion pattern is modified to the phase associated with the impact time so that the pattern can be synchronized to this real-time interaction. The phase resetting scheme proposed here was applied to the network depicted in fig. 3.2 in order to show a practical application in a real robot. The response time was set to 10 ms to ensure a fast reaction whenever the phase resetting mechanism is applied to the system. Figure 4.14 shows the phase resetting curve and the corresponding phase transition curve that were chosen to ensure correct synchronization between the robot's feet and the floor. The PRC used in this practical example is given in (4.14). The goal of this function is to define the phase shifts that must be applied to the system so that the current phase can be changed for the correct phase associated with the real interaction between the feet and the floor.

As can be appreciated in the PTC shown in fig. 4.14, the system synchronizes the locomotion pattern at the two instants that each foot is in contact with the floor. Figure 4.15 shows an example of the phase resetting mechanism applied to
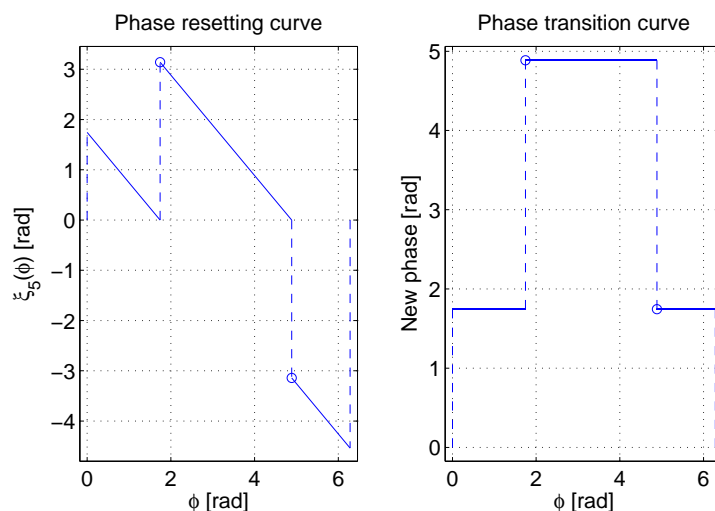
Figure 4.14: Example of phase resetting curve and corresponding phase transition curve for bipedal locomotion
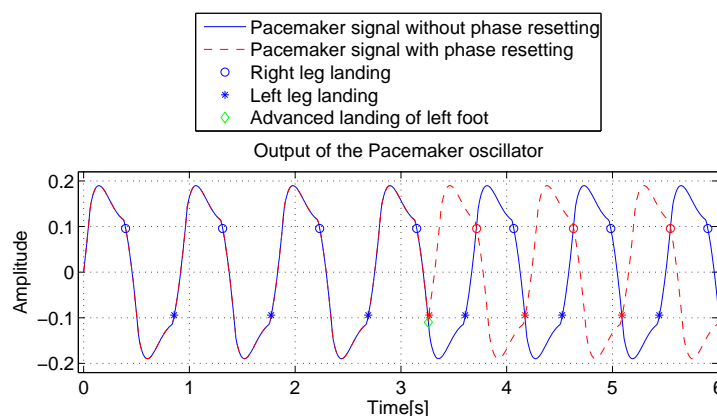
Figure 4.15: Phase resetting example for the pacemaker oscillator of the network shown in fig. 3.2

the pacemaker oscillator of the network shown in fig. 3.2. A sequence of snapshots showing the performance of the system in a NAO humanoid robot can be seen in fig. 4.16 (top) with no phase resetting and fig. 4.16 (bottom) with the proposed phase resetting scheme. When phase resetting is not active, the robot falls down when trying to walk over an obstacle. Alternatively, with phase resetting, the robot manages to negotiate the obstacle safely. The full video sequences with the NAO robot in simulation and on a real setup are shown in the companion website.[1]

---

[1]Companion website: http://deim.urv.cat/%7Erivi/NAO%5F2015.html
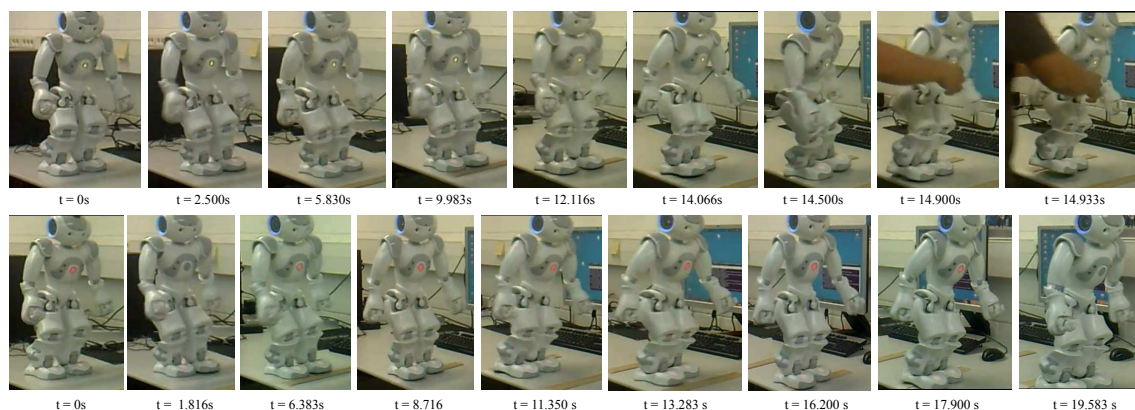
Figure 4.16: System behaviour without (top) and with (bottom) phase resetting

$$
\xi_5(\phi) = \begin{cases} -\phi + \frac{5\pi}{9} & 0 \le \phi \le \frac{5\pi}{9} \;\; \text{or} \;\; \frac{14\pi}{9} < \phi \le 2\pi \\[2em] -\phi + \frac{14\pi}{9} & \frac{5\pi}{9} < \phi \le \frac{14\pi}{9} \end{cases}
\tag{4.14}
$$

4.4.3   Application to bipedal locomotion: Fast balance recovery

This section discusses a practical application of the proposed phase resetting scheme to closed-loop locomotion control of biped robots for recovering balance after external perturbations. In particular, phase resetting is a fast and simple feedback strategy that has also been used to change the phase of the locomotion pattern generated by the control system in order to recover the robot's balance whenever an external perturbation is applied to the robot's body (Nakanishi et al., 2006; Nomura et al., 2009). This effective feedback strategy is suitable for humanoid robots with reduced computational capability since it does not require a complex processing of data. In this section, a simple experiment is presented to show the suitability of the second locomotion control scheme proposed in this thesis along with the proposed phase resetting mechanism for fast recovery of balance in biped robots.

The closed-loop system for locomotion control of biped robots with phase resetting must detect the external force applied to the robot's body through the fast analysis and tracking of the measures provided by the robot's sensors. Once

the external perturbation is detected by the system, it must react by activating the phase resetting mechanism in order to quickly recover balance.

The phase resetting mechanism proposed in this chapter synchronizes the neurons' output signals in order to modify the current phase of the locomotion pattern generated by the system to a desired phase given an external event or stimulus, such as the external force applied to the robot's body. The aim of this mechanism is the generation of a force in the direction opposite to the one of the force generated by the external perturbation by changing the phase of the current locomotion pattern in order to guarantee the fast recovery of balance.

The information provided by the 3-axis accelerometer is used to detect the instant at which the external force is applied to the robot's body and also to estimate the magnitude and direction of the external force applied to the robot's body. According to the current phase of the generated locomotion pattern and the external force applied to the robot, the phase resetting controller must react by changing the current phase of the locomotion pattern to another phase that allows the robot to recover its balance. The phase change is effective after Δt seconds, as was explained in this chapter.
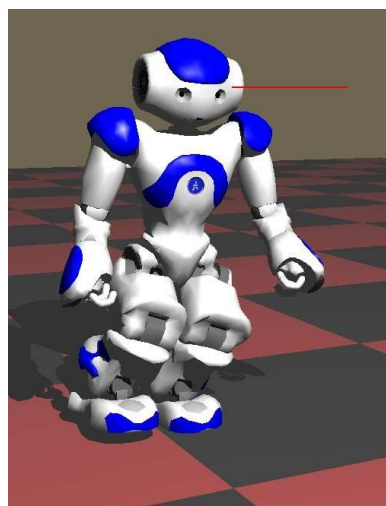
Figure 4.17: Instant at which the external perturbation is applied to the robot's head

In the experiment described below, the external force was considered to be applied to the robot's head along a known direction defined manually. This force guarantees that the robot will fall down when the feedback mechanism is not
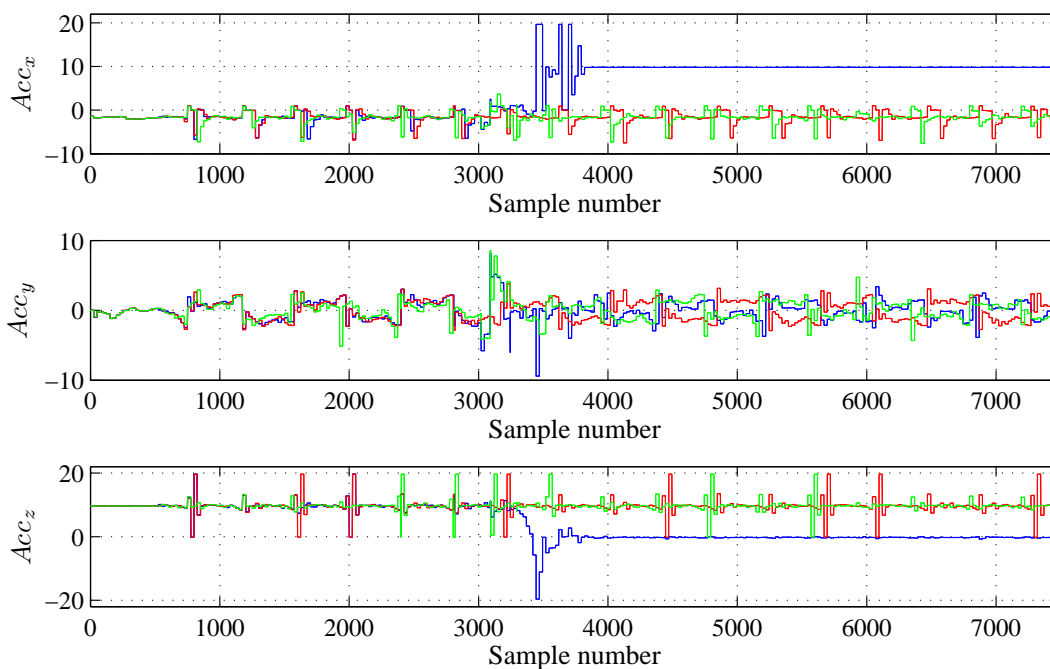
Figure 4.18: Measures provided by the accelerometer located in the robot's trunk. The measures are in $\frac{m}{s^2}$. In the plots, the red line represents the system response when there is no external force applied to the robot's body. Thus, the robot is just walking. The blue line represents the behaviour when the external force is applied to the robot's head and the phase resetting controller is not activated. Finally, the green line represents the behaviour when the phase resetting controller is activated and the external force is applied to the robot's head.

activated. Therefore, it has been used to test the system operating in both open and closed loop. The simulator allows the definition of the exact point in the robot's body in which the force is applied, as well as its desired magnitude and direction. The external force was also applied at a known phase of the locomotion pattern and at the same point on the robot's body in order to test the system under the same dynamic conditions.

The external force was applied at the instant in which the robot is standing on a single foot (right foot at the highest position and left foot supporting the full robot's weight). This pose was chosen as an example to validate that the control system is able to deal with unstable situations. Figure 4.17 represents the instant at which the external force is applied to the robot's head while the robot is standing on its left foot.

The locomotion pattern was generated by means of the second proposed
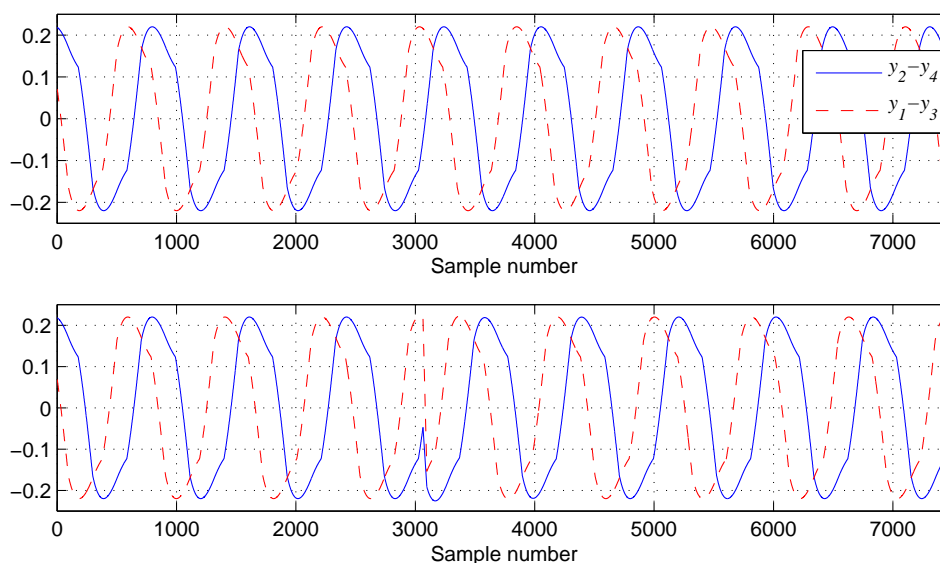
Figure 4.19: Output signals of the 4-neuron CPG network shown in fig. 2.15. The plots represent the system's response without (top) and with (bottom) the proposed phase resetting mechanism.

CPG-joint-space control scheme, with the parameters found for the straight-line locomotion pattern by considering a walking speed of 5 cm/s. That speed is similar to the one used by Nakanishi et al. (2006). The phase resetting mechanism proposed in this chapter was used to change the current locomotion pattern's phase. In the experiment, the controller's response time (Δt) was set to 40 ms. However, this time could be smaller according to the desired system's response.

Figure 4.18 represents the measures provided by the robot's accelerometer for 3 possible situations, namely, the system response in open-loop without any external force applied to the robot's head (red), the system response in open loop with the external force applied to the robot's head (blue) and, finally, the system response in closed-loop with the external force applied to the robot's head (green). The sampling time was set to 1.7 ms. The information provided by the robot's accelerometer was used in order to determine the instant in which the external force is applied to the robot's body and thus the phase resetting controller is activated. The effect of the phase resetting mechanism in the output signals generated by the CPG network (see fig. 2.15) used to control the generated locomotion pattern is shown in fig. 4.19. From these figures it can be observed the fast and stable response produced by the
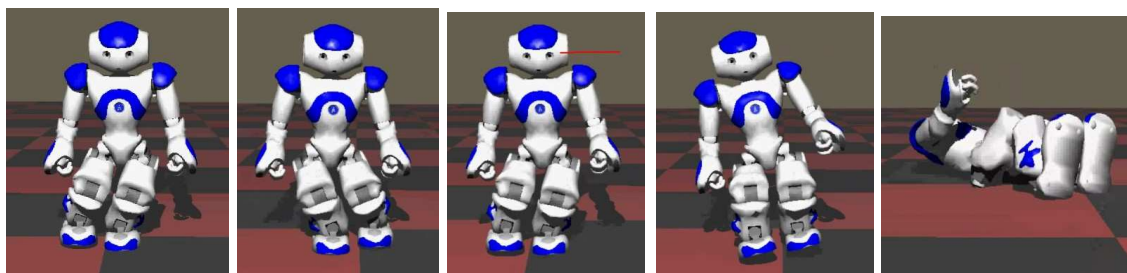
Figure 4.20: System behaviour with phase resetting off.
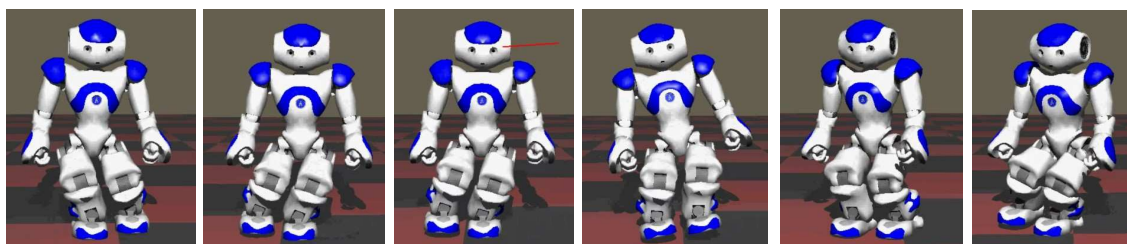
Figure 4.21: System behaviour with phase resetting on.

system.

The effect of the phase resetting mechanism can be appreciated in fig. 4.19 and in the plots shown in fig. 4.18. The external force is detected by the system in sample number 3064. The feedback mechanism is activated at that instant. After the controller's response time (40 ms) the system compensates for the external force applied to the humanoid robot's head through a fast motion that generates a force in the opposite direction. This minimizes the effect of the external perturbation and manages to recover balance quickly.

A sequence of snapshots showing the performance of the robot when phase resetting is off and on are shown in fig. 4.20 and fig. 4.21, respectively. These experiments have shown that the closed-loop response is fast and effective, which makes this system suitable for humanoid robots with reduced processing capabilities. This system can also deal with larger forces than those tackled by other control strategies.

A video with some sequences that show the system behaviour for both open and closed-loop with the NAO humanoid robot in simulation can be found in the companion website.[2]

---

[2]Companion website: https://www.youtube.com/watch?v=lnQTjFjP-VM

4.5   Summary

A new phase resetting mechanism for CPG networks consisting of interconnected Matsuoka's neuron models has been proposed. It allows control systems to change the current phase of rhythmical output signals generated by CPG networks in real-time and in a stable and well characterized way through a single-pulse perturbation. This mechanism can be applied to robotics control and adaptive control systems which require phase resetting with a bounded response time.

By adapting the PRCs, the proposed phase resetting scheme can define a wide range of controllers that properly react according to sensory feedback provided by force and inertial sensors. These curves can also be modified through on-line learning. In addition, with this approach, several CPG networks can effectively interact with one another to carry out specific tasks.

This feedback strategy was designed so that it could be introduced into the proposed control systems based on CPGs networks implemented with Matsuoka's neuron model. Experiments performed with the humanoid robot indicate the effectiveness of this feedback into the system. Future work will include the detailed study of feedback controllers that use the phase resetting mechanism, particularly for the system proposed in section 3.3, to cope with balance recovery in complicated unstable situations for the humanoid robot. Some initial experiments similar to those performed by Nakanishi et al. (2006) indicate that the system proposed in section 3.3 in combination with the phase resetting mechanism proposed in this chapter will allow the robot to deal with more challenging situations.

CHAPTER 5

Conclusions

"The basis of success is to insist, persist, resist and never desist."

Two closed-loop control architectures based on CPG-joint-space control methods have been proposed and tested by using a simulated and a real NAO humanoid robot. The locomotion control systems were implemented using CPG networks based on Matsuoka's neuron model. The first control architecture identified some important features that a CPG-joint-space control scheme must have if a useful locomotion pattern is to be described. On the basis of this analysis, the second control architecture was proposed to describe well-characterized locomotion patterns. The new system, characterized by optimized parameters obtained with a GA, effectively generated and controlled locomotion patterns for biped robots.

To improve how the system behaves in closed loop, a phase resetting mechanism for CPG networks based on Matsuoka's neuron model has been proposed. It makes it possible to design and study feedback controllers that can quickly modify the locomotion pattern generated by the response described by a phase resetting curve.

The results are similar to those previously presented in chapter 2 of this thesis. Even though the costly inverse kinematics is not solved, the system still describes a well-characterized omnidirectional locomotion pattern that can be modulated quickly at any time so that complex situations can be coped with. The results show that CPG-joint-space control schemes can yield well-characterized locomotion patterns with a fast response suitable for humanoid robots with a reduced processing capability. Initial experiments indicate that the phase resetting controllers enable the robot to respond quickly and robustly, and to cope with complex situations. A summary with the main contributions of this thesis and some suggestions for future research directions are presented below.

5.1   Summary of contributions

5.1.1   CPG-joint-space control schemes for generating and controlling well-characterized locomotion patterns for biped robots on flat terrain

Two closed-loop control architectures based on a CPG network have been proposed for generating and controlling locomotion patterns for biped robots. These control schemes work in the CPG-joint-space, which means that response is fast and the inverse kinematics problem does not have to be solved. The CPG networks were modelled using the well-known model proposed by Matsuoka. Some feedback mechanisms have been incorporated into the system so that a variety of terrains can be dealt with. The systems were designed in such a way that the number of control parameters was minimized.

Many of the studies mentioned above use CPG networks to describe the motion in the task space because that makes it easier to understand the signal generation process and guarantee well-characterized locomotion patterns so that correct control strategies can be developed. However, the computation of the inverse kinematics delays the system's response since it is a very time-consuming process. Thus, the CPG-joint-space control scheme proposed in section 3.3 was designed so that the system would describe well-characterized locomotion patterns that can be modulated quickly without having to solve the inverse kinematics and make it easy to understand the signal generation process and the effect of each variable on the locomotion pattern generated by the system. It is important to have a detailed understanding of the effect of each variable on the system because only in this way can the system be constantly improved (for instance, by adding more useful controllers).

The control system discussed in section 3.3 describes well-characterized locomotion patterns whose behaviour is represented by a few parameters found by a GA. Many previous approaches use numerous parameters and complex networks, which makes it very difficult to analyse the signal generation process and incorporate useful feedback controllers. The well-characterized locomotion pattern generated by the system and its fast response together with the well-known effect of each variable on the system's output signals means that the locomotion pattern can be modulated on-line so that the current gait can be changed. The experiments performed in section 3.3 demonstrate that the locomotion patterns generated allow the robot to freely navigate by activating the omnidirectional controller and deal with different walking surfaces. The results are similar to those presented in previous studies but the response is faster because there is no need to continuously solve the inverse kinematics.

5.1.2 Well-characterized CPG-joint-space control scheme for the locomotion control of biped robots on inclined terrain

The results obtained with the control system proposed in section 3.3 made it possible to deal with inclined surfaces up to $+/-$ 10 degrees. As can be seen from table 2.1, this indicates that the control system produces locomotion patterns comparable to other state-of-the-art systems for humanoid robots with similar kinematic structures. Similar studies have previously been carried out with the same humanoid robot and CPG-based locomotion control on sloped surfaces. However, the most robust of these previous approaches need to solve the costly inverse kinematics problem (Liu et al., 2013b; Song and Hsieh, 2014), and the other approaches do not ensure stable interaction with the floor, since the robot tends to drag its feet when walking, which is very likely to lead to falls on uneven terrain (Nassour et al., 2013). The results presented in this thesis were obtained by means of a control scheme in the CPG-joint-space that generates well-characterized locomotion patterns, which reduce the processing requirements and enable the robot to react faster and walk on inclined surfaces.

5.1.3   Phase resetting mechanism for CPG networks implemented with Matsuoka's neuron model

The detailed study of Matsuoka's neuron model and the proposed CPG networks built using this model led to the proposal of a useful mechanism for resetting the phase of the neurons' output signals. Although this mechanism was used in this thesis for the closed-loop control of biped locomotion it can also be used in biomedical and other control applications in which the phase resetting mechanism is a useful feedback strategy. This is because of the fast response of this feedback mechanism which makes it suitable for real-time systems.

In addition, with this approach, several CPG networks can effectively interact with one another to carry out specific tasks. Thus, the proposed phase resetting scheme can be used to implement a control scheme that can learn and generate complex signals for reproducing various complex rhythmical patterns, such as those proposed by Gams et al. (2009).

5.1.4 Well-described system for the detailed study of phase resetting controllers for quick recovery after loss of balance

The control scheme presented in section 3.3 in combination with the phase resetting mechanism presented in chapter 4 establish a system for studying and characterizing phase resetting controllers. By combining this control scheme and the phase resetting mechanism that allows a quick reaction, optimal phase resetting controllers can be defined that can cope with more complex situations (for instance, external forces from different directions applied directly to the robot's body). Initial experiments performed with the robot indicate that phase resetting controllers are the best way of getting the robot to react quickly and compensate for external disturbances.

5.2 Future research lines

5.2.1 Detailed analysis of the parameters that characterize the second control scheme proposed

Future research work will include a rigorous study of the variation in the internal parameters of the system proposed to control the locomotion of biped robots. The aim is to establish mathematical models that enable the system to automatically determine optimal parameters and the relationship between them for any desired locomotion pattern specified by a required walking speed and direction.

5.2.2 Detailed analysis of phase resetting controllers for the locomotion control of biped robots

The detailed analysis of phase resetting controllers will be useful to design additional feedback controllers so that robots can cope with more complex types of terrain and deal with unknown external perturbations.

For example, a detailed study will be carried out, first in simulation and then in a real robot, of the phase resetting mechanism for unknown external forces applied directly to the robot's structure from different directions. This study makes it possible to characterize the phase resetting controllers that improve the system's behaviour because they will react faster in unpredictable situations. Therefore, it is very important to make a quick analysis of the information provided by the robot's sensors because the effect of the current sensory information on the system will guarantee a fast and appropriate system response.

The feedback controllers that use the phase resetting mechanism will be studied in detail for the system proposed in section 3.3 in combination with the phase resetting mechanism proposed in chapter 4. This will make it possible to define phase resetting controllers that can cope with balance recovery after loss of balance due to complicated unstable situations for the humanoid robot. Initial experiments have been performed similar to those presented in (Nakanishi et al., 2006), which indicated that the system proposed in section 3.3 in combination with the phase resetting mechanism proposed in chapter 4 allow the robot to react quickly and deal with more challenging situations. Future work will include the detailed analysis and characterization of these controllers.

5.2.3   On-line learning of phase resetting controllers

Some experiments performed with the control system proposed in section 3.3 and the phase resetting mechanism in chapter 4 indicate that the phase resetting controllers improve the system's behaviour. Thus, it could be interesting to use on-line learning of feedback controllers in order to redefine the fixed phase resetting curve that characterizes the behaviour of the phase resetting mechanism. A control scheme must be defined that incorporates learning by redefining the PRC in real-time in accordance with the real-time analysis of the sensory information and the real robot's response.

5.3 Publications derived from this thesis

5.3.1 Journals

1. **Julián Cristiano**, Miguel Ángel García, Domènec Puig, Deterministic phase resetting with predefined response time for CPG networks based on Matsuoka's oscillator, *Robotics and Autonomous Systems* 74, Part A, pp. 88-96. (2015). (Cristiano et al., 2015a). Impact factor: 1.256. Robotics (Q2).

2. **Julián Cristiano**, Domènec Puig, Miguel Ángel García, Efficient locomotion control of biped robots on unknown sloped surfaces with central pattern generators, *Electronics Letters*, 51 (3), pp. 220-222. (2015). (Cristiano et al., 2015b). Impact factor: 0.930. Engineering, electrical and electronic (Q3).

5.3.2 Book chapters from international conferences proceedings

3. **Julián Cristiano**, Domènec Puig, Miguel Ángel García, Locomotion control of a biped robot through a feedback cpg network. In Armada, M. A., Sanfeliu, A., and Ferre, M., editors, *ROBOT2013: First Iberian Robotics Conference*, Advances in Intelligent Systems and Computing, volume 252, pages 527-540. Springer International Publishing. 2014. (Cristiano et al., 2014)

4. Jainendra Shukla, **Julián Cristiano**, David Amela, Laia Anguera, Jaume Vergés-Llahí, Domènec Puig, A Case Study of Robot Interaction among Individuals with Profound and Multiple Learning Disabilities. *International Conference on Social Robotics, ICSR 2015*. Lecture Notes in Computer Science, volume 9388, pp. 613-622. Springer International Publishing. 2015 (Shukla et al., 2015).

5. Jainendra Shukla, **Julián Cristiano**, Laia Anguera, Jaume Vergés-Llahí, Domènec Puig, A Comparison of Robot Interaction with Tactile Gaming Console Stimulation in Clinical Applications, Accepted for publication in *ROBOT2015: Second Iberian Robotics Conference*, Advances in Intelligent

Systems and Computing.

5.3.3   Spanish conferences

6. **Julián Cristiano**, Domènec Puig, Miguel Ángel García, On the maximum walking speed of NAO humanoid robots, in proceedings of *XII Workshop of Physical Agents*, Albacete, España, pp. 3-7. ISBN: 978-84-694-6730-5, 2011. (Cristiano et al., 2011)

7. **Julián Cristiano**, Domènec Puig, Miguel Ángel García, Locomotion control of biped robots on uneven terrain through a feedback CPG network, in proceedings of *XIV Workshop of Physical Agents*, Madrid, España, pp. 1-6. ISBN: 978-84-695-8319-7, 2013. (Cristiano et al., 2013)

References

Aoi, S., Egi, Y., Sugimoto, R., Yamashita, T., Fujiki, S., and Tsuchiya, K. (2012a). Functional Roles of Phase Resetting in the Gait Transition of a Biped Robot From Quadrupedal to Bipedal Locomotion. *IEEE Transactions on Robotics*, 28(6):1244–1259.

Aoi, S., Katayama, D., Fujiki, S., Kohda, T., Senda, K., and Tsuchiya, K. (2012b). Cusp catastrophe embedded in gait transition of a quadruped robot driven by nonlinear oscillators with phase resetting. In *ROBIO*, pages 384–389.

Aoi, S., Ogihara, N., Funato, T., Sugimoto, Y., and Tsuchiya, K. (2010). Evaluating functional roles of phase resetting in generation of adaptive human bipedal walking with a physiologically based model of the spinal pattern generator. *Biological Cybernetics*, 102(5):373–387.

Aoi, S. and Tsuchiya, K. (2005). Locomotion Control of a Biped Robot Using Nonlinear Oscillators. *Autonomous Robots*, 19(3):219–232.

Aoi, S. and Tsuchiya, K. (2006). Stability analysis of a simple walking model

driven by an oscillator with a phase reset using sensory feedback. *Robotics, IEEE Transactions on*, 22(2):391–397.

Aoi, S. and Tsuchiya, K. (2007). Adaptive behavior in turning of an oscillator-driven biped robot. *Autonomous Robots*, 23(1):37–57.

Bekey, G. A. (2005). *Autonomous Robots: From Biological Inspiration to Implementation and Control.* Intelligent Robotics and Autonomous Agents series, MIT Press.

Bicanski, A., Ryczko, D., Knuesel, J., Harischandra, N., Charrier, V., Ekeberg, Ö., Cabelguen, J.-M., and Ijspeert, A. (2013). Decoding the mechanisms of gait generation in salamanders by combining neurobiology, modeling and robotics. *Biological Cybernetics*, 107(5):545–564.

Choi, Y., Kim, D., Oh, Y., and You, B.-J. (2007). Posture/Walking Control for Humanoid Robot Based on Kinematic Resolution of CoM Jacobian With Embedded Motion. *Robotics, IEEE Transactions on*, 23(6):1285–1293.

Crespi, A. and Ijspeert, A. (2008). Online Optimization of Swimming and Crawling in an Amphibious Snake Robot. *Robotics, IEEE Transactions on*, 24(1):75–87.

Cristiano, J., García, M. A., and Puig, D. (2015a). Deterministic phase resetting with predefined response time for CPG networks based on Matsuoka's oscillator. *Robotics and Autonomous Systems*, 74, Part A:88–96.

Cristiano, J., Puig, D., and García, M. (2011). On the maximum walking speed of NAO humanoid robots. In *XII Workshop of Physical Agents*, pages 3–7.

Cristiano, J., Puig, D., and García, M. (2013). Locomotion control of biped robots on uneven terrain through a feedback CPG network. In *XIV Workshop of Physical Agents*, pages 1–6.

Cristiano, J., Puig, D., and García, M. (2014). Locomotion Control of a Biped Robot through a Feedback CPG Network. In Armada, M. A., Sanfeliu, A.,

and Ferre, M., editors, *ROBOT2013: First Iberian Robotics Conference*, volume 252 of *Advances in Intelligent Systems and Computing*, pages 527–540. Springer International Publishing.

Cristiano, J., Puig, D., and García, M. (2015b). Efficient locomotion control of biped robots on unknown sloped surfaces with central pattern generators. *Electronics Letters*, 51(3):220–222.

Danion, F., Varraine, E., Bonnard, M., and Pailhous, J. (2003). Stride variability in human gait: the effect of stride frequency and stride length. *Gait and Posture*, 18(1):69–77.

Dietz, V. (2003). Spinal cord pattern generators for locomotion. *Clinical Neurophysiology*, 114(8):1379–1389.

Ding, M. and Glanzman, D. (2011). *The Dynamic Brain: An Exploration of Neuronal Variability and Its Functional Significance.* Oxford University Press.

Endo, G., Morimoto, J., Matsubara, T., Nakanishi, J., and Cheng, G. (2008). Learning CPG-based Biped Locomotion with a Policy Gradient Method: Application to a Humanoid Robot. *The International Journal of Robotics Research*, 27(2):213–228.

Endo, G., Morimoto, J., Nakanishi, J., and Cheng, G. (2004). An Empirical Exploration of a Neural Oscillator for Biped Locomotion Control. In *ICRA*, pages 3036–3042. IEEE.

Endo, G., Nakanishi, J., Morimoto, J., and Cheng, G. (2005). Experimental Studies of a Neural Oscillator for Biped Locomotion with QRIO. In *Robotics and Automation, 2005. ICRA 2005. Proceedings of the 2005 IEEE International Conference on*, pages 596–602.

Galán, R. F., Ermentrout, G. B., and Urban, N. N. (2005). Efficient Estimation of Phase-Resetting Curves in Real Neurons and its Significance for Neural-Network Modeling. *Phys. Rev. Lett.*, 94:158101.

Gams, A., Ijspeert, A., Schaal, S., and Lenarčič, J. (2009). On-line learning and modulation of periodic movements with nonlinear dynamical systems. *Autonomous Robots*, 27(1):3–23.

Gouaillier, D., Collette, C., and Kilner, C. (2010). Omni-directional closed-loop walk for NAO. In *Humanoid Robots (Humanoids), 2010 10th IEEE-RAS International Conference on*, pages 448–454.

Gouaillier, D., Hugel, V., Blazevic, P., Kilner, C., Monceaux, J., Lafourcade, P., Marnier, B., Serre, J., and Maisonnier, B. (2009). Mechatronic design of NAO humanoid. In *Robotics and Automation, 2009. ICRA '09. IEEE International Conference on*, pages 769–774.

Granada, A., Hennig, R., Ronacher, B., Kramer, A., and Herzel, H. (2009). Chapter 1 Phase Response Curves: Elucidating the Dynamics of Coupled Oscillators. In Johnson, M. L. and Brand, L., editors, *Computer Methods, Part A*, volume 454 of *Methods in Enzymology*, pages 1–27. Academic Press.

Ha, I., Tamura, Y., and Asama, H. (2011). Gait pattern generation and stabilization for humanoid robot based on coupled oscillators. In *Intelligent Robots and Systems (IROS), 2011 IEEE/RSJ International Conference on*, pages 3207–3212.

Huang, W., Chew, C.-M., and Hong, G.-S. (2008). Coordination between oscillators: An important feature for robust bipedal walking. In *Robotics and Automation, 2008. ICRA 2008. IEEE International Conference on*, pages 3206–3212.

Ijspeert, A. J. (2008). Central pattern generators for locomotion control in animals and robots: a review. *Neural Networks*, 21(4):642–653.

Inada, H. and Ishii, K. (2003). Behavior generation of bipedal robot using central pattern generator(CPG) (1st report: CPG parameters searching method by genetic algorithm). In *Intelligent Robots and Systems, 2003. (IROS 2003). Proceedings. 2003 IEEE/RSJ International Conference on*, volume 3, pages 2179–2184 vol.3.

Kajita, S., Kanehiro, F., Kaneko, K., Fujiwara, K., Harada, K., Yokoi, K., and Hirukawa, H. (2003). Biped walking pattern generation by using preview control of zero-moment point. In *Robotics and Automation, 2003. Proceedings. ICRA '03. IEEE International Conference on*, volume 2, pages 1620–1626 vol.2.

Kajita, S., Kanehiro, F., Kaneko, K., Fujiwara, K., Yokoi, K., and Hirukawa, H. (2002). A realtime pattern generator for biped walking. In *Robotics and Automation, 2002. Proceedings. ICRA '02. IEEE International Conference on*, volume 1, pages 31–37 vol.1.

Kamimura, A., Kurokawa, H., Yoshida, E., Murata, S., Tomita, K., and Kokaji, S. (2005). Automatic locomotion design and experiments for a Modular robotic system. *Mechatronics, IEEE/ASME Transactions on*, 10(3):314–325.

Kimura, H., Fukuoka, Y., and Cohen, A. H. (2007). Adaptive Dynamic Walking of a Quadruped Robot on Natural Ground Based on Biological Concepts. *I. J. Robotic Res.*, 26(5):475–490.

Lewis, M., Tenore, F., and Etienne-Cummings, R. (2005). CPG Design using Inhibitory Networks. In *Robotics and Automation, 2005. ICRA 2005. Proceedings of the 2005 IEEE International Conference on*, pages 3682–3687.

Liu, C., Chen, Q., and Wang, D. (2011). CPG-Inspired Workspace Trajectory Generation and Adaptive Locomotion Control for Quadruped Robots. *Systems, Man, and Cybernetics, Part B: Cybernetics, IEEE Transactions on*, 41(3):867–880.

Liu, C., Chen, Q., and Wang, G. (2013a). Adaptive walking control of quadruped robots based on central pattern generator (CPG) and reflex. *Journal of Control Theory and Applications*, 11(3):386–392.

Liu, C., Wang, D., and Chen, Q. (2013b). Central Pattern Generator Inspired Control for Adaptive Walking of Biped Robots. *Systems, Man, and Cybernetics: Systems, IEEE Transactions on*, 43(5):1206–1215.

Matos, V. and Santos, C. P. (2012). Central Pattern Generators with Phase Regulation for the Control of Humanoid Locomotion. In *IEEE-RAS International Conference on Humanoid Robots*, Japan.

Matsuoka, K. (1985). Sustained oscillations generated by mutually inhibiting neurons with adaptation. *Biological Cybernetics*, 52(6):367–376.

Matsuoka, K. (1987). Mechanisms of frequency and pattern control in the neural rhythm generators. *Biological Cybernetics*, 56(5-6):345–353.

Matsuoka, K. (2011). Analysis of a neural oscillator. *Biological Cybernetics*, 104(4-5):297–304.

McGeer, T. (1990). Passive Dynamic Walking. *The International Journal of Robotics Research*, 9(2):62–82.

Michel, O. (2004). Webots: Professional Mobile Robot Simulation. *Journal of Advanced Robotics Systems*, 1(1):39–42.

Miyakoshi, S., Taga, G., Kuniyoshi, Y., and Nagakubo, A. (1998). Three dimensional bipedal stepping motion using neural oscillators-towards humanoid motion in the real world. In *Intelligent Robots and Systems, 1998. Proceedings., 1998 IEEE/RSJ International Conference on*, volume 1, pages 84–89 vol.1.

Morimoto, J., Endo, G., Nakanishi, J., and Cheng, G. (2008). A Biologically Inspired Biped Locomotion Strategy for Humanoid Robots: Modulation of Sinusoidal Patterns by a Coupled Oscillator Model. *Robotics, IEEE Transactions on*, 24(1):185–191.

Nakada, K., Asai, T., Hirose, T., and Amemiya, Y. (2005). Analog current-mode CMOS implementation of central pattern generator for robot locomotion. In *Neural Networks. IJCNN. Proceedings of the 2005 IEEE International Joint Conference on*, volume 1, pages 639–644.

Nakada, K. and Matsuoka, K. (2012). Integrated Circuit Implementation of Piecewise Linear Oscillators and its Application to Phase Reset Control. *Technical report of IEICE. ICD*, 111(497):1–6.

Nakada, K., Sato, Y., and Matsuoka, K. (2011). Tuning time scale parameter of piecewise linear oscillators for phase resetting control.

Nakada, K., Sato, Y., and Matsuoka, K. (2013). Theoretical Analysis of Phase Resetting on Matsuoka Oscillators. In *Advances in Cognitive Neurodynamics (III)*, pages 531–536. Springer Netherlands.

Nakanishi, J., Morimoto, J., Endo, G., Cheng, G., Schaal, S., and Kawato, M. (2004). Learning from demonstration and adaptation of biped locomotion. *Robotics and Autonomous Systems*, 47:79–91.

Nakanishi, M., Nomura, T., and Sato, S. (2006). Stumbling with optimal phase reset during gait can prevent a humanoid from falling. *Biological Cybernetics*, 95(5):503–515.

Nassour, J., Hugel, V., Ouezdou, F., and Cheng, G. (2013). Qualitative Adaptive Reward Learning With Success Failure Maps: Applied to Humanoid Robot Walking. *Neural Networks and Learning Systems, IEEE Transactions on*, 24(1):81–93.

Nomura, T., Kawa, K., Suzuki, Y., Nakanishi, M., and Yamasaki, T. (2009). Dynamic stability and phase resetting during biped gait. *Chaos: An Interdisciplinary Journal of Nonlinear Science*, 19(2):026103(1–12).

Oliveira, M., Matos, V., Santos, C. P., and Costa, L. (2013). Multi-objective parameter CPG optimization for gait generation of a biped robot. In *Robotics and Automation (ICRA), 2013 IEEE International Conference on*, pages 3130–3135.

Park, C.-S., Hong, Y.-D., and Kim, J.-H. (2010). Full-body joint trajectory generation using an evolutionary central pattern generator for stable bipedal

walking. In *Intelligent Robots and Systems (IROS), 2010 IEEE/RSJ International Conference on*, pages 160–165.

Park, J. and Youm, Y. (2007). General ZMP Preview Control for Bipedal Walking. In *Robotics and Automation, 2007 IEEE International Conference on*, pages 2682–2687.

Passino, K. M. (2004). *Biomimicry for Optimization, Control and Automation.* Springer International Publishing, 1 edition.

Righetti, L. and Ijspeert, A. (2006). Programmable central pattern generators: an application to biped locomotion control. In *Robotics and Automation, 2006. ICRA 2006. Proceedings 2006 IEEE International Conference on*, pages 1585–1590.

Sakagami, Y., Watanabe, R., Aoyama, C., Matsunaga, S., Higaki, N., and Fujimura, K. (2002). The intelligent ASIMO: system overview and integration. In *Intelligent Robots and Systems, 2002. IEEE/RSJ International Conference on*, volume 3, pages 2478–2483 vol.3.

Shukla, J., Cristiano, J., Amela, D., Anguera, L., Vergés-Llahí, J., and Puig, D. (2015). A Case Study of Robot Interaction Among Individuals with Profound and Multiple Learning Disabilities. In Tapus, A., André, E., Martin, J.-C., Ferland, F., and Ammi, M., editors, *Social Robotics*, volume 9388 of *Lecture Notes in Computer Science*, pages 613–622. Springer International Publishing.

Song, K.-T. and Hsieh, C.-H. (2014). CPG-based control design for bipedal walking on unknown slope surfaces. In *Robotics and Automation (ICRA), 2014 IEEE International Conference on*, pages 5109–5114.

Sugihara, T., Nakamura, Y., and Inoue, H. (2002). Real-time humanoid motion generation through ZMP manipulation based on inverted pendulum control. In *Robotics and Automation, 2002. Proceedings. ICRA '02. IEEE International Conference on*, volume 2, pages 1404–1409 vol.2.

Taga, G. (1995). A model of the neuro-musculo-skeletal system for human locomotion. *Biological Cybernetics*, 73(2):113–121.

Taga, G., Yamaguchi, Y., and Shimizu, H. (1991). Self-organized control of bipedal locomotion by neural oscillators in unpredictable environment. *Biological Cybernetics*, 65(3):147–159.

Tass, P. (1999). *Phase Resetting in Medicine and Biology: Stochastic Modelling and Data Analysis.* Springer series in synergetics. Springer Verlag.

Vukobratović, M. and Borovac, B. (2004). Zero-Moment Point - Thirty five years of its life. *International Journal of Humanoid Robotics*, 01(01):157–173.

Williamson, M. M. (1999). *Robot Arm Control Exploiting Natural Dynamics.* PhD thesis.

Xu, W., Fang, F. C., Bronlund, J., and Potgieter, J. (2009). Generation of rhythmic and voluntary patterns of mastication using Matsuoka oscillator for a humanoid chewing robot. *Mechatronics*, 19(2):205–217.

Yu, J., Tan, M., Chen, J., and Zhang, J. (2014). A Survey on CPG-Inspired Control Models and System Implementation. *Neural Networks and Learning Systems, IEEE Transactions on*, 25(3):441–456.

Zhang, D., Poignet, P., Widjaja, F., and Ang, W. T. (2011). Neural oscillator based control for pathological tremor suppression via functional electrical stimulation. *Control Engineering Practice*, 19(1):74–88.